

ER-2989

A COMPARISON OF HYDRAULIC  
FRACTURE TREATMENTS  
FOR THE MUDDY "J" SAND  
WATTENBERG FIELD, COLORADO

By

R. L. Zahner

ProQuest Number: 10782645

All rights reserved

INFORMATION TO ALL USERS

The quality of this reproduction is dependent upon the quality of the copy submitted.

In the unlikely event that the author did not send a complete manuscript and there are missing pages, these will be noted. Also, if material had to be removed, a note will indicate the deletion.



ProQuest 10782645

Published by ProQuest LLC (2018). Copyright of the Dissertation is held by the Author.

All rights reserved.

This work is protected against unauthorized copying under Title 17, United States Code  
Microform Edition © ProQuest LLC.

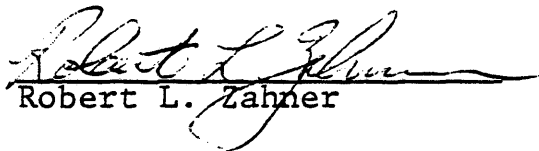
ProQuest LLC.  
789 East Eisenhower Parkway  
P.O. Box 1346  
Ann Arbor, MI 48106 – 1346

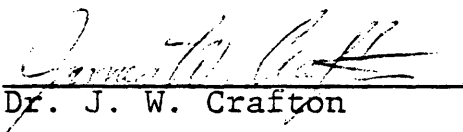
ER-2989

A thesis submitted to the Faculty and the Board of Trustees of the Colorado School of Mines in partial fulfillment of the requirements for the degree of Master of Engineering (Petroleum Engineer).

Golden, Colorado

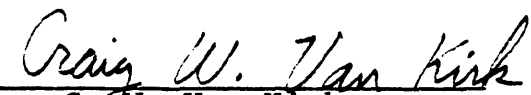
Date NOVEMBER 28, 1984

Signed:   
Robert L. Zahner

Approved:   
Dr. J. W. Crafton

Golden, Colorado

Date Nov. 28, 1984

  
Dr. C. W. Van Kirk  
Department Head  
Petroleum Engineering

ABSTRACT

A data base of production, fracture treatment, and volumetric data of wells in T2N/R65W, Wattenberg gas field, is used to evaluate the long-term (eight year) performance of hydraulic fracture treatments. Short-term (two year) data is used to compare the performance of polymer emulsions versus cross-linked gels, pillar-fractures versus packed fractures, and low fluid loss fluids versus high fluid loss fluids. Fracture dimensions are calculated using the procedure proposed by H.O. McLeod, with modifications. The validity of the modified McLeod method is investigated.

Fracture design optimization must consider several variables in light of the general uncertainty of formation properties and created fracture shape and dimensions. Operators with limited leasehold positions generally cannot justify the expense of rigorous optimization methods incorporating finite difference simulators. However, the results presented here strongly suggest that some type of optimization procedure is required to reduce the economic risk in drilling and completing wells in the Muddy "J" formation.

TABLE OF CONTENTS

	<u>Page</u>
Abstract . . . . .	iii
List of Figures . . . . .	vii
List of Tables . . . . .	x
Acknowledgements . . . . .	xi
Introduction . . . . .	1
Conclusions . . . . .	6
Recommendations for Future Research . . . . .	9
Review of Pertinent Literature	
Evolution of Fracture Design in the Wattenberg Field . . . . .	11
Review of Fracture Design Optimization Methods . . . . .	18
Calculation of Gas in Place	
Geology and Field Description . . . . .	25
Volumetric Calculations . . . . .	29
Calculation of Fracture Dimensions	
Selection of a Fracture Model . . . . .	34
Determination of Fracture Height . . . . .	35
Selection of Fluid Properties . . . . .	36
Modification of the McLeod Method . . . . .	38
Determination of Performance Indicators . . . . .	47
The Effect of Volumetric Parameters and Fracture Length on Well Performance . . . . .	51

	<u>Page</u>
First-Order versus Second-Order Polynomial Best Fit Curves . . . . .	52
The Validity of the Modified McLeod Method . . . . .	53
The Effect of Net Pay and Porosity on Performance . . . . .	57
The Effect of Fracture Length on Well Performance . . . . .	61
Comparisons of Fluid Systems and Proppant Schedules	
Comparison of Polymer Emulsions and Cross- linked Gels . . . . .	71
Comparison of Pillar and Conventional Packed Fractures . . . . .	77
Comparison of Low and High Fluid Loss Treatments . . . . .	79
Discussion of the Variations in Well Performance	
Formation Damage Due to Fluid Invasion . . . . .	93
The Concept of Effective Fracture Length . . . . .	94
Other Factors Which Affect Performance . . . . .	97
Discussion of Fracture Design Optimization Procedures . . . . .	98
Nomenclature . . . . .	100
References . . . . .	103
Appendices	
A. The McLeod Method of Fracture Dimension Calculations . . . . .	110
B. Modifications to the McLeod Method . . . . .	115

	<u>Page</u>
C. Fracture Treatment Data and Fracture Dimensions . . . . .	121
D. Procedure for Economic Calculations . . .	134
E. Structure of the 1022 Data Base Used for this Study . . . . .	136
F. Procedure to test for Parallelsim of Slopes . . . . .	139

LIST OF FIGURES

	<u>Page</u>
1. Regional location of the Wattenberg field . .	2
2. Location of Township 2N/65W within the Wattenberg field . . . . .	3
3. Southwest-northeast cross-section of Muddy "J" resistivity logs. . . . .	26
4. Interpretation of depositional environment of well 173, Sec. 24, T2N/65W, Wattenberg . .	27
5. Example of net pay selection for well 173 . .	28
6. Net pay isopach, T2N/65W, Wattenberg . . . .	30
7. Gas porosity isopach, T2N/65W, Wattenberg . .	31
8. Fracture conductivity vs. areal and concen- tration, for 10-20 and 20-40 sand . . . . .	44
9. Propped vs. created fracture length for a hypothetical Wattenberg fracture design. Second order best-fit curves . . . . .	56
10. Propped vs. created fracture length for fracture treatments studied in this report .	58
11. Average daily rate (first year) vs. net pay .	59
12. Average daily rate (first year) vs. hydro- carbon gas porosity . . . . .	60
13. Eight-year net present value vs. propped fracture length. Second order best-fit curve . . . . .	62
14. Eight-year cumulative production vs. propped fracture length. Second order best-fit curve . . . . .	63
15. Eight-year cumulative recovery vs. propped fracture length. Second order best-fit curve . . . . .	64

	<u>Page</u>
16. Eight-year undiscounted profit/investment ratio length. Second order best-fit curve . . . . .	65
17. Average daily producing rates for wells with short (0 to 800 ft), medium (1500 to 2200 ft) and long (2400 to 3600 ft) fracture lengths . . . . .	67
18. Two-year net present value vs. propped fracture length. Second order best-fit curve . . .	69
19. Two-year profit/investment ratio vs. propped fracture length. Second order best-fit curve . . . . .	70
20. Comparison of initial producing rates vs. proppant weight for polymer emulsions and cross-linked gels. First order best-fit curves . . .	73
21. Comparison of NPV vs. proppant weight for polymer emulsions and cross-linked gels. First order best-fit curves . . . . .	74
22. Comparison of initial producing rates vs. fluid volume for polymer emulsions and cross-linked gels. First order best-fit curves . . .	75
23. Comparison of NPV vs. fluid volume for polymer emulsions and cross-linked gels. First order best-fit curves . . . . .	76
24. Comparison of initial producing rates vs. proppant weight for packed and pillar fracs. First order best-fit curves . . . . .	80
25. Comparison of NPV vs. proppant weight for packed and pillar fracs. First order best-fit curves . . . . .	81
26. Comparison of initial producing rates vs. fluid volume for packed and pillar fracs. First order best-fit curves . . . . .	82

	<u>Page</u>
27. Comparison of NPV vs. fluid volume for packed and pillar fracs. First order best-fit curves . . . . .	83
28. Fluid efficiency vs. fluid loss coefficient for the treatments included in this report. Second order best-fit curve . . . . .	84
29. Created fracture length vs. fluid volume for high fluid loss and low fluid loss jobs. First order best-fit curve . . . . .	86
30. Comparison of initial producing rate vs. propped weight for high and low fluid loss. First order best-fit curves . . . . .	89
31. Comparison of NPV vs. proppant weight for high and low fluid loss. First order best-fit curve . . . . .	90
32. Comparison of initial producing rates vs. fluid volume for high and low fluid loss. First order best-fit curves . . . . .	91
33. Comparison of NPV vs. fluid volume for high and low fluid loss. First order best-fit curves . . . . .	92

LIST OF TABLES

	<u>Page</u>
1. Fracture Dimensions of Wattenberg Wells Reported by Roberts (5) . . . . .	17
2. Comparisons of Design and History Match Fracture Lengths for Various Wells, Reported by Holditch (6) . . . . .	22
3. Summary of Fracture Treatments from 2N/65W which are included in this Report . . . . .	45
4. Summary of Calculated Fracture Dimensions for Treatments included in this Report . . . . .	46
5. Parameters used in Economic Calculations . . . . .	49
6. Comparisons of Hydraulic and Propped Fracture Lengths of Modified McLeod Method and Results of Harp (4), with Cross-linked Gel . . . . .	54
7. Variation of Fracture Dimensions with Fluid Loss Coefficient, using Modified McLeod Method . . . . .	87

ACKNOWLEDGEMENTS

I would like to thank the following operators and service companies, who have been very helpful in providing data for this study:

Amoco Production Co.  
Coors Energy Co.  
Halliburton Services  
Macey & Mershon Oil, Inc.  
MGF Oil Corp.  
Panhandle Eastern Pipeline Co.  
Petroleum Information  
Vessels Oil & Gas Co.  
Western Co.

I would like to thank Dr. James Crafton, my advisor, for his many suggestions and insight of the topics covered here.

The efforts of Dee Brown, the petroleum engineering secretary, and Linda Hasty, my typist, in completing this report are appreciated very much. Finally, my wife, Debbie, deserves special mention for her continuous understanding and support during this endeavor.

## INTRODUCTION

Commercial development of the Muddy "J" sandstone in the Wattenberg gas field began in the early 1970's. The field encloses 978 square miles northeast of Denver, in the Colorado portion of the Denver Basin (Fig. 1). The geology of the Muddy "J" sand is well documented: It is a Cretaceous age delta front blanket-sand of large areal extent(1). Initially, this formation presented a substantial economic risk due to the uncertainty of fracturing techniques required to obtain commercial production rates. In order to recover the anticipated gas in place, operators in the area initiated a major development program which resulted in the evolution of successful fracturing treatments.

With over eight years of production history and a wide range of fracture treatment sizes, the Wattenberg field provides a unique opportunity to evaluate fracture design optimization for tight gas sands. To that end, this report compares calculated fracture dimensions, based on actual fracture job data from 71 treatments in Township T2N/R65W, with performance indicators such as cumulative production and net present value (NPV). Wells from T2N/R65W (Fig. 2) were selected for the following reasons:

- 1) the township is close to the center of the Wattenberg field;
- 2) all wells produce only from the Muddy "J" sand;  
and

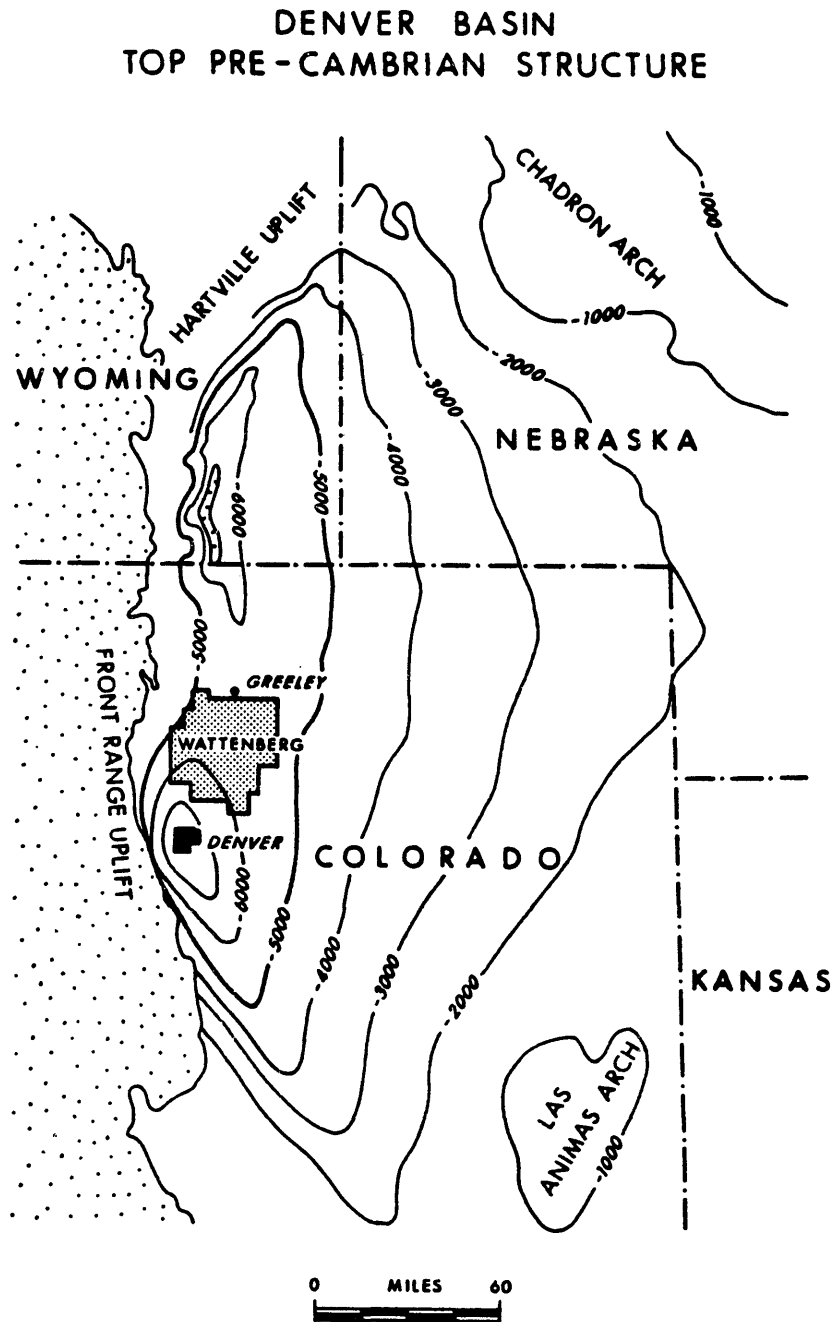


Figure 1. Regional location of the Wattenberg field. After Matuszczak (1).

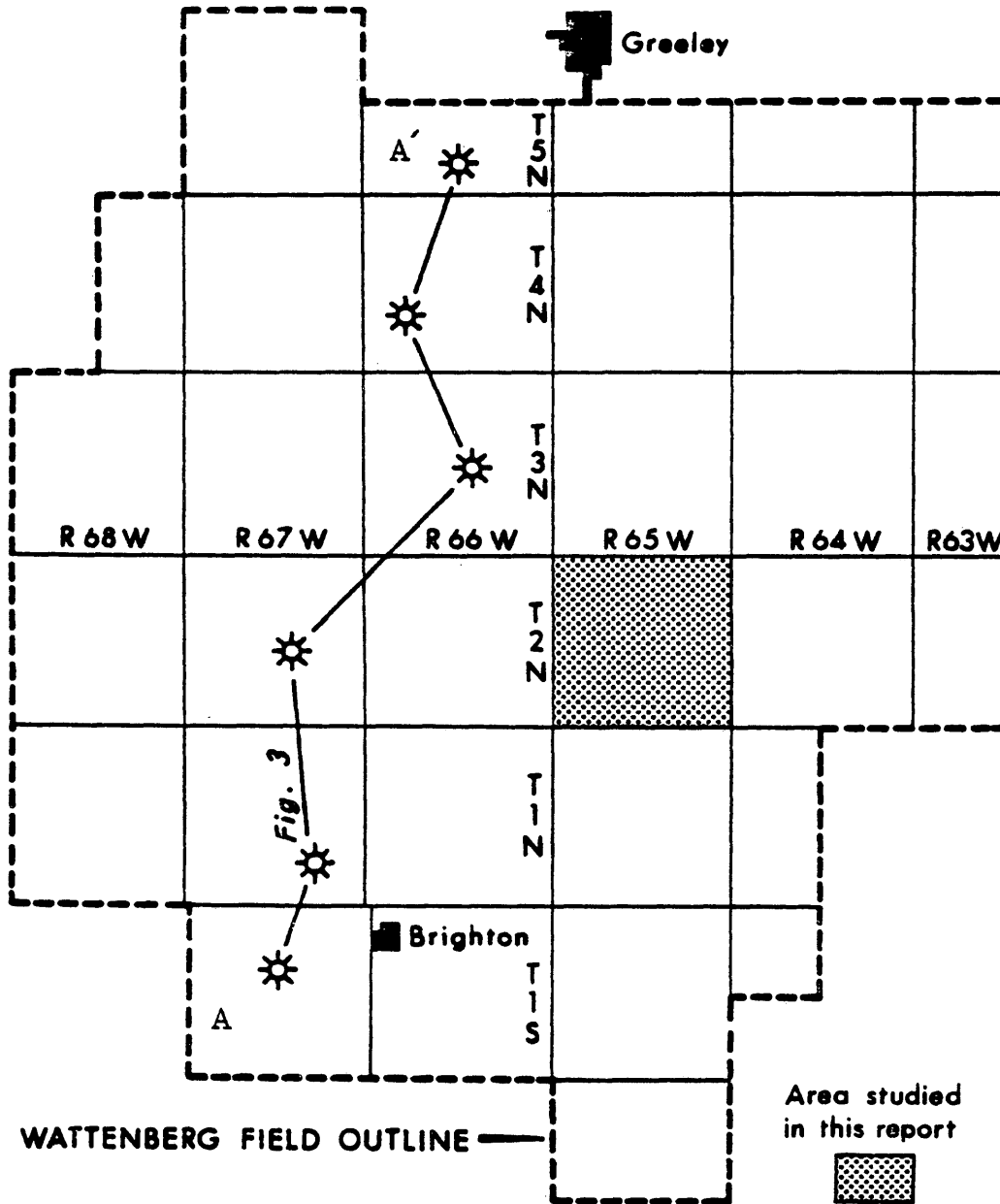


Figure 2. Location of Township 2N/65W within the Wattenberg field. After Matuszczak (1). Cross-section A-A' Shown in Fig. 3.

- 3) all wells produce mostly dry gas with little or no liquid production.

The current fracture design commonly used in the Wattenberg field has evolved over many years through a trial-and-error process and operators' research particularly Amoco's. While the experience gained in the Wattenberg field is valuable, it does not directly allow selection of job sizes for other fields. Moreover, optimum job sizes may vary from well to well within the Wattenberg field. Finite difference simulators are available to permit optimization of fracture design for specific wells, but their cost can be prohibitive. Small to medium size operators with only a few wells to fracture must often use a "standard" design without any indication that it is near optimum.

Fracture design optimization, in the simplest sense, means maximizing NPV. To that end, there are several variables to be considered:

- 1) treatment fluid volume;
- 2) proppant volume (weight) and concentration;
- 3) treatment fluid rheology;
- 4) design created fracture length;
- 5) design propped fracture length;
- 6) effective fracture length;
- 7) total job cost;
- 8) expected production stream;
- 9) formation permeability, porosity, and net pay

A fracture design optimization method must ultimately account for all of these variables. Effective fracture

length is defined here as the length determined by well testing methods, and that which provides an accurate forecast of production rates. Thus, it is the link between the fracture design and the expected results (i.e., production). Note that the effective fracture length is not necessarily equal to the propped length.

It must be stated emphatically that the results presented in this report are not intended to represent absolute magnitudes of actual economic performance, nor predict future performance for specific fracture treatments. The purpose of this report is to evaluate the effects of design fracture lengths and treatment sizes on actual well performance, with the intent of comparing all wells in a consistent manner.

### CONCLUSIONS

Based on the derivations of the fracture dimension equations presented here and on the comparisons of actual production data from Township T2N/R65W, several conclusions can be drawn:

1. There is a wide variation of well performance within T2N/R65W, which cannot be attributed to the volumetric factors of net pay, porosity, and water saturation.
2. Well productivity is influenced by variations in hydraulic fracture treatment size and fracture length. However, using the calculation method presented here, propped fracture lengths longer than 2000 feet have substantially increased economic risk. There is virtually no correlation between economic performance and propped fracture length for larger treatments.
3. Simple modifications to the fracture design method proposed by McLeod (9) account for fracture fluid efficiency, average created width, and viscosity increases due to proppant. The modified McLeod method predicts more realistic fracture dimensions than the original method.
4. The modified McLeod method appears to be capable of predicting sandouts in the fracture. It is not suitable for fluid systems with low viscosity and high

fluid leak-off. The limits of application are approximately 100 cp and  $0.002 \text{ ft}/(\text{min})^{\frac{1}{2}}$ , respectively.

5. Wells treated with cross-linked gels have higher initial producing rates than those treated with equivalent volumes of polymer emulsion fluids. There is no difference in initial rates when the comparison is based on equivalent total proppant weights. All comparisons are based on a significance level of 5%, or confidence interval of 95%.
6. Normalized two-year net present values are equivalent for cross-linked gels and polymer emulsions. Constant unit costs and gas prices are used for all economic evaluations.
7. Conventional packed fracture treatments resulted in higher initial rates than pillar fracture treatments, based on equal fluid volumes. There is no difference in initial production for equivalent total proppant weights. The pillar fracture treatments generally had lower average sand concentrations than packed fracture treatments.
8. The normalized two-year net present values are equivalent for packed and pillar fracture treatments.
9. Wells fractured with high fluid-loss treatments (fluid loss coefficient greater than  $0.001 \text{ ft}/(\text{min})^{\frac{1}{2}}$ ) have

ER-2989

calculated fracture lengths which are approximately one half the lengths of low fluid-loss treatments (fluid loss coefficient less than  $0.001 \text{ ft/min}^{\frac{1}{2}}$ ), for equal fluid volumes. Fracture widths and dimensionless fracture conductivities are generally larger for the high fluid loss treatments.

10. There are not enough data points to make definitive comparisons of low fluid loss and high fluid loss treatments. However, the available data indicates there is no difference in initial producing rates for low and high fluid loss treatments. Low fluid loss treatments include both cross-linked gels and polymer emulsions.
11. Available data indicates the normalized two-year net present values are equivalent for high fluid loss and low fluid loss treatments.
12. The addition of 5% or more of hydrocarbon to a cross-linked gel can reduce the fluid loss coefficient by 30 to 90%.

### RECOMMENDATIONS FOR FUTURE RESEARCH

The data base assembled for this study provides an opportunity for the research of the long-term results of hydraulic fracture treatments. Moreover, fracture design optimization procedures can be evaluated using this historical data. Some specific proposals are as follows:

1. Do a history match using long-term production data and well test data, where available. The objective would be to determine effective fracture lengths and permeability for each well.
2. Use the results from history-matching to forecast production rates and compare with historical data. Compare the suitability of finite-conductivity and uniform-flux fracture models.
3. Evaluate the design optimization procedure proposed here. Compare the expected results with historical results.
4. Compare the fracture dimension predictions of the modified McLeod method with those of a finite difference fracture simulator.
5. Investigate the effect of permeability variations on well performance.
6. Investigate the effect of proppant size, scheduling, and concentration on well performance.

ER-2989

7. Evaluate the success of refracturing treatments in T2N/R65W, in order to establish general criteria for justifying refractures.
8. Use multi-variate analysis techniques to further evaluate the results presented here.

### REVIEW OF PERTINENT LITERATURE

There is a significant volume of literature on the evolution of fracture treatments in the Wattenberg field. Most notable are the works of Fast, Holman, and Covlin (2), Parrot and Long (3), and Harp (4), and Roberts (5). These papers provide an excellent history of Wattenberg fracture treatments. Holditch et al (6), Crafton et al (7), Crowell and Jennings (8), and McLeod (9) present specific procedures for optimizing fracture design.

#### Evolution of Fracture Design in the Wattenberg Field

Fast, Holman and Covlin (2) present an excellent history of hydraulic fracture design optimization through 1976. Five wells were completed in the Muddy "J" sand in 1970 to mark the discovery of the Wattenberg field. A drilling program consisting of 100 wells followed to evaluate the potential of the area. These initial wells were treated with 30,000 to 50,000 gallons of gelled water, with proppant concentrations of 1 to 3 lb/gal. Although 72 of the 100 wells produced gas, there was still an uncertainty of the economic success with these treatments. In 1973, four wells were treated with 132,000 to 180,000 gallons of polymer emulsion with about 200,000 lbs of proppant. The productivity of these wells was 3 to 4 times better than the earlier

ER-2989

wells, and proved the economic feasibility of developing the Wattenberg field.

Four fracture fluids were tested to find the one with the best combination of (1) low fluid loss, (2) high viscosity, (3) low formation damage, (4) high-temperature stability, and (5) low cost. The fluids tested were:

- 1) polymer emulsion (2/3 condensate, 1/3 guar-gum gel);
- 2) cross-linked gelled condensate;
- 3) cellulose-gum water gel; and
- 4) high temperature guar-gum gel.

The polymer emulsion was chosen on the basis of its low fluid loss, viscosity stability and low to moderate formation damage.

The standard treatment in late 1976 consisted of 100 mesh, 20-40 mesh, and 10-20 mesh sand, pumped in that order. Final sand concentrations were 6 lb/gal. The "pillar fracture" technique (10) was used extensively, but the authors reported no conclusions had been reached as to its effectiveness compared to packed fractures.

Of particular interest in the work of Fast, Holman, and Covlin is the discussion of field results. Three areas in adjacent townships were evaluated to determine optimum treatment volume. Area A and area C each contained four wells, and were found to have permeabilities which varied by as much as 10-fold. Cumulative production for equivalent

ER-2989

300,000 gal polymer emulsion treatments varied accordingly.

The results are as follows:

<u>Area</u>	<u>Minimum Permeability, md</u>	<u>Cumulative Production (20 Months), MMSCF</u>
A	0.05	490
B	Not Reported	150
C	0.005	275

The sand volumes used in areas B and C were not reported, but apparently were the same as area A. Net pays, porosities, or water saturations were not reported for any of the wells. The authors concluded that the optimum treatment size had not been reached in area A, but areas B and C might be uneconomic, regardless of treatment size, due to low permeability.

Parrot and Long (3) reported that by 1979 the maximum economic treatment size in the Wattenberg field had not been determined, in spite of jobs with up to 623,000 gallons fluid and 1,041,300 lbs sand. Their work reported the results of refracturing 29 wells which originally had received 50,000-gal gelled water fracture treatments, including the areas described by Fast, Holman, and Covlin (FHC) above. It is especially pertinent to note that areas A, B, and C described by FHC are all grouped into a single area A by Parrot and Long. Moreover, areas B and C of FHC, which were considered marginally economic by them, were reported to be

ER-2989

successfully refractured. Higher gas prices certainly make the economics of refracturing more favorable for marginal wells. Nonetheless, areas considered significantly different by FHC are considered by Parrot and Long to have comparable refracture performance. The implication here is that while reservoir permeability affects well performance, the areal variation of reservoir quality may be more gradual and/or fracture treatments have more impact than suspected by FHC. Parrot and Long report that refracture treatments in areas north and south of area A were unsuccessful. These areas were characterized by poor productivity following initial completions.

Crosslinked gelled water became the preferred fracture treatment fluid in the late 1970's. Parrot and Long suggest that the lengthy recovery times were the primary reason for switching to the crosslinked gel. Although these cross-linked gels also had long recovery times, it was reasoned that the wells began producing "new" condensate much sooner. Harp (4) similarly states that the long recovery time for condensate was a major reason for discontinuing polymer emulsion treatments. Two other reasons are also given by him: 1) polymer emulsions were considered to be a banking fluid, resulting in much shorter propped fracture lengths than originally expected, and 2) friction loss is approxi-

mately 2.8 times higher for polymer emulsions, compared to crosslinked gel. The author does not explain why a polymer emulsion is considered a banking fluid, but does suggest that a crosslinked gel without temperature stabilizers also becomes a banking fluid. Production results are given to support the author's view. Harp argues that propped length is more important than fracture conductivity, in maximizing production in tight gas reservoirs, citing the work of McGuire and Sikora (11) to support this idea. However, the author reports that Amoco had decided to eliminate "pillar fractures," and use higher sand concentrations, which would tend to result in shorter, higher conductivity fractures.

Roberts (5) discusses several aspects of fracture optimization in the Wattenberg field up to 1981 and presents results of field research. Five reasons are given for using cross-linked gel rather than polymer emulsions:

- 1) less formation damage
- 2) higher sand concentrations possible
- 3) less cost
- 4) much faster load recovery
- 5) not flammable

The author reports that the optimum fracture length was determined to be 3900 feet, based on computer simulation, and would require 300,000 gallons of polymer emulsion or 180,000 gallons of cross-linked gel. The optimum proppant volume is considered to be the maximum concentration that

ER-2989

could be pumped without causing a screenout.

Fracture lengths calculated by modeling and type curve-matching are presented for ten Wattenberg wells. The results are reproduced in Table 1. Roberts reports that fracture height is attained in the early stages of treatment. Fractures were found to extend approximately four feet into the shale above and below the Muddy "J" sand. The standard deviation of fracture height for wells listed in Table 1 is 14.5% of the mean. This compares to a standard deviation of net pay/fracture height ratio which is 32.9% of the mean, and suggests that selecting a fracture height based on gross pay is more appropriate than using a fracture height/net pay ratio. The comparison of "modeled  $x_f$ ", and "type curve  $x_f$ ", which must be based on performance, indicates that the effective length averages approximately 85% of the design length. This difference between the design fracture length and effective fracture length, and its implication with respect to optimization, is not addressed by the author. One final point to note is that the mean modeled efficiency, which is taken to be fracture fluid efficiency, is 64.5% and 49.5% for cross-linked gels and polymer emulsions, respectively.

Veatch and Crowell (12) present a comprehensive review of Amoco's field research program, including some results

Table 1

Well	Treatment Size		Fluid Type	h (ft)	h <sub>f</sub> (ft)	h/h <sub>f</sub>	Fracture Length, ft		Modeled Fluid Eff.	
	Fluid (M gal)	Sand (M lb)					Modeled	TC/Mod. Curve		
1	323	709	XLG	27	111	0.24	5200	5730	1.102	0.55
2	362	701	XLG	36	121	0.30	5000	3761	0.752	0.57
3	200	804	XLG	32	116	0.28	3800	3588	0.944	0.71
4	167	848	XLG	20	130	0.15	3400	2379	0.700	0.75
5	600	1363	XLG	25	116	0.22	10300	7333	0.712	0.64
6	622	1041	PE	27	105	0.26	9600	7862	0.819	0.50
7	206	494	XLG	20	91	0.22	5400	5139	0.952	0.67
8	325	738	XLG	10	103	0.10	6400	5606	0.876	0.64
9	315	735	PE	30	114	0.26	4600	3600	0.783	0.49
10	300	760	XLG	17	150	0.11	4200	3621	0.862	0.63

\* XLG = Cross-linked gel; PE = Polymer emulsion

Table 1. Fracture dimensions of Wattenberg wells reported by Roberts (5).

ER-2989

from Wattenberg, as follows:

Elastic Modulus, $10^6$ psi	2 to 7
Net fluid-loss interval, ft	30 to 50
Estimated fracture height, ft	100 to 180
Fluid-loss coefficients, $\text{ft}/(\text{min})^{1/2}$	
Field data	0.0005 to 0.0007
Laboratory data	0.0003 to 0.0007

The research program was directed at obtaining reliable values for use in design calculations, such as fracture height, fluid loss coefficient, in-situ stress, rock properties and fracture orientations. The authors conclude that fracturing design parameters may vary widely throughout the same tight gas reservoir.

#### Review of Fracture Design Optimization Methods

The work of Holditch, et al (6) is one of the first to specifically discuss fracture design optimization. The authors present a design model which uses the equations of Geertsma and deKlerk (13) and the power-law viscosity equation to simultaneously solve for width, length, and viscosity. Well performance is then predicted using the analytical solutions of Gringarten et al (14) for an infinite conductivity fracture. Present value economic calculations are used to determine the optimum fracture design and/or well spacing for a particular application. There are several assumptions used in this early model which limit its

ER-2989

practical use. A partial list of these assumptions is as follows:

- 1) constant producing rate;
- 2) infinite fracture conductivity; and
- 3) the propped fracture length is assumed to be equal to the distance to the pad remaining in the fracture at the end of pumping.

In spite of these assumptions, the procedure is a good one, and can provide the framework for a practical optimization method.

A significant milestone in performance prediction of hydraulically fractured wells was achieved in the work of Agarwal, Carter, and Pollock (15). They developed type curves for finite conductivity fractures which can be used for history-matching to determine effective fracture length. Another set of type curves can then be used to predict production rates, given fracture length and conductivity, and reservoir permeability. The lack of wide-spread acceptance of this method is probably due to the fact that permeability must be known in order to obtain a unique curve-fit for history-matching.

Crowell and Jennings (8) use the finite conductivity type curves discussed above to analyze performance of fractured wells, and select refracturing candidates. An example of the analysis for a Wattenberg well indicates that the effective fracture length (from the type curve match) is

79.5% of the design length of 748 feet. The authors conclude that such a discrepancy between effective and design lengths implies that a "problem area" exists with respect to the fracture treatment. They do not suggest what this problem area might be. The authors also note that pressure transient analysis methods using an infinite-conductivity fracture model will result in much shorter effective fracture lengths than obtained with a finite-conductivity model.

The argument of finite versus infinite fracture conductivity is considered by Crafton et al (7) to be unimportant, with respect to fracture optimization. They present an optimization procedure which uses the uniform-flux fracture model of Gringarten et al (14). A uniform-flux fracture assumes high, but not infinite conductivity, and the authors readily admit that a finite conductivity fracture would appear to be shorter with their model. However, they report very good history matches and accurate production forecasts. The model can predict productivity with good accuracy because the forecasts are based on an effective fracture length and reservoir permeability which the model "sees" from history matching. The model also has the distinct advantage of not requiring an independent estimate of formation permeability, because it is found by iterative regression. The authors note that if histories from several

ER-2989

wells in one area are available, effective fracture lengths can be compared with net present value (NPV) performance to obtain an optimum job size. Results from history matching using the analytical model (AM) and a finite difference simulator (FDS) are as follows:

<u>Case</u>	Effective Length, ft		Res. Permeability, md	
	<u>FDS</u>	<u>AM</u>	<u>FDS</u>	<u>AM</u>
I	256	160	0.16	0.175
II	780	750	0.007	0.015
III	325	325	1.00	0.525

Note that the analytical model indicates an effective fracture length which is 62.5% of the FDS length, for an equivalent permeability (case I).

The most significant comparison of fracture lengths to date can be found in the work of Holditch and Lee (16). They present the results of calculating fracture lengths and formation permeabilities for 13 wells, using several different methods. A finite-difference history match is used to obtain the most representative estimates of effective fracture length and conductivity, which are compared to design lengths. No details of the design calculations are given, but the method is assumed to be similar to that used in Ref. 6. The results of these comparisons are shown in Table 2. Note that the average of effective fracture lengths is 68.4% of the average design lengths for 10 of the 13 wells. Wells

Table 2

Well	Est. Frac Height(ft)	Frac* Fluid	Volume (M Gal)	Proppant (M lbs)	Ld (ft)	History Match Lhm (ft)	History Match $F_c$ (md-ft)	Lhm/Ld (%)
1	350	NP	100	210	400	50	400	12.5
2	300	SP	154	196	700	400	400	57.1
3	140	NP	100	135	640	150	307	23.4
4	215	NP	160	230	900	550	227	61.1
5	110	NP	320	410	1500	200	540	13.3
6	300	GA	65	96	500	400	400	80.0
7	100	SP	250	170	1500	1000	800	66.7
8	80	SP	110	110	1000	500	50	50.0
9	400	NP	640	1200	1500	1500	500	100.0
10	300	NP	150	250	700	500	20	71.4
11	250	NP	200	350	1000	600	300	60.0
12	200	Foam	190	230	800	700	20	87.5
13	200	NP	100	340	800	400	250	50.0
Mean (excluding 1,3,5)								68.4

\*NP = Natural polymer; SP = Synthetic polymer; GA = Gelled 5% acid

Ld = Design fracture length; Lhm = History-match fracture length

Table 2. Comparisons of design and history match fracture lengths for various wells, reported by Holditch (6).

ER-2989

1, 3, and 5 are considered to be anomalies, with average effective/design length ratios of 12.5, 23.4, and 13.3%, respectively. The effective lengths in each case are for finite conductivity fractures. The authors conclude that fracture jobs should be slightly oversized to account for this difference in effective and design fracture lengths. They also note that they had difficulty obtaining unique solutions when using type curves for history matching.

If the analytical model of Crafton et al (7) can be used to forecast production for hydraulically fractured wells, a simple and reasonably accurate method of calculating propped fracture lengths can complete a cost-effective optimization procedure. The work of McLeod (9) presents such a method for computing fracture dimensions. He reports that his design method has been used successfully for numerous treatments in south Texas. Assumptions inherent in this method include:

- 1) the treatment fluid is a "perfect transport" fluid; i.e. no proppant settling occurs;
- 2) the fluid loss coefficient is approximately 0.001 ft/ min or less;
- 3) the fracture fluid behaves as a power-law fluid;
- 4) there is no fluid loss;
- 5) fracture height is constant

The current state-of-the-art cross-linked gels meet most of these assumptions, so this method applies to treatments

ER-2989

commonly performed today. The equations and method outlined by McLeod are presented in Appendix A. The author suggests that the work of McGuire and Sikora (11) can be used to forecast production increases and ultimately arrive at an optimum fracture treatment size. As shown in Appendix A, the McGuire and Sikora method applies only to steady-state flow and is generally not applicable to tight-gas reservoirs.

CALCULATION OF GAS IN PLACE

Geology and Field Description

The Muddy "J" sand is a marginal marine blanket-type reservoir of Cretaceous age (1, 17). The stratigraphic trap which dominates the accumulation of hydrocarbons was formed in a prograding delta front environment. The delta front and transgressive marine sequence interpretation is shown in Figure 3.

The reservoir characteristics are reported in the literature (2) as follows:

Initial Reservoir Pressure, psia	2900
Reservoir Temperature, °F	260
Gross Sand, ft	50-150
Net Sand, ft	10-50
Porosity, percent	8-12
Permeability, md	0.05-0.005

Examination of typical logs from T2N/R65W (Figures 4 and 5) reveals the transition from marine shale at the base to sandstone at the top. Interbedded shales and matrix clays combine to result in low permeability, and reduce the net pay/gross pay ratio. This ratio was found to vary considerably within T2N/R65W, but the gross sand interval is fairly constant. Results of log analysis from 20 wells indicate the following:

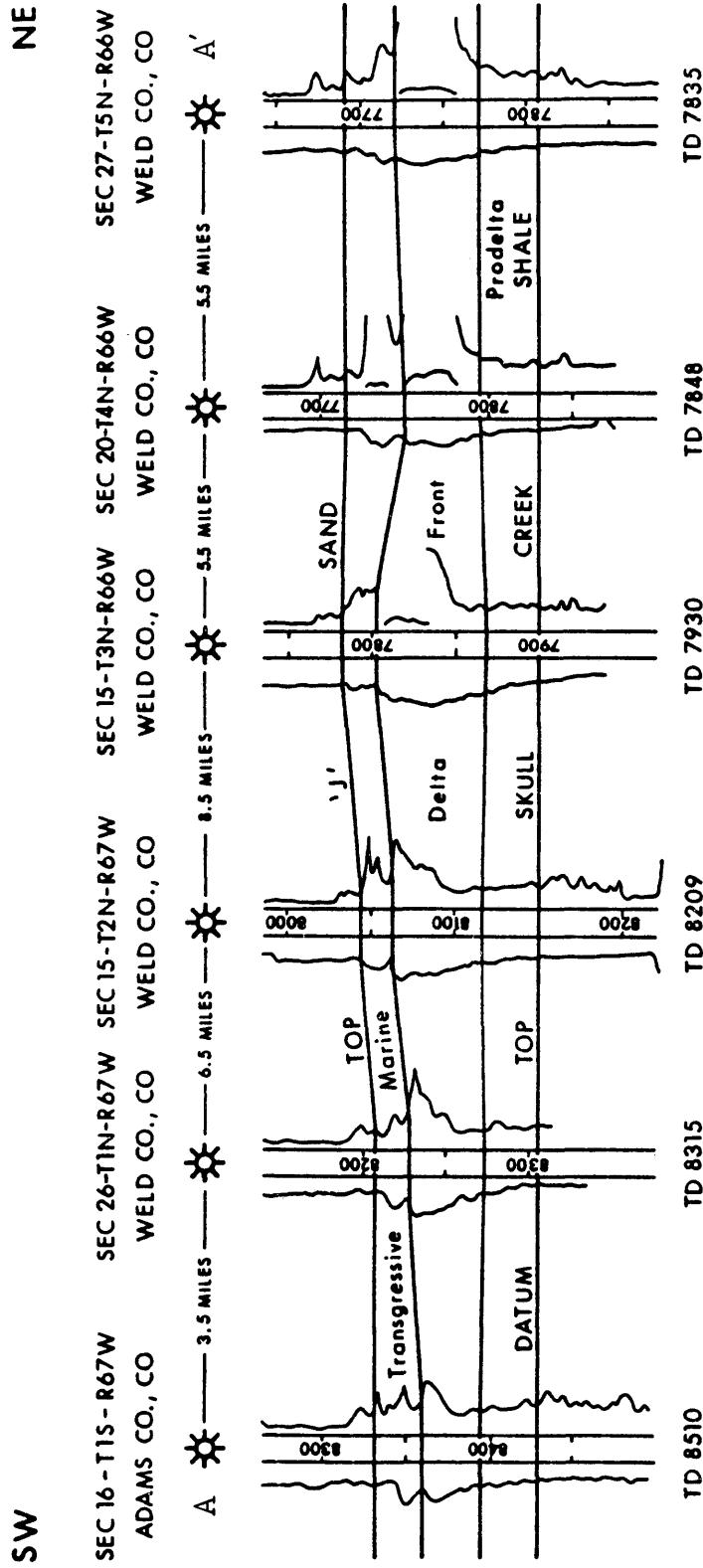


Figure 3. Southwest-northeast cross-section of Muddy "J" resistivity logs. After Matuszczak (1).

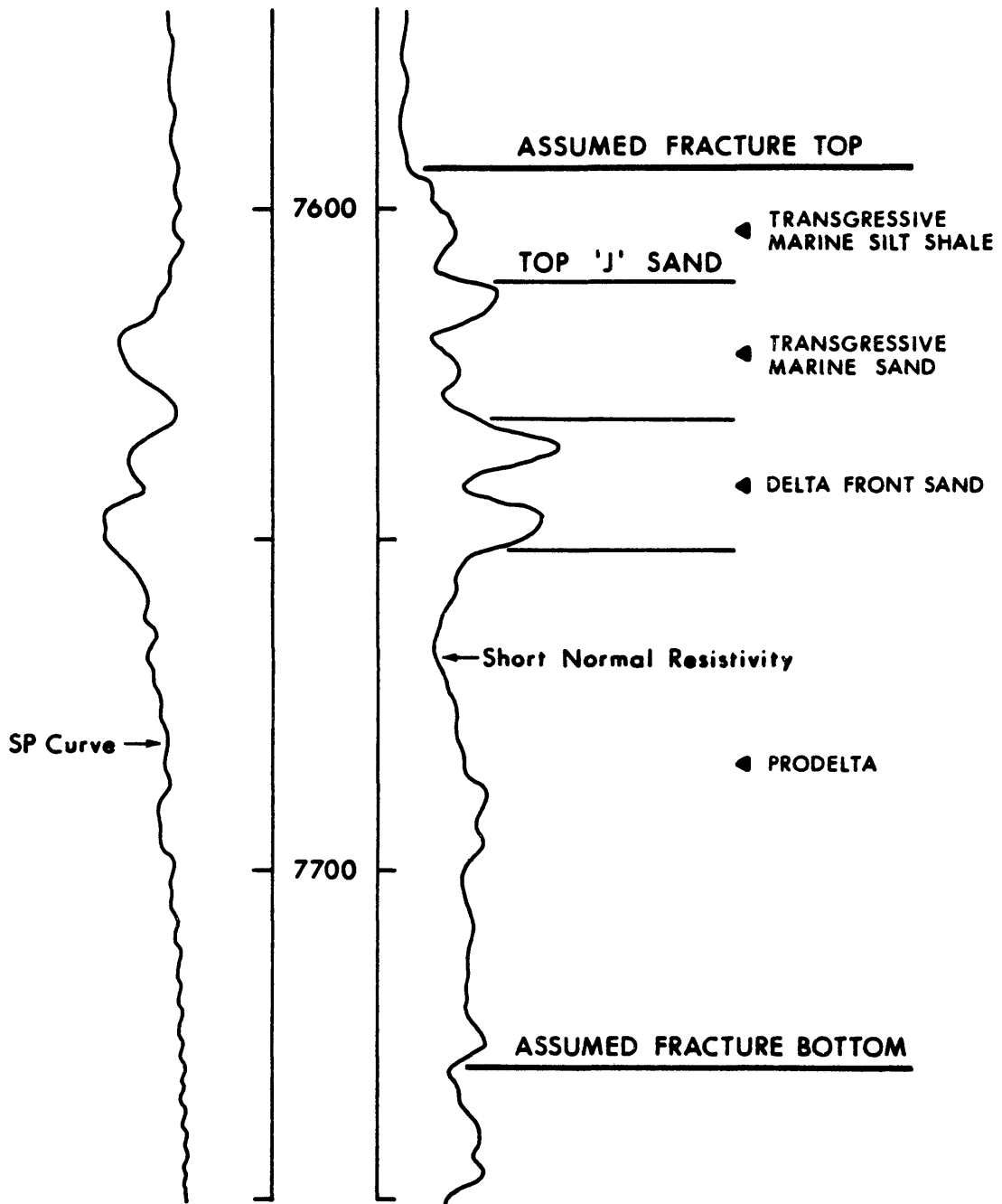


Figure 4. Interpretation of depositional environment of well 173, Sec. 24, T2N R65W, Wattenberg. After Matuszc-  
zak (1).

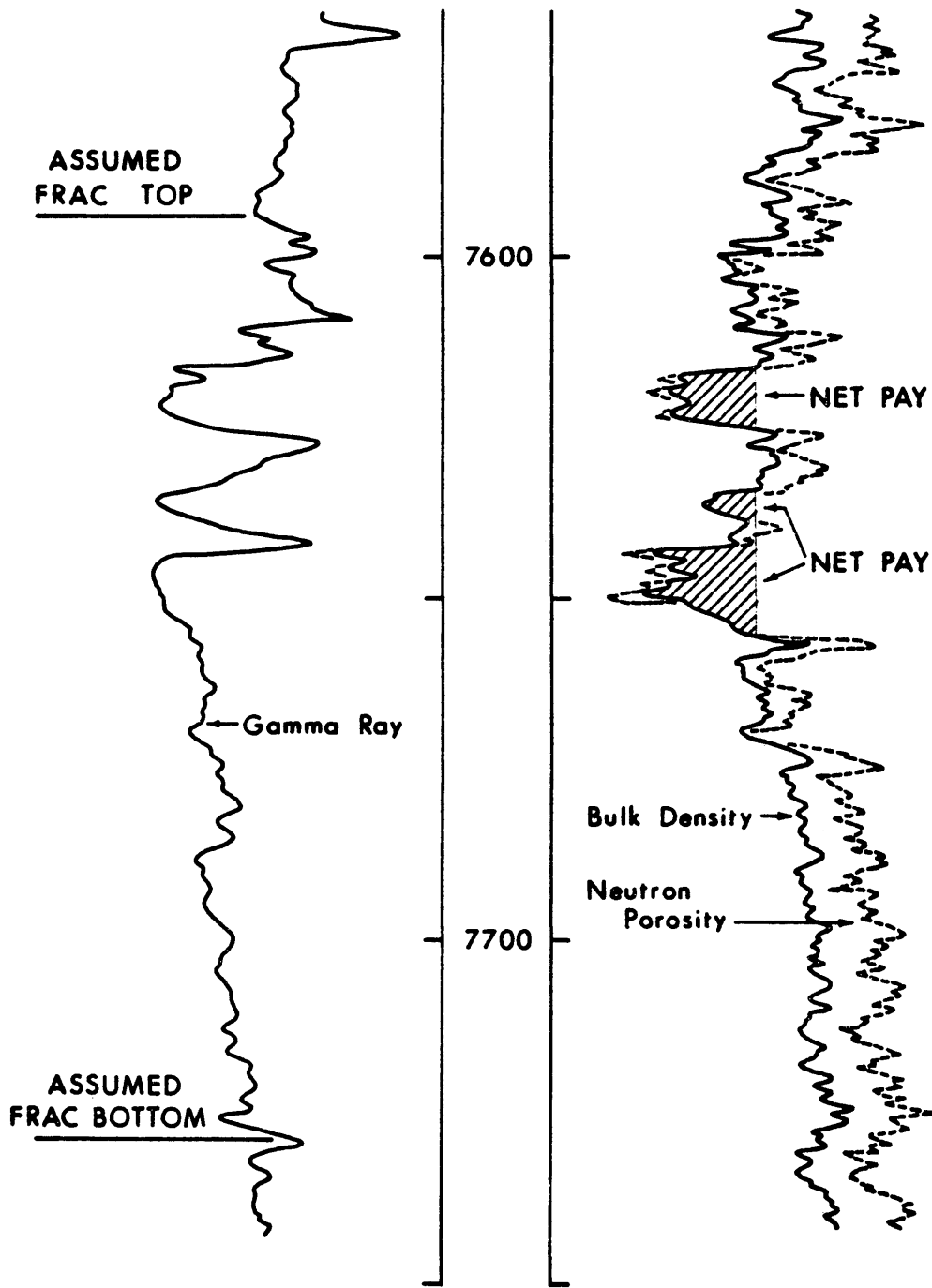


Figure 5. Example of net pay selection for well 173.

	<u>Mean</u>	<u>Standard Deviation</u> <u>Value</u>	<u>Percent of Mean</u>
Net Pay/Gross Pay	0.174	0.024	13.8
Gross Pay, feet	135	4.9	3.6

The Muddy "J" sand has been penetrated numerous times since 1949, when development of the Denver Basin began in earnest. Gas was known to be present in the Wattenberg field, but flowrates were generally too low to be measured. In 1967 a discovery in Roundup field, near Wattenberg, provided encouragement for the development of the Muddy "J" sand. The well produced 2700 MSCFD after a fracture treatment (1). Development of T2N/R65W began in 1970, and as of January 1, 1984 there were 98 Muddy "J" sand completions in this township. All wells are currently on 160-acre spacing.

#### Volumetric Calculations

Net pay counts, porosity, and water saturations of selected wells have been determined and used to construct net pay isopach and effective (hydrocarbon) porosity maps (Fig. 6 and 7). A porosity cutoff of 8% is used to select net pay counts. Net pay and effective porosity for all wells in T2N/R65W are taken from the maps presented as Figures 6 and 7. Frequency statistics of these variables are:

ER-2989

WATTENBERG FIELD  
MUDDY 'J' SAND

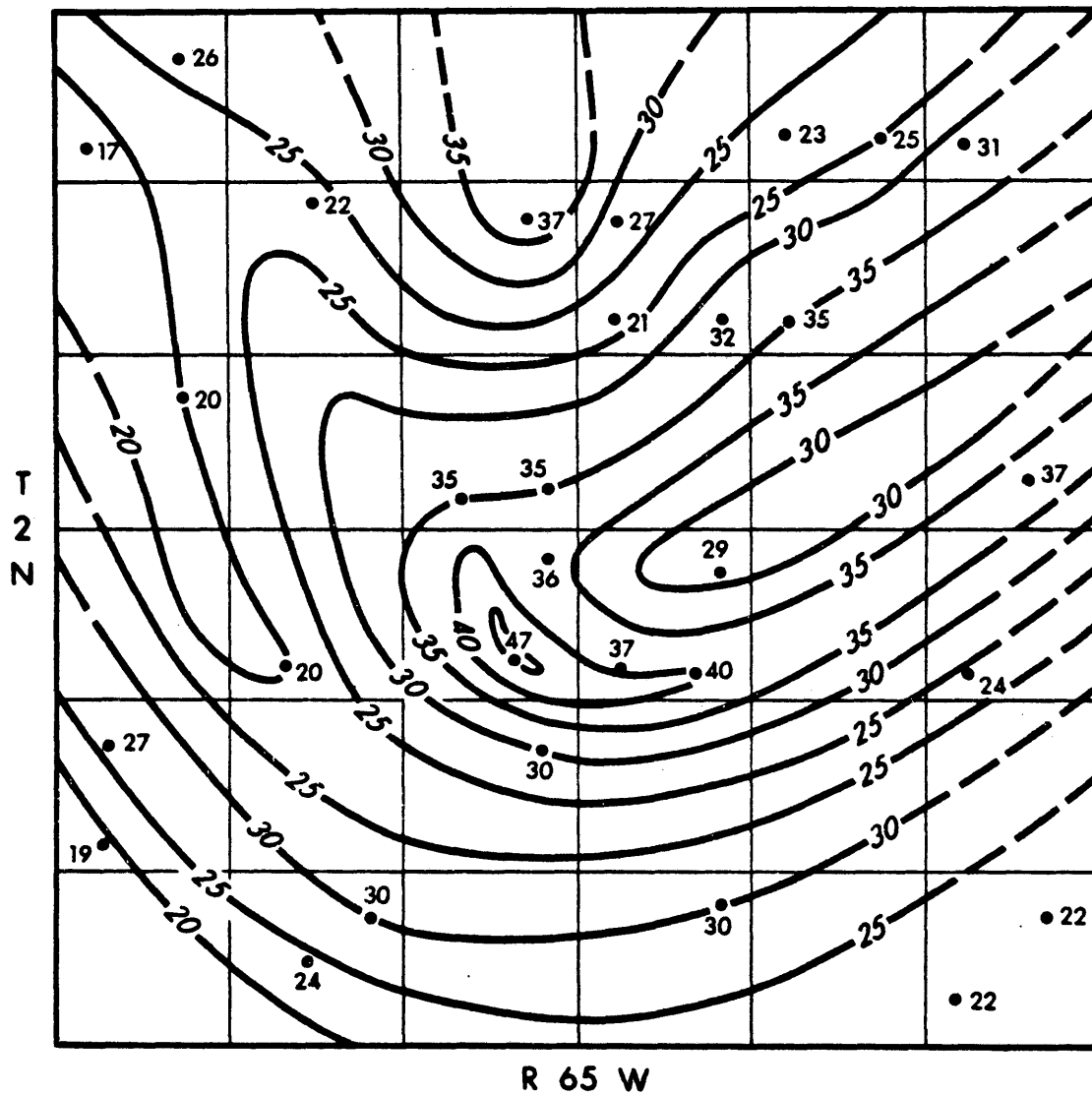


Figure 6. Net pay isopach, T2N/R65W Wattenberg.  
All values have units of feet.

WATTENBERG FIELD  
MUDDY 'J' SAND

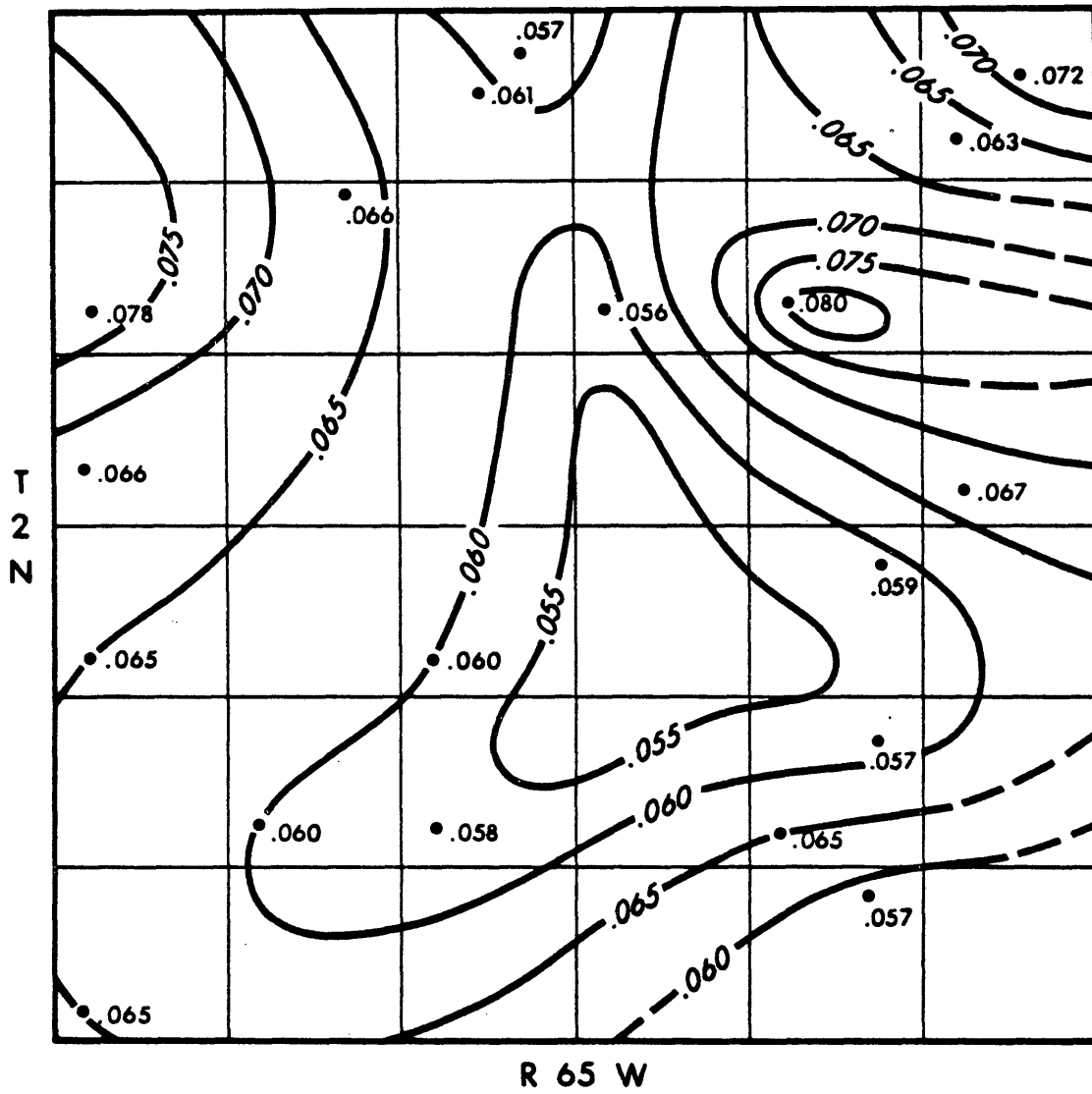


Figure 7. Gas porosity isopach, T2N/R65W, Wattenberg.

	<u>Net Pay</u> <u>(Ft.)</u>	<u>Porosity</u> <u>(%)</u>	<u>Water Sat.</u> <u>(%)</u>
Minimum	17	9.7	38
Maximum	47	14.0	55
Mean	29.1	11.8	46
Std. Deviation			
Value	5.48	0.86	3.3
% of Mean	18.8	7.2	7.2

Net pay clearly has the most variation of these three variables, as shown by statistics. No attempt is made to determine variations of initial reservoir pressure and temperature or drainage area throughout T2N/R65W. The following values are assigned to each well:

Initial Reservoir Pressure, psia	2900
Reservoir Temperature, of	260
Drainage area, acres	160

Produced gas analysis from several wells indicates that the following values are constant throughout the Township T2N/R65W:

Specific Gravity (Air=1.00)	0.70
CO <sub>2</sub> , percent	3.6
N <sub>2</sub> , percent	0.6
H <sub>2</sub> S, percent	0.0

Using these values and the Hall and Yarborough method, the Z-factor at 2900 psia is 0.927. Volumetric gas-in-place is computed using this Z factor, the values from Figures 6 and 7, reservoir pressure and temperature of 2900 psia and 260°F,

and 160-acre spacing.

There is some question within the industry as to whether calculated water saturations from the Muddy "J" truly represent water within the pore space, or reflect bound water in clays. Production from the Muddy "J" is essentially dry gas with little or no water (after fracture clean up). Calculated water saturations of 50% might suggest some water would be produced. However, references 18 and 19 report that in tight gas sands, the flowing phase is primarily gas until water saturation is greater than 50%. This is reinforced by capillary pressure data for the Muddy "J" sand which indicate irreducible water saturation is between 15 and 40 percent. For purposes of this study, the objective is to compare all wells on an equal basis and the magnitudes of volumetric parameters are of secondary importance.

The results of the volumetric calculations are as follows:

	<u>Gas-in-place*</u> <u>MMSCF</u>
Minimum	1214.06
Maximum	3066.89
Mean	1994.83

\* Per 160 acres

CALCULATION OF FRACTURE DIMENSIONS

Selection of a Fracture Model

The two fracture geometry models commonly used today are those described by Perkins-Kern-Nordgen (PKN) (20,21) and Khristianovich-Geertsma-deKlerk (KGD) (13, 22). There is no definite consensus in industry on how to decide which model is more appropriate for a particular situation. Moreover, some companies use only one model for all applications. The selection of a model is important because the PKN geometry results in fractures which are narrower and longer than the KGD model would indicate, for equivalent treatments. The width equations of PKN and KGD, respectively, are:

$$\text{PKN: } w(o,t) = 0.38926 \left[ \frac{q\mu L(1-\nu)}{G} \right]^{\frac{1}{4}} \quad [1]$$

$$\text{KGD: } w(o,t) = 0.2945 \left[ \frac{q\mu L^2(1-\nu)}{Gh} \right]^{\frac{1}{4}} \quad [2]$$

Where

$w(o,t)$  = maximum created width at the wellbore, in.

$q$  = total injection rate, bpm

$\mu$  = fracture fluid viscosity, cp

$L$  = fracture half-length, ft.

$\nu$  = Poisson's ratio

$G$  = shear modulus

$h$  = fracture height, ft.

ER-2989

The results of a detailed study of bottom-hole pressures recorded during fracture treatments are reported by Erdle et al (23). They found both PKN and KGD-type behavior in the same formation, although the authors thought that horizontal fractures may have occurred in some cases. McLeod (9) suggests that the PKN model is more suitable for most Rocky Mountain formations, where there is a long and heterogeneous transition from clean net pay to bounding shale beds. Barree (24) reports that the PKN model yields accurate results for length/height ratios greater than one, and the KGD model is accurate for length/height ratios less than one. All of the treatments examined in this report have length/height ratios greater than one, therefore the PKN model is used.

#### Determination of Fracture Height

Fracture heights are selected with the help of Amoco's considerable research on the subject. Temperature profiles run after Wattenberg frac treatments indicate fracture heights range from 100 to 180 feet (12). Height containment is generally assumed to occur after moderate growth, as the fracture penetrates the shales bounding the Muddy "J" sand (25). As noted earlier, gross sand thickness in T2N/R65W is fairly constant, with a mean value of 135 feet. Although

fracture height can be expected to be tapered away from the wellbore (26), a constant value of 135 feet is used for width and length calculations. It is recognized that calculated fracture lengths presented in this report may be considerably different from those reported by others. However, the main objective is to compare all wells in this study on an equal basis.

#### Selection of Fluid Properties

Characterization of fracture fluids used in the treatments proved to be difficult. The McLeod calculation method inherently assumes that fluid properties remain constant for the entire job, in conflict with the temperature and/or time-dependent nature of most fracture fluids. Initially, an average fluid temperature of 150°F was used, based on a service company graph. Pump time for most jobs was four hours. An average exposure time of two hours for the entire fluid volume was used.

One reason polymer emulsion (PE) fluids were used extensively in the mid-1970's was due to their low fluid loss coefficients (FLC), compared to simple gelled water systems (2). Nolte reports an FLC of  $0.00053 \text{ ft}/(\text{min})^{\frac{1}{2}}$  calculated from a mini-frac test using a polymer emulsion fluid in the Muddy "J" sand of the Wattenberg field

ER-2989

(27). He states that the FLC should be similar for treatments of a given zone for similar fluids. Since virtually all of the polymer emulsion fluids used in T2N/R65W are based on the system licensed by Exxon Production Research, FLC values are fairly uniform. Data presented by Halliburton and Western for  $n'$  and  $K'$  of polymer emulsion (50 lb/gal gel) agrees very closely and is used in this report.

The water-base cross-linked gels (CLG) developed in the late 1970's are much more difficult to characterize than the polymer emulsion fluids for three reasons:

- 1) each service company appears to have independently developed their own crosslinked gel;
- 2) the rheology of CLG's is much more time-dependent than for polymer emulsions; and
- 3) non-standard testing of fluid.

Values for  $n'$ ,  $K'$ , and FLC of each fluid used are selected from service company data, based on an average temperature of 150°F and one-half the total pump time (typically four hours). The Western Company literature indicates that FLC of cross-linked gels is reduced by a factor of 10 with the addition of 5% hydrocarbon (HC). Other references (25,28,29,30,31) cite FLC reductions of 30 to 90 percent with the addition of 5% HC. Nolte (27) reports a mini-frac calculated FLC of  $0.00076 \text{ ft}/(\text{min})^{\frac{1}{2}}$  for a cross-linked gel with 5% HC in the Muddy "J" sand. This compares to a minimum

FLC of .0022 for cross-linked gels without hydrocarbon. Western considers the difference in FLC significant enough to use different names for their cross-linked gels with and without 5% HC. The cross-linked gel treatments performed by Halliburton and Dowell are assumed to contain no hydrocarbon, unless the treatment report specifically notes that hydrocarbon was used. A total of 14 treatments contained no hydrocarbon.

The selection of FLC is important because of its impact on fluid efficiency, and thus fracture length. Fluid efficiency has been reported to decrease from 90% to 30% when FLC is increased from 0.0001 to 0.001(31).

#### Modification of the McLeod Method

With all the necessary fluid properties determined, the McLeod method was used to determine fracture dimensions. The initial computation indicated that more than 25 wells had longer propped lengths than created lengths. The initial effort to correct this problem was directed at refining fracture fluid  $n'$ ,  $K'$ , and FLC values. Halliburton supplied a fluid temperature profile that indicated the average temperature during a typical job is closer to 200°F, and this value is used for the results of this report. Halliburton also provided computer-generated fluid rheology properties for the treatments encountered in this study. The revised fluid

property data resulted in a reduction of incorrect propped/created length ratios, but not an elimination of ratios over 1.0. Most of the ratios over 1.0 were for jobs without hydrocarbon in the treatment fluid, and thus higher fluid loss coefficients and lower fluid efficiencies.

The source of the error in the propped/created length ratio is considered to be in the assumptions used to compute propped fracture width, as proposed by McLeod. Although not specifically stated, McLeod apparently assumes there is no fluid loss, as indicated by his statement that this method is applicable for fracture fluids with a FLC of 0.001 or less. Indeed, the propped/created length ratio using the McLeod method is greater than one for all jobs with a FLC greater than 0.0010. The equations, used to derive the propped width equation can be stated as follows:

$$V_{si} = V_{fc} \quad [3]$$

where  $V_{si}$  = volume of slurry injected  
 $V_{fc}$  = volume of created fracture

and,

$$V_{pi} = V_{fp}(1-\phi_f) \quad [4]$$

where  $V_{pi}$  = volume of proppant injected  
 $V_{fp}$  = volume of propped fracture

$\phi_f$  = in-situ porosity of proppant in fracture

Combining these two equations results in McLeod's equation for propped width (see Appendix A). The equation for propped length follows from the volumetric relationship of height (h), width ( $w_p$ ) and length ( $L_p$ ).

Details of the modified McLeod method used in this report are presented in Appendix B. There are three basic modifications used in an attempt to improve the McLeod method:

- 1) the propped width equation is derived using the entire fluid volume and calculated fluid efficiency;
- 2) the average created width is determined by integrating the analytical expressions of width, over the height and length; and
- 3) frac fluid viscosity is corrected for proppant volume, using the chart of Perkins and Kern (20).

Fluid efficiency is defined here as the ratio of fracture volume created by slurry to the volume of slurry pumped. The fluid efficiency of the slurry is calculated using the following equations:

$$E_f = V_{ct}/V_{li} \quad [5]$$

$$V_{cs} = (E_f V_{li} + V_p) - E_f V_{pi} \quad [6]$$

where

$E_f$  = overall frac fluid efficiency

$V_{ct}$  = volume of fracture created by slurry + pad

$V_{li}$  = total volume of liquid injected

$V_{cs}$  = volume of fracture created by slurry

ER-2989

$V_p$  = total volume of proppant

$V_{pi}$  = volume of pad injected during job

The slurry fluid efficiency is then,

$$E_s = V_{cs}/V_{si} \quad [7]$$

where  $V_{si}$  = volume of liquid and proppant in slurry

The fluid efficiency of the pad fluid will generally be lower than the overall fluid efficiency. However, the pad volume is usually a small percentage of the total volume injected, so the error in Equation 6 is not significant.

The average sand concentration in the slurry is used here, rather than the final sand concentration used by McLeod. The propped fracture shape is implicitly assumed to be similar to the created fracture shape, with a corresponding variation in areal sand concentration. Thus, the vertical cross-section of the propped fracture has the shape of an ellipse (viewed from the wellbore) for a PKN-type model, as used here. Complete mixing of fluid and proppant is assumed for "pillar fracture" treatments, with the result of lower average sand concentrations than conventional jobs with equivalent fluid volumes. Reasons for using this assumption are presented in the discussion of the "pillar fracture" technique.

As previously noted, the McLeod method assumes a perfect-

transport fracturing fluid, i.e. no proppant settling occurs. It can be argued that polymer emulsion fluids do not meet this criteria, in spite of their high apparent viscosity. Kasperit (32) notes that fluids may have a high viscosity without being a perfect transport fluid. However, polymer emulsions are considered to behave as a perfect transport fluid for this report.

The following values of rock properties are used for all fracture dimension calculations:

Young's modulus, psi	5.0 E6
Poisson's ratio	0.25
Permeability, md	0.01

Constant values are used due to a lack of definitive data for individual wells. It is recognized that reservoir permeability may vary from well to well, but the effect of these variations on well performance is not addressed in this report.

Fracture conductivities are determined from charts such as that shown in Figure 8, for a given areal proppant concentration, and a closure stress of 4000 psi. Dimensionless fracture conductivities are calculated as follows:

$$F_{cd} = (k_f w_f) / (k_R L_f) \quad [8]$$

where  $F_{cd}$  = dimensionless fracture conductivity  
 $(k_f w_f)$  = fracture conductivity, md-ft

$k_R$  = reservoir permeability, md

$L_f$  = fracture length, ft

A summary of fracture treatments included in this report is presented in Table 3. Table 4 presents a summary of fracture dimensions calculated with the modified McLeod method. The fracture treatment data and dimensions of the individual wells are presented in Appendix C.

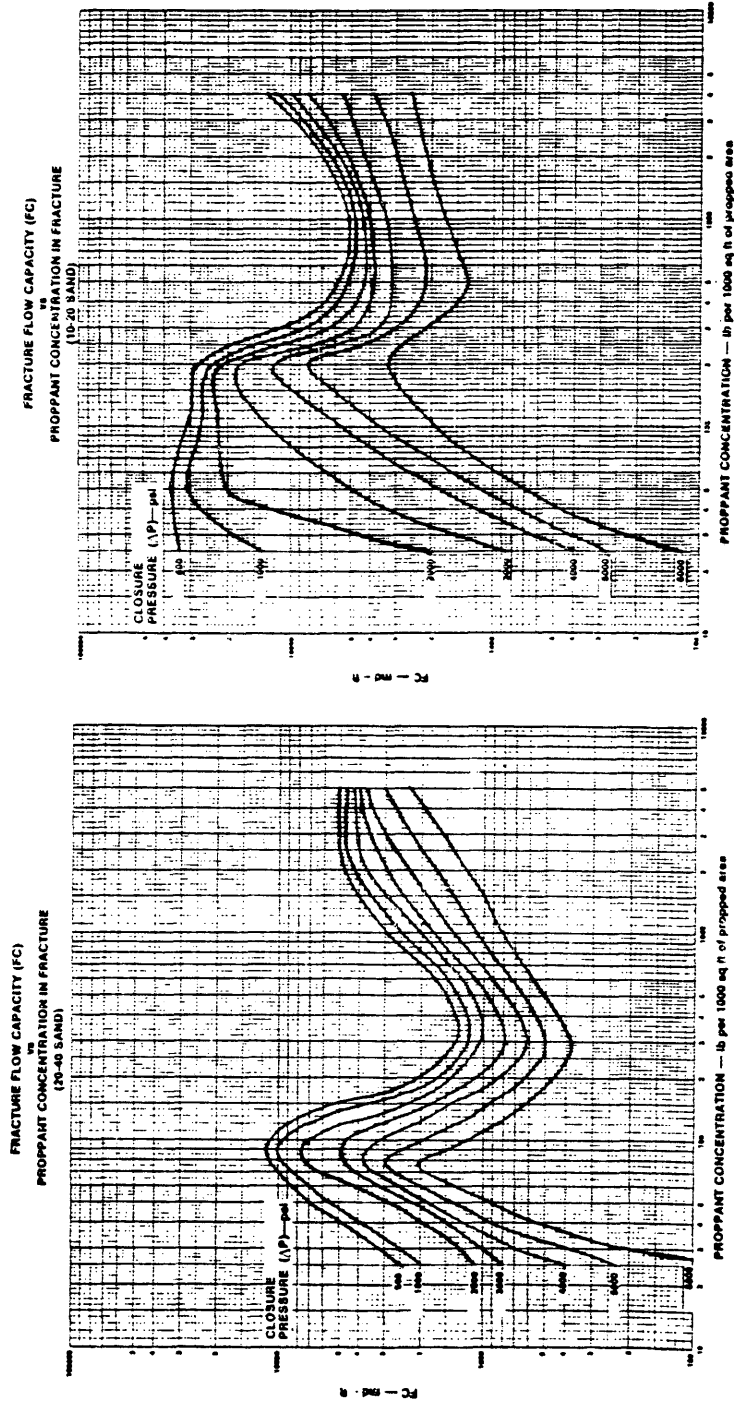


Figure 8. Fracture conductivity vs. areal and concentration, for 10-20 and 20-40 sand.

Table 3

	<u>Number</u>			
Initial fracture treatment	71			
Treatment fluid types				
Polymer emulsion	29			
Cross-linked gel	37			
Other	5			
Proppant schedules				
Conventional packed fracture	38			
Pillar-fracture	33			
Fluid-loss coefficients				
Less than .001	60			
Greater than .001	11			
<u>Treatment sizes</u>	<u>Min.</u>	<u>Max.</u>	<u>Mean</u>	<u>Std. Dev.</u>
Frac Fluid volume, M gal	30	316	182.8	73.0
Pad volume, 1000 gal	5	83	27.9	13.4
Proppant weight, M lb	28	971	560.1	255.6
Max. prop. concen., lb/gal	1.0	9.0	5.6	1.64
Avg. prop. concen., lb/gal	0.9	6.2	3.1	1.44

Table 3. Summary of fracture treatments from T2N/R65W which are included in this report.

ER-2989

Table 4

	<u>Min.</u>	<u>Max.</u>	<u>Mean</u>
Apparent visc., cp	2.1	1315	393
Fluid loss coeff., ft/(min) <sup>1/2</sup>	.00028	.00281	.00061
Fluid efficiency, %	9.1	80.1	59.3
<u>Fracture Widths</u>			
Maximum created, in	0.101	0.811	0.545
Avg. propped*, in	0.026	0.153	0.092
<u>Fracture Lengths</u>			
Created, ft (CL)	397	3857	2325
Propped*, ft (PL)	412	3400	2299
PL/CL*	.751	.994	.9429
<u>Calculated Fracture Conductivities</u>			
F <sub>c</sub> <sup>*</sup> , md-ft	337	4694	1452
F <sub>cd</sub> <sup>*</sup> , dimensionless	17	720	90.9

\* Excluding 11 wells with Propped Length/Created Length ratios greater than 1.

Table 4. Summary of calculated fracture dimensions for treatments included in this report.

DETERMINATION OF PERFORMANCE  
INDICATORS

Historical production data for all but two wells in T2N/R65W has been provided by Panhandle Eastern Pipeline Co. The data for each well consists of monthly gas production in MSCF, average line pressure in PSIG, number of days on line during the month, and average daily rate for the month in MSCFPD. The time span of the data is from late 1974 through November, 1983. Although several wells were drilled prior to 1974, production was apparently delayed due to the lack of a collection system. There were no significant production restrictions prior to 1984.

Production streams for all wells are converted to a common basis by calculating yearly cumulative production from the start of the first month of production. Cumulative recoveries are determined using the volumetric gas-in-place calculated for each well. Average daily rates for the first year are calculated by dividing the first year cumulative production by the number of producing days.

Economic evaluations of all wells are normalized to a common time frame. That is, all treatment costs are calculated using current (1984) costs, one gas price is used for all cases, and all production streams are treated as if they had begun at the same time. Refracturing treatments

are not included in any performance comparisons due to the uncertainty of depletion at the time of refracturing. Net present values (NPV), and undiscounted profit/investment ratios (PI) are calculated using the normalized data. Drilling costs are considered sunk costs for this report, and are not included in any economic calculations. The economic variables used are summarized in Table 5.

The summation of four components is used to determine a fracture treatment cost for each well:

- 1) fixed set-up cost;
- 2) volume of fluid used;
- 3) total proppant weight;
- 4) hydraulic horsepower.

Fluid costs are broken down to include water-base gel, hydrocarbon, and methanol. All proppant weights are assigned one cost, and hydraulic horsepower is calculated from average treating rates and pressures during the job.

An operating cost and gas price of \$1100/mo. and \$2.35/MSCF, respectively, are used, based on an average of values reported by two operators. Advalorem and severance taxes of 10% and 5%, respectively, are the best estimates of current rates. All costs and gas prices are unescalated, and mid-year discounting with a 10% rate is used. The revenue interest is assumed to be 80%, and working interest 100%. Profit/investment ratios are undiscounted. Details of the

Table 5

Fracture Treatment Costs

Fixed set-up cost, \$	15,000
Cross-linked gel, \$/gal	0.35
Hydrocarbon, \$/bbl	28
Methanol, \$/gal	1.00
Proppant, \$/100 lb	6.65
Hydraulic Horsepower, \$/hhp	3.55

Operating Costs

Direct operating cost, \$/well-mo	1100
Severance tax, % of revenues	10
Advalorem tax, % of revenues	5
Gas price, \$/MSCF	2.35
Net revenue interest, %	80
Working interest, %	100
Discount factor, %	10

Table 5. Parameters used in economic calculations.

economic calculation procedure are presented in Appendix D.

A 1022 Data Base Management System on the Colorado School of Mines DEC-10 computer is used to store the data assembled for this study. The wells in T2N/R65W have been assigned a number, beginning with 101. Several data sets are included in the data base, and well numbers are used to cross-reference data as required. The data base allows data to be assembled with virtually any desired parameters. Further details of the data base are presented in Appendix E, for reference by future researchers.

THE EFFECT OF VOLUMETRIC PARAMETERS  
AND FRACTURE LENGTH ON WELL PERFORMANCE

Several combinations of fracture treatment sizes, fluid systems, proppant sizes, and proppant scheduling have been tried in the development of the Wattenberg field. The data collected for this study is used to subjectively evaluate the effectiveness of the fracture treatments performed in T2N/R65W. A large number of cases is used in an effort to provide a significant sample of data points and account for the numerous parameters which affect well performance.

The comparison method employed is to cross-plot all significant combinations of variables to determine first-order or second-order polynomial best-fit curves. In this type of analysis, the researcher must generally have some idea of cause-and-effect relationships in order to decide how to combine variables for cross-plots and to evaluate the results. Thus, the analysis is at least somewhat subjective.

Again, the reader is reminded that the results presented in this report are not intended to represent absolute magnitudes of actual economic performance, nor predict future performance for specific fracture treatments. As will be shown, in most cases, there is too much data scatter to use these results for forecasts. Moreover, all comparisons are bi-variate, considering only two variables.

### First-Order versus Second-Order Polynomial Best-Fit Curves

A first-order polynomial best-fit curve is, by definition, a straight line, and can be used on virtually any data set. The strength of the linear relationship between two variables is indicated by the squared correlation coefficient ( $R^2$ ), with 1.0 being a perfect linear fit and 0.0 being a complete lack of fit. A "perfect" fit means all data points lie on the fitted straight line. However,  $R^2$  is not a measure of the validity of the straight-line model.

The analysis of a second-order polynomial best-fit curve is slightly more complex. There are three possibilities for such a curve: concave downward, straight line, and concave upward. Furthermore, a concentration of points over a narrow range on the x-axis can strongly influence the location of the apex and the magnitude of its curvature. Two steps are taken to help produce realistic curve fits:

1. where appropriate, the curve is forced through zero by plotting 50 points at the origin;
2. the curve is terminated at or before the maximum available x-value.

Wattenberg wells typically produce little or no gas without fracture treatments, so that all performance indicators are assumed to be zero for zero fracture length. In spite of these two steps, the validity of second-order curves can be questionable if data scatter is significant. Moreover, some curves must be neglected due to obviously false con-

ER-2989

clusions, while others are at least logically plausible. For example, a curve of average daily rate versus propped fracture length which is concave downward can be extrapolated to a producing rate of zero for a large fracture length. Interpretation of second-order curves is much more subjective than for first-order curves. Their use is limited to the analysis of performance versus fracture length in this report. First-order curves are used when comparing fluid types and proppant schedules.

#### The Validity of the Modified McLeod Method

Propped fracture length is an important component in the evaluation of hydraulic fracture treatments. It is important to establish the validity of the modified McLeod method used to calculate propped fracture lengths in order to give credibility to the comparisons presented. The equations for created length, created width and average fluid viscosity are accepted and routinely used in industry. Assuming that fluid properties have been selected correctly, created fracture widths and lengths are reasonable.

Dimensions of several hypothetical fracture designs have been computed to compare created and propped fracture lengths. The results presented in Table 6 are for a typical cross-linked gel treatment fluid with various job sizes. Harp (4) reports calculated fracture lengths for actual jobs

Table 6

Source	Fluid (M gal)	Proppant (M lb)	Created Length (ft)	Propped Length (ft)	PL/CL*
Modified McLeod	50	150	1081	955	0.883
	100	300	1564	1380	0.882
	150	450	2066	1837	0.889
	200	600	2513	2360	0.939
	250	750	2923	2836	0.970
	300	900	3304	3278	0.992
<hr/>					
Harp (4)	618	1250	5398	5067	0.939
	316	735	3423	3232	0.944
	180	672	2672	2515	0.941

\* Propped length/created length ratio

Table 6. Comparisons of hydraulic and propped fracture lengths of modified McLeod method and results of Harp (4), with cross-linked gel.

in the Wattenberg field, also shown in Table 6. He does not report details of fluid rheology or the model used to calculate dimensions. The relationship of propped to created fracture length is entirely linear in Harp's work, with an  $R^2$  value of 1.000. The modified McLeod method also predicts that this relationship is virtually linear. Using the hypothetical data, the  $R^2$  value is 0.997 for six treatment sizes, as shown in Figure 9.

Roberts (5) reports calculated fracture lengths for 3 hypothetical Wattenberg fracture designs using cross-linked gels and a fracture height of 120 ft. Again, no details of fluid rheology or the fracture model are given. Results from the modified McLeod method, using an assumed fluid rheology, are compared to those of Roberts:

<u>Treatment Size</u>		<u>Propped Length, ft.</u>	
<u>M gal.</u>	<u>M lb.</u>	<u>Roberts (5)</u>	<u>this report</u>
183	832	3900	3115
315	735	4800	3757
370	1250	10000	6197

The results of fracture dimension calculations from 76 treatments in T2N/R65W indicate 11 propped/created length ratios greater than 1.0, using the modified McLeod method. Nine of these 11 have apparent fracture fluid viscosities less than 55 cp, which would suggest they didn't behave as

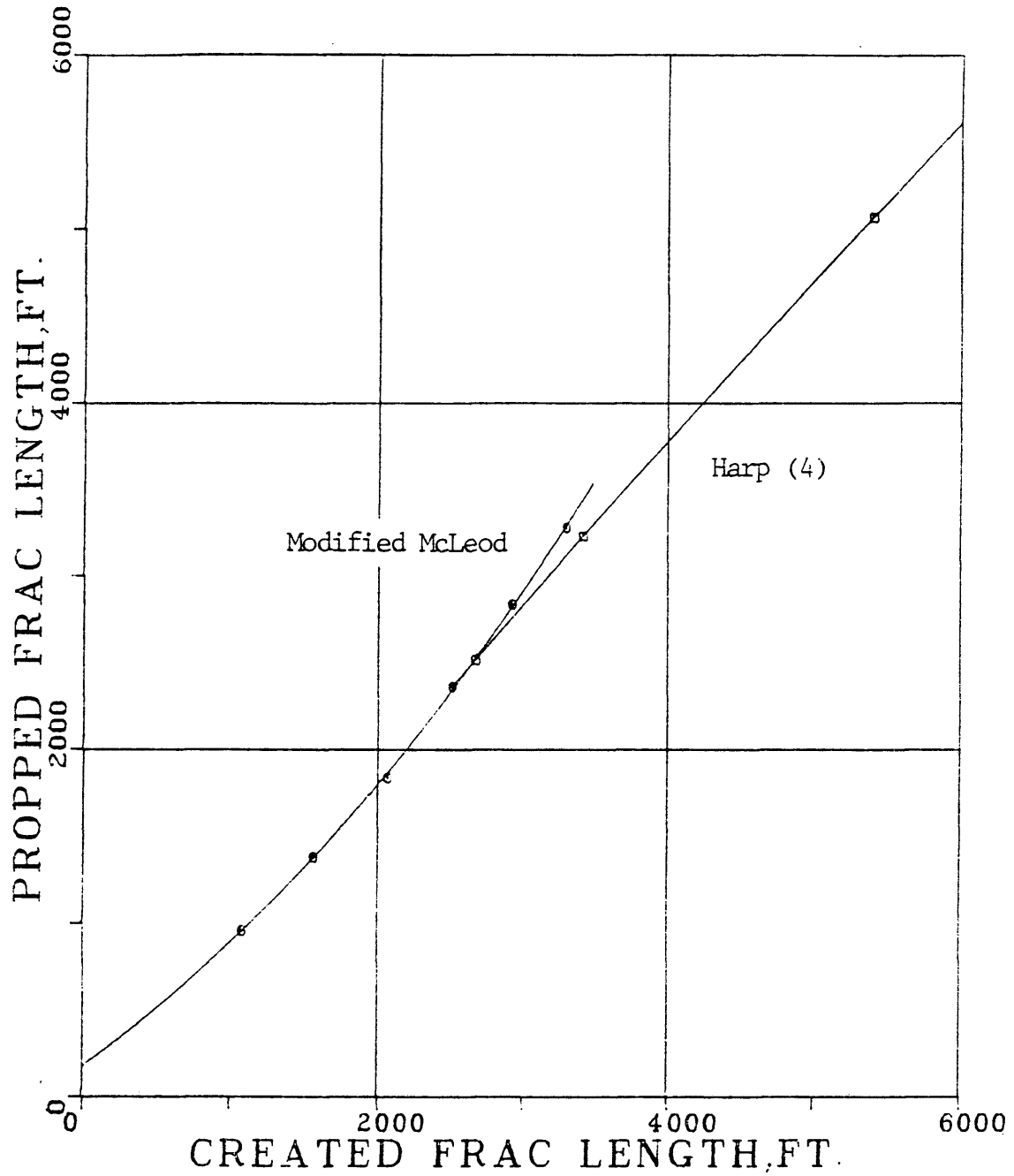


Figure 9. Propped vs. created fracture length for a hypothetical Wattenberg fracture design. Second order best-fit curves.

perfect transport fluids. Another treatment contained 21 tons CO<sub>2</sub>, which could have altered fluid rheology and/or fluid loss behavior. Finally, one of the 11 wells sanded-out at the end of the job. The calculated propped/created length ratio of 1.008 for this job would predict a sand-out, so this result strongly supports the validity of the modified McLeod method.

Figure 10 presents propped fracture length versus created fracture length for 71 fracture treatments in T2N/R65W.

#### The Effect of Net Pay and Porosity of Performance

The effect of net pay and porosity on well performance is investigated in Figures 11 and 12. Both plots indicate that there is virtually no correlation between initial producing rates and net pay or hydrocarbon (gas) porosity. There is a narrow concentration of points on the x-axis of both plots, yet a wide variation on the y-axis. The frequency statistics for the average daily rate during the first year are as follows:

Minimum, MSCFD	47
Maximum, MSCFD	817
Mean, MSCFD	382
Standard Deviation	
Value	169
% of Mean	44

Figures 11 and 12 clearly show that there is virtually no correlation between net pay and initial rates or porosity

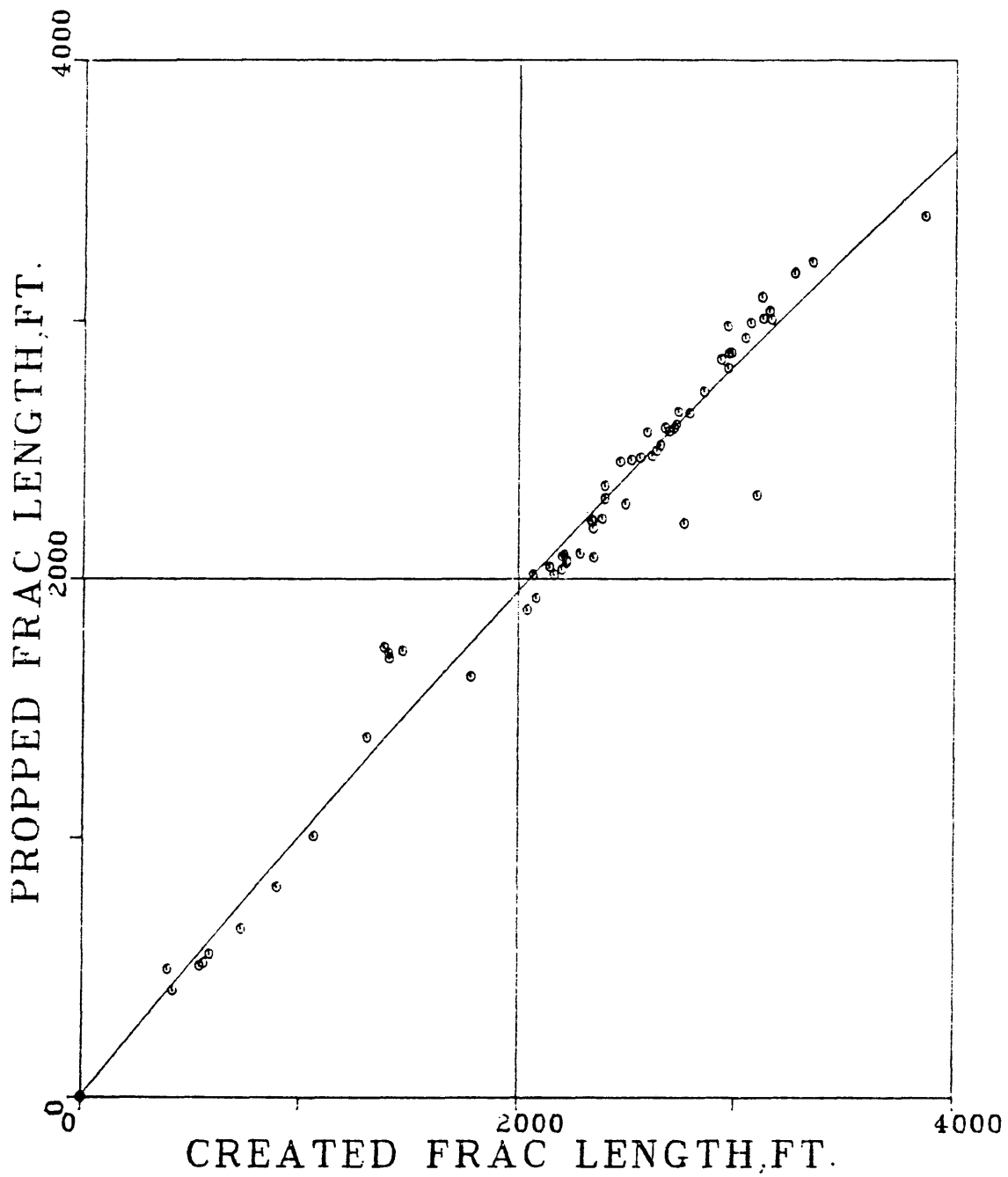


Figure 10. Propped vs. created fracture length for fracture treatments studied in this report.

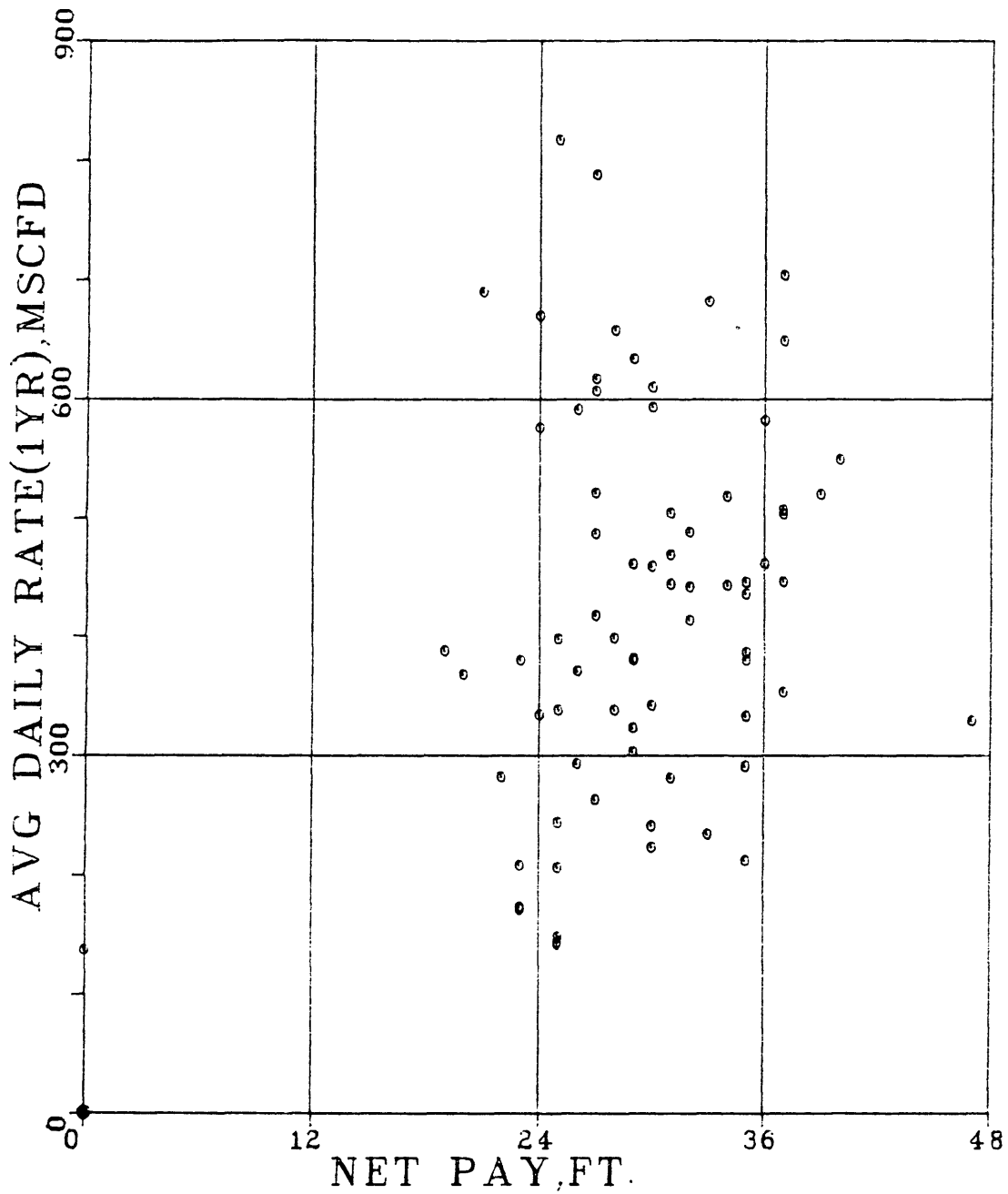


Figure 11. Average daily rate (first year) vs. net pay.

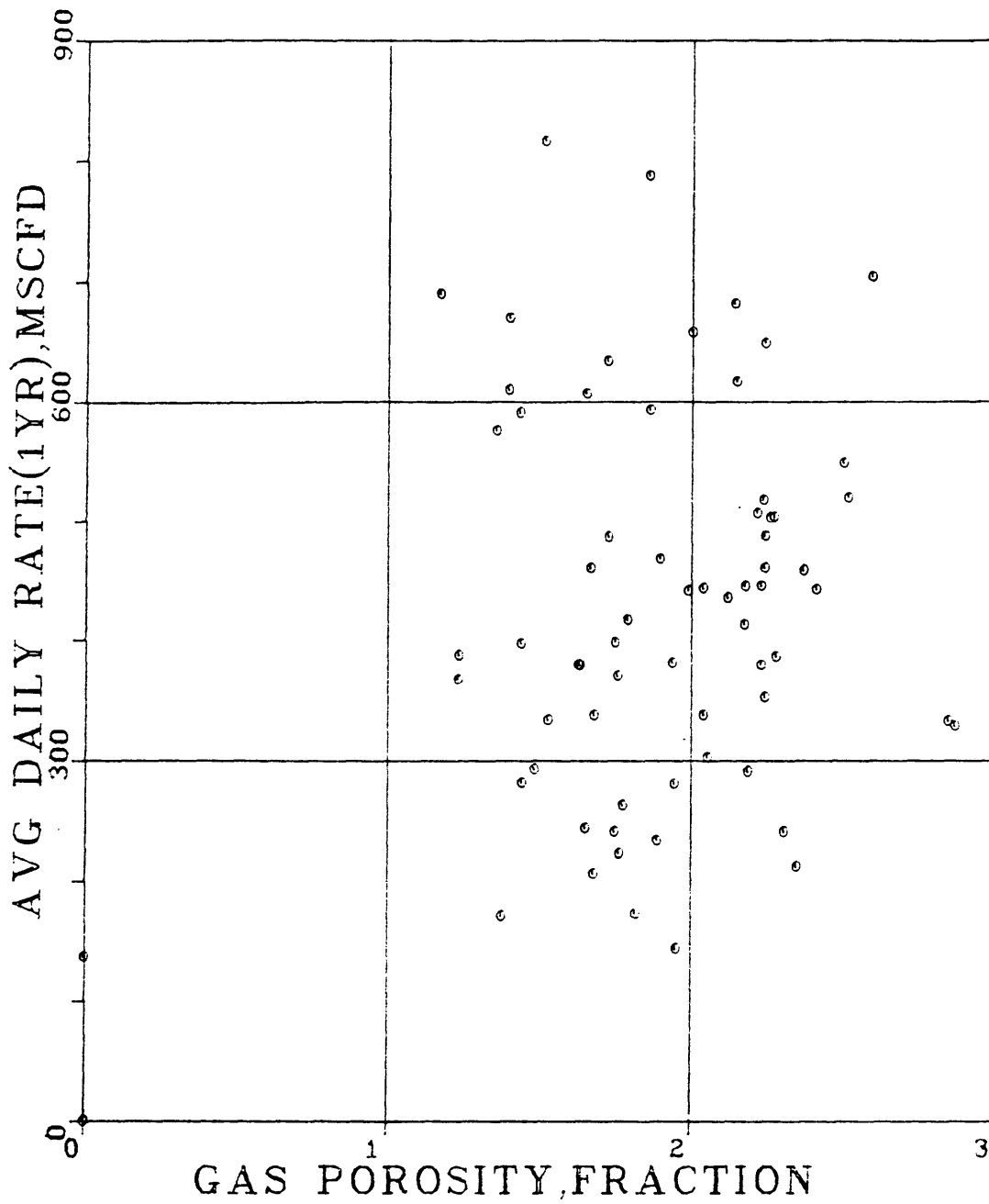


Figure 12. Average daily rate (first year) vs. hydrocarbon gas porosity.

and initial rates. No attempt is made in this report to account for the effect of permeability variations on performance.

### The Effect of Fracture Length on Well Performance

Well performance indicators are grouped in short term (two year), and long term (eight year) categories. The long term data offers the advantage of being fairly homogeneous, as all early jobs were done with polymer emulsion. The short term data provides a larger sample for comparison of different fluid systems.

Figures 13, 14, 15, and 16 show that there is virtually no correlation of performance and propped fracture length for propped lengths greater than 2000 feet. The plot of cumulative recovery is slightly concave upward, due to 3 wells (126, 141, 175) with eight-year recoveries of better than 35%, and concentrated between 2800 and 3000 feet fracture length. The cumulative production of these 3 wells is also above average (Fig. 14). The wells are not close to each other, and there are no significant differences in their fracture treatments to explain their superior performance, compared to the other wells in T2N/R65W. Apparently, there are other factors besides fracture treatment design and volumetric parameters which have improved their performance.

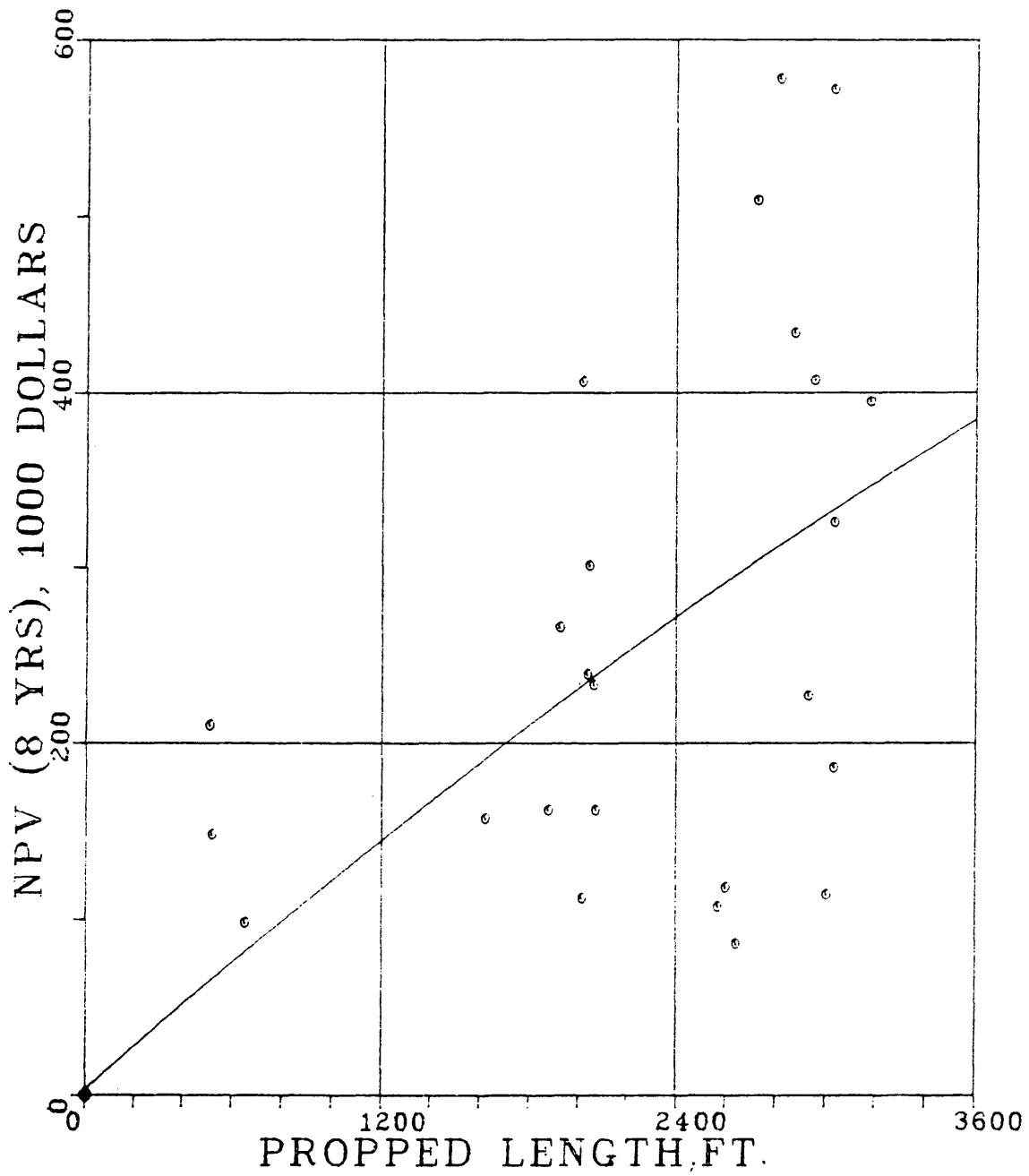


Figure 13. Eight-year net present value vs. propped fracture length. Second order best-fit curve.

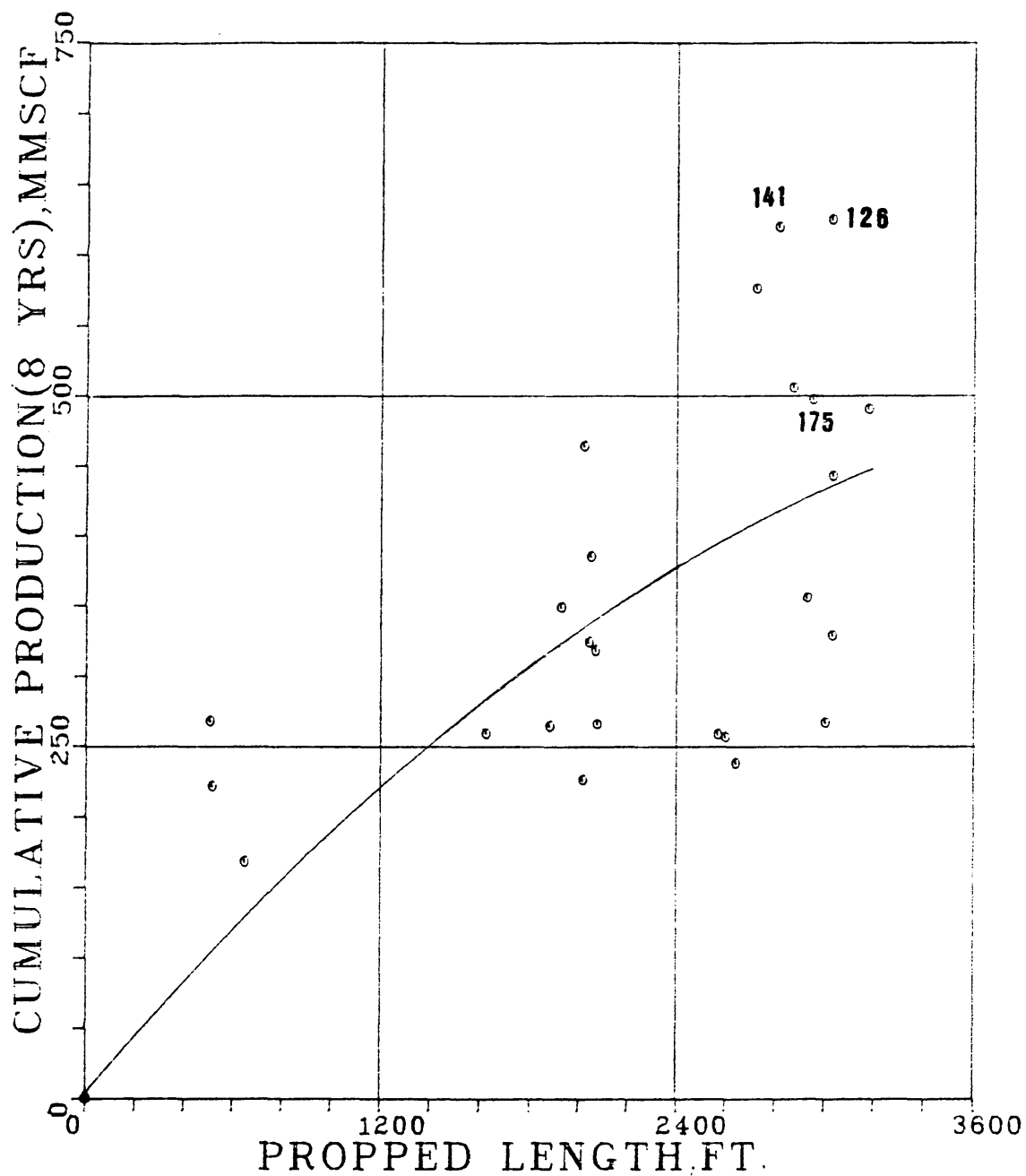


Figure 14. Eight-year cumulative production vs. propped fracture length. Second order best-fit curve.

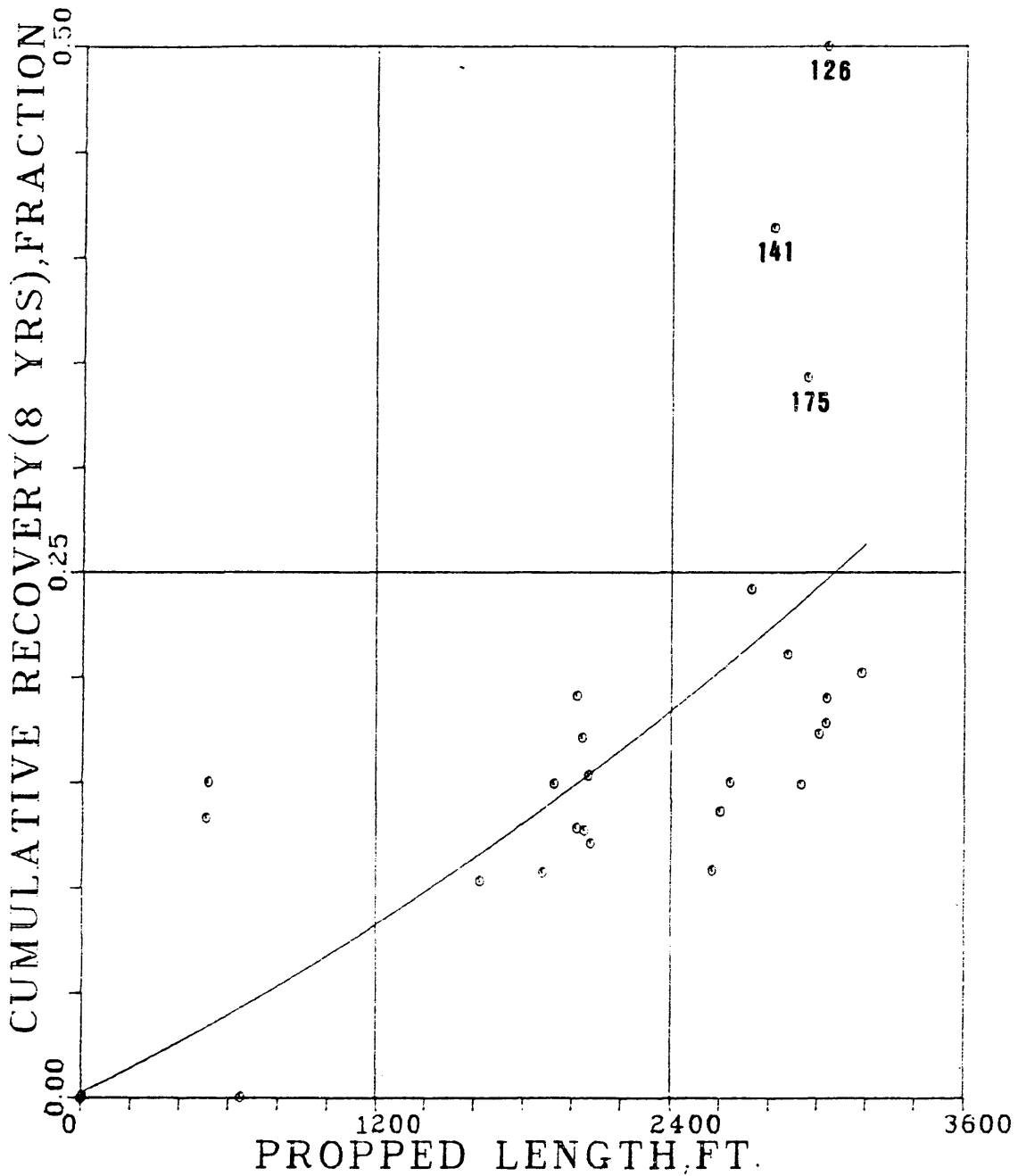


Figure 15. Eight-year cumulative recovery vs. propped fracture length. Second order best-fit curve.

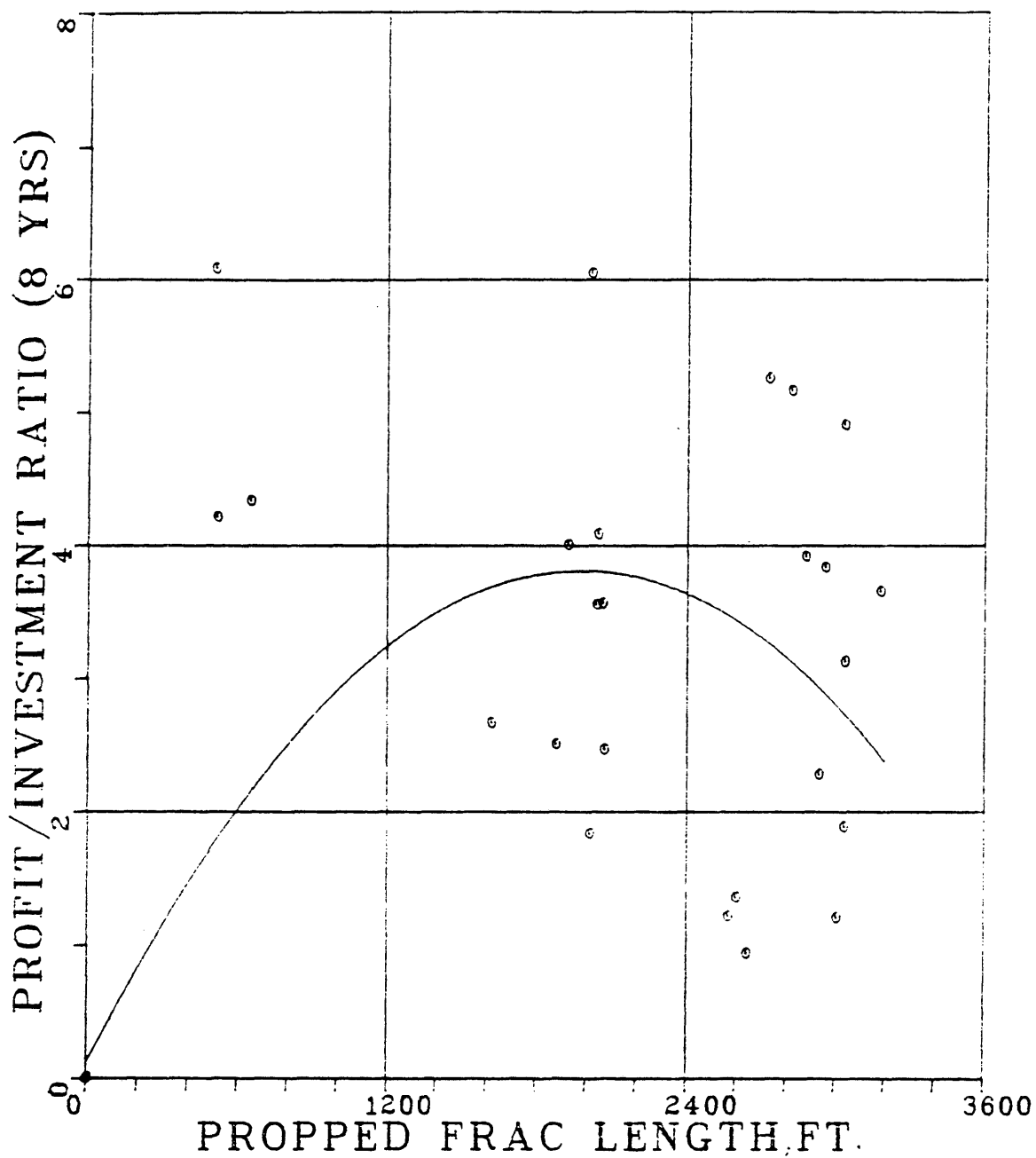


Figure 16. Undiscounted P/I (8 Years) vs. propped fracture length. Second order best-fit curve.

One possible explanation for the performance of wells 126, 141, and 175 is that they were drilled and completed after the pipeline system was in operation. Thus, they were on production immediately after completion. Other wells had to wait months or even years before they could be produced into the gathering system. As Crafton and Wilderson (32) suggest, it is quite likely that wells which are able to clean up immediately following their fracture treatments may restore relative gas permeability more quickly than those wells which lay dormant for several months. The shut-in wells may have suffered permanent formation damage from fracturing fluids. Moreover, if these shut-in wells had large fracture treatments, the effective/propped fracture length ratios would be low.

Figure 16 indicates that the optimum propped fracture length is approximately 2000 feet, based on undiscounted profit/investment ratio. This result contradicts Figure 13, which shows eight-year net present values increasing up to at least 3000 feet of propped length. The discrepancy may be due to discounting. Figure 17 shows that initial producing rates are much higher for those wells with propped lengths greater than 2400 feet. After the first year, the longer fracture lengths produce only slightly more than the medium-length (1500 to 2200 feet) fractures.

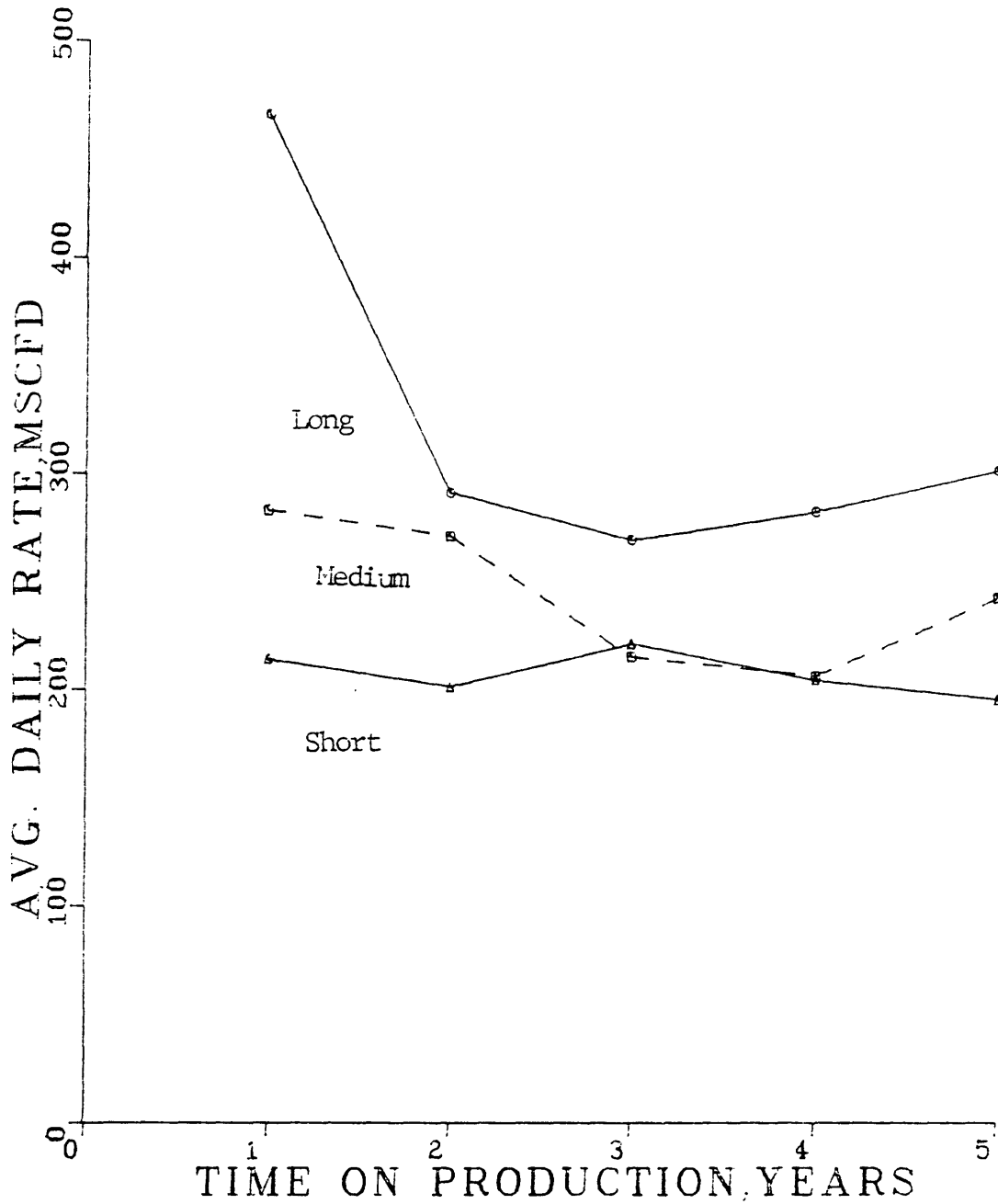


Figure 17. Average daily producing rates for wells with short (0 to 800 ft), medium (1500 to 2200 ft) and long (2400 to 3600 ft) fracture lengths.

Recall that this discussion pertains to polymer emulsion jobs only.

Figures 18 and 19 present two-year net present values and profit/investment ratios, respectively, plotted against fracture length. This data contains all wells with two or more years of production history, and thus includes various combinations of fluid types, proppant scheduling, and fluid loss characteristics. Figure 18 provides no clear indication of optimum fracture length. However, note that the range of net present value increases as fracture length increases, and many wells with fracture lengths over 2000 feet would fail to pay for fracture treatment costs after two years.

The conclusion to be drawn is that while longer fracture lengths may increase net present value, they also present substantially greater risk. Figure 19 verifies this conclusion. It indicates that the optimum propped fracture length occurs at 1400 to 1800 feet, based on undiscounted profit-investment ratios. Values of zero profit-investment ratio are for those wells with a negative two-year net present value.

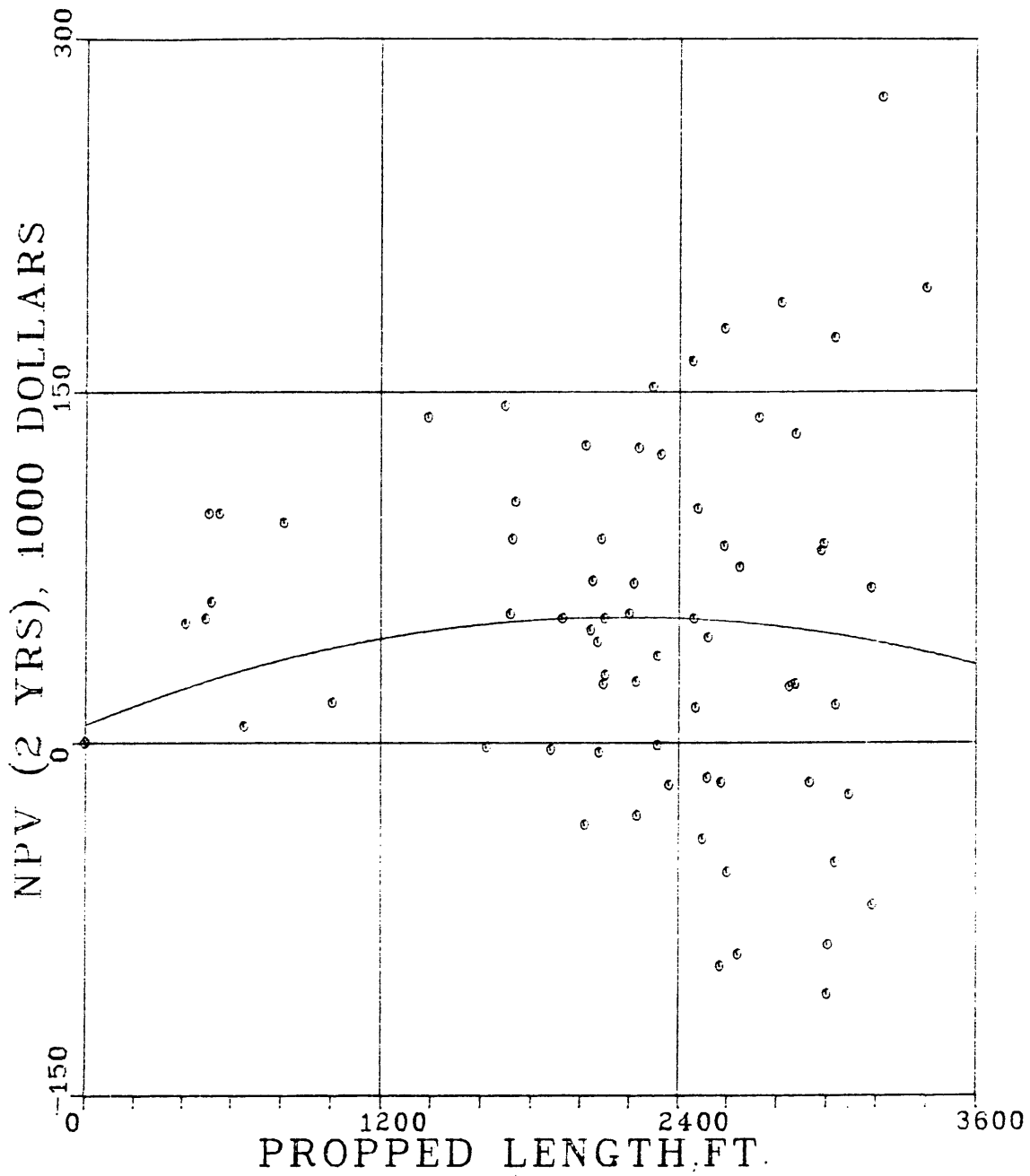


Figure 18. Two-year net present value vs. propped fracture length. Second order best-fit curve.

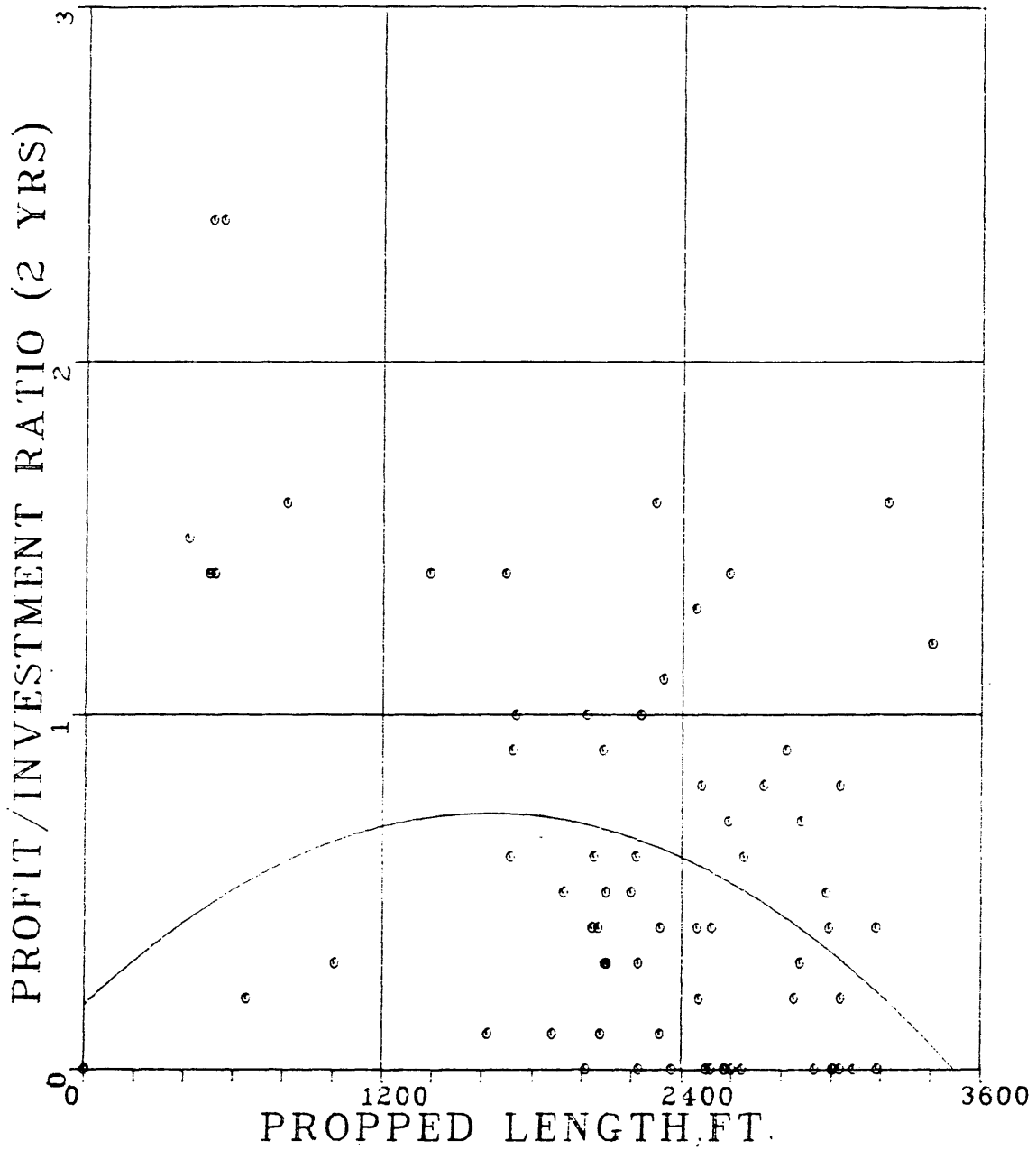


Figure 19. Two-year profit/investment ratio vs. propped fracture length. Second order best-fit curve.

COMPARISONS OF FLUID SYSTEMS AND  
PROPPANT SCHEDULES

The data collected for this study provides an excellent opportunity to compare the following treatments:

Polymer emulsions and cross-linked gels  
Packed fractures and pillar fractures  
Low fluid loss and high fluid loss

Comparisons are made by cross-plotting average daily production rates and two-year net present values (NPV) against total treatment volumes and total proppant weights. First order curve-fits are used for each data set, with 50 points plotted at the origin. Producing rates and net present values are assumed to be zero for all wells, without fracture treatments. The results show that all best-fit lines have an intercept at or near zero, so that the slopes can be used to compare performance. Each pair of slopes is tested for parallelism to determine if the slopes are truly different within a confidence interval of 95%. A confidence interval of 95% means that there are two boundary points between which there is a 95% level of confidence that the slopes are equal. In repeated sets of samples, each of the same size, the slopes would be expected to be equal in 95% of all intervals calculated (33). Specific results of the tests for equal slopes are presented in Appendix F.

Comparison of Polymer Emulsions and Cross-Linked Gels

The use of cross-linked gels has been a major development in hydraulic fracture treatments in the Wattenberg

ER-2989

field. The cross-linked gel (CLG) treatments included in this study had higher average sand concentrations than polymer emulsions (PE), as shown by the mean values:

	<u>CLG</u>	<u>PE</u>
Avg. sand concentration (lb/gal)	4.10	2.13
Job cost/sand wt., (\$/lb)	0.20	0.41
Job cost/fluid vol., (\$/gal)	0.82	0.86

The job cost/sand weight ratios reflect the higher cost of hydrocarbons used in polymer emulsions, and the greater fluid volumes for equivalent total proppant weights.

Figures 20 and 21 indicate that initial rates and NPV are equivalent for cross-linked gels and polymer emulsions, based on total sand weight. The test for parallelism verifies that there is essentially no difference in slopes.

Figures 22 and 23 indicate that cross-linked gels are superior to polymer emulsions, based on fracture fluid volume. Recall that average sand concentrations of cross-linked gels are almost twice those of polymer emulsions. The test for parallelism reveals the slope of cross-linked gels in Figure 22 is higher for a 95% confidence interval. The slopes of Figure 23 are different for a 90% confidence interval, but not for a 95% confidence interval.

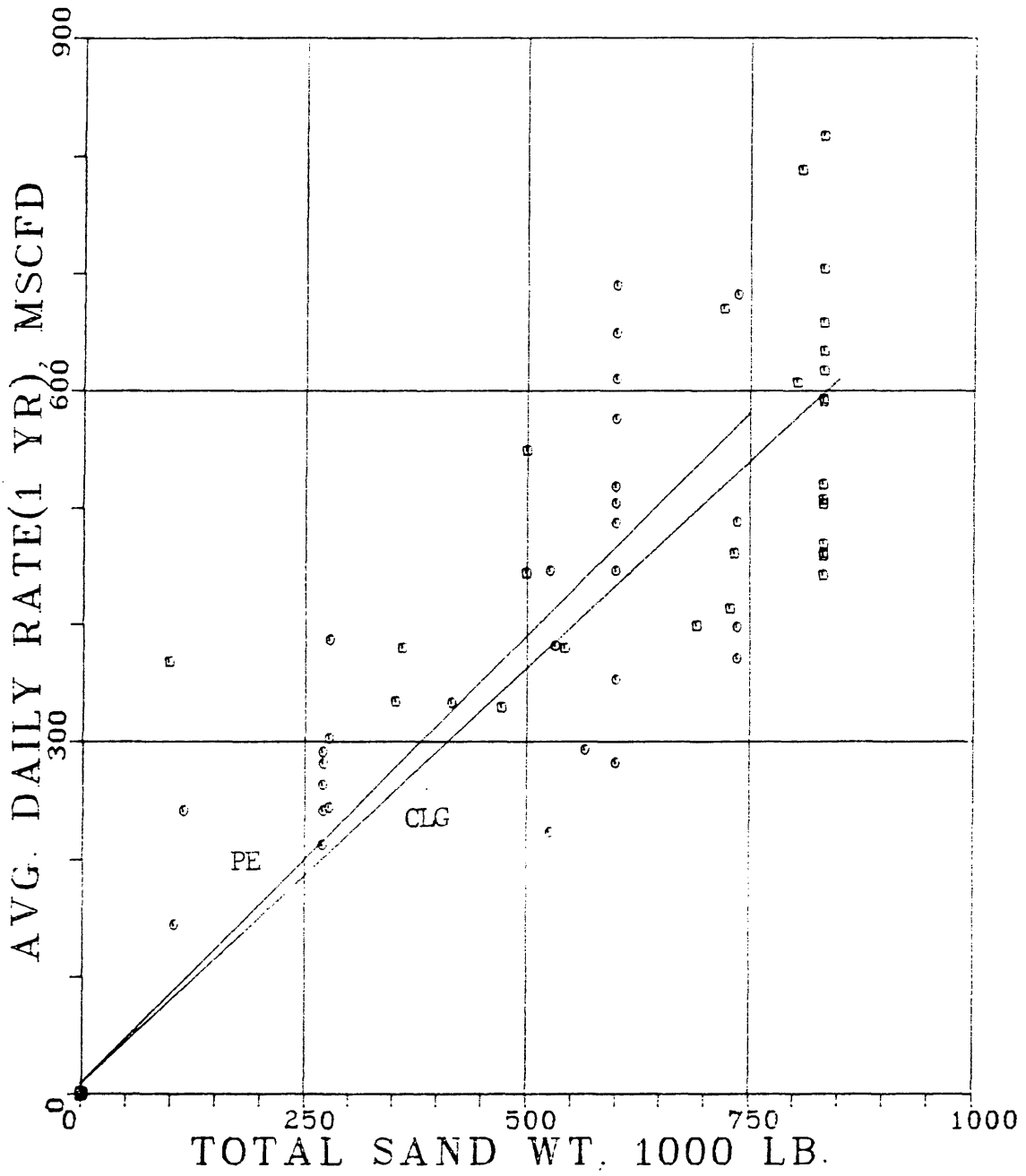


Figure 20. Comparison of initial producing rates versus proppant weight for polymer emulsions and cross-linked gels. First order best-fit curves.

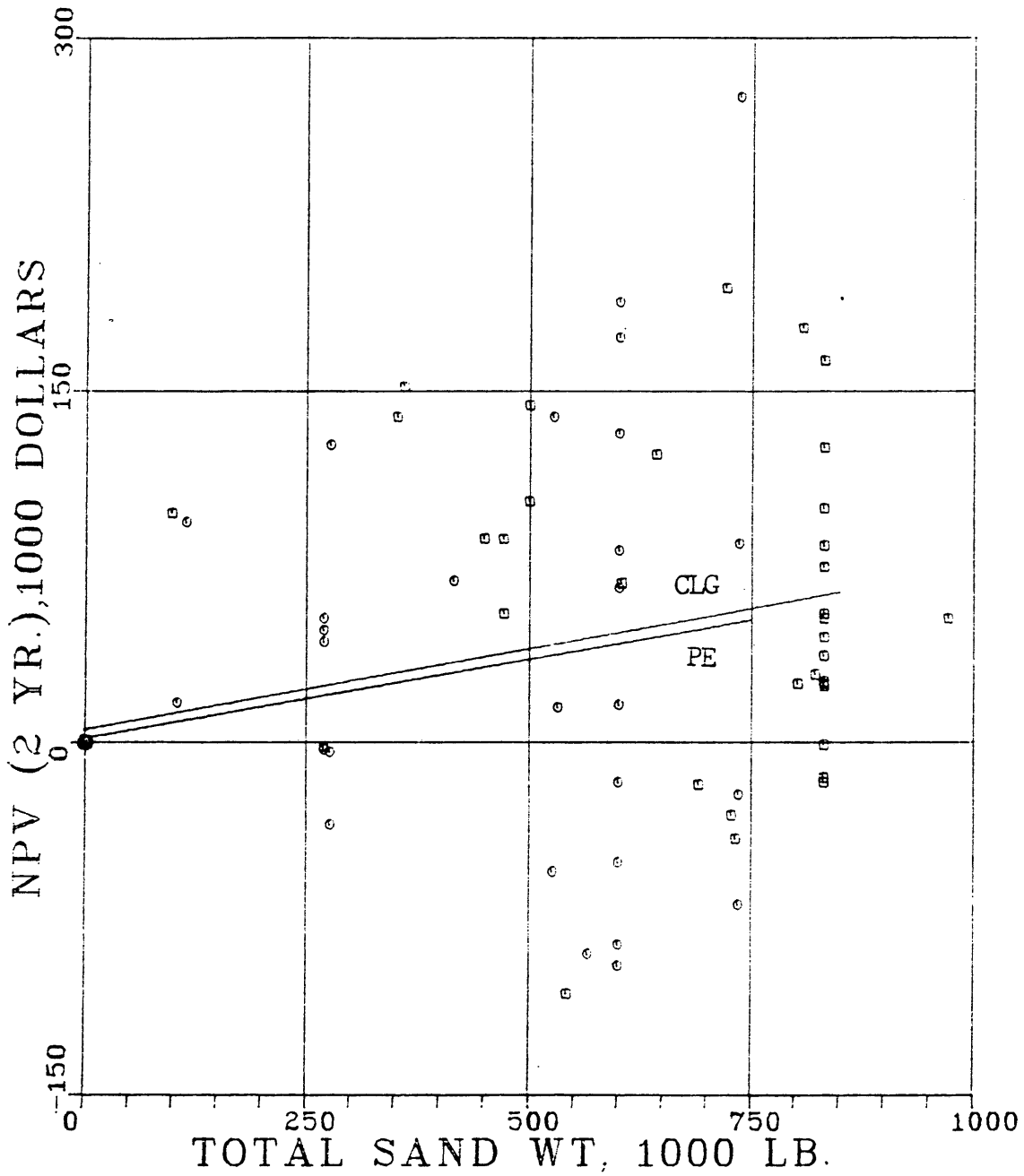


Figure 21. Comparison of NPV versus proppant weight for polymer emulsions and cross-linked gels. First order best-fit curves.

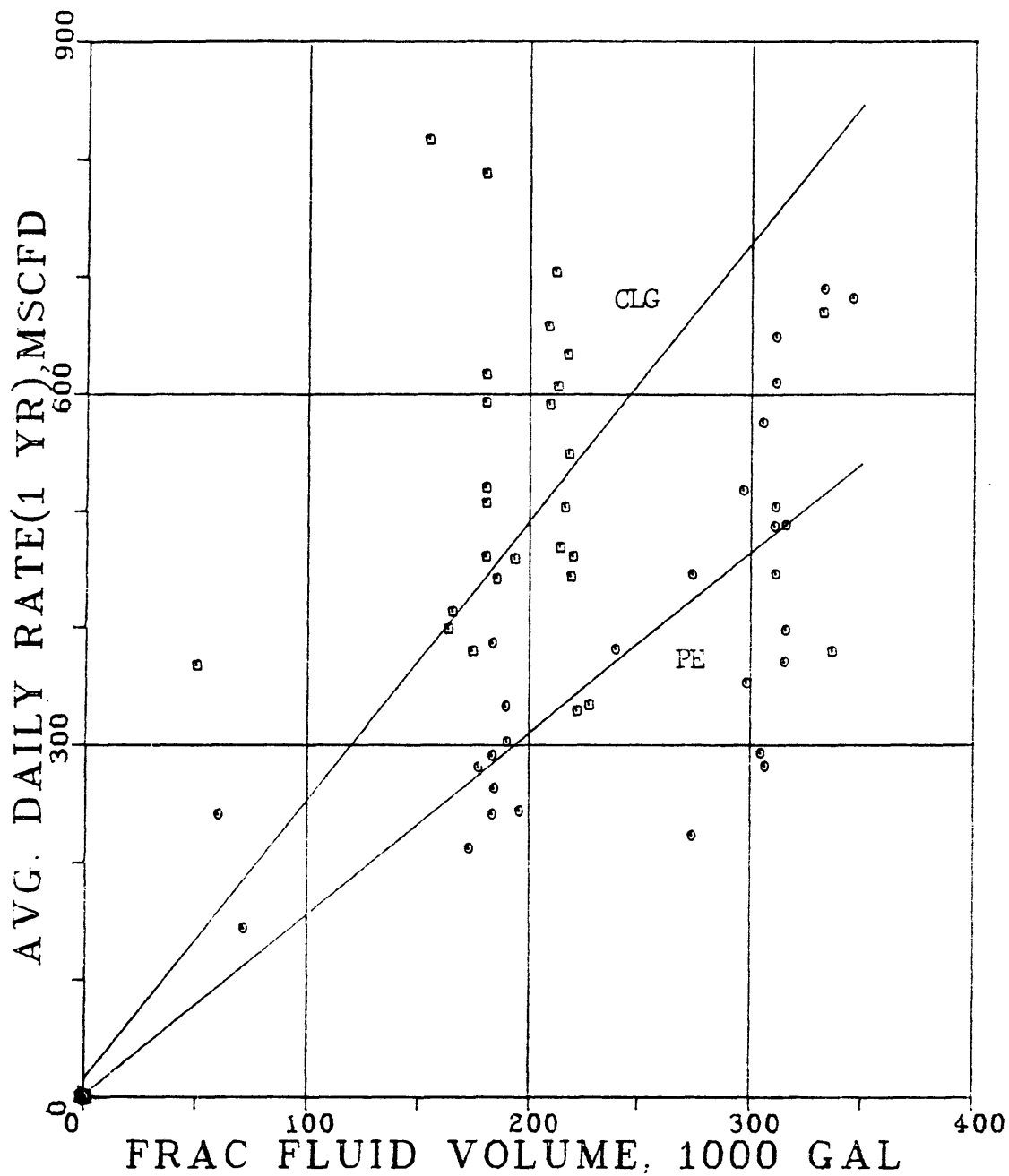


Figure 22. Comparison of initial producing rates versus fluid volume for polymer emulsions and cross-linked gels. First order best-fit curves.

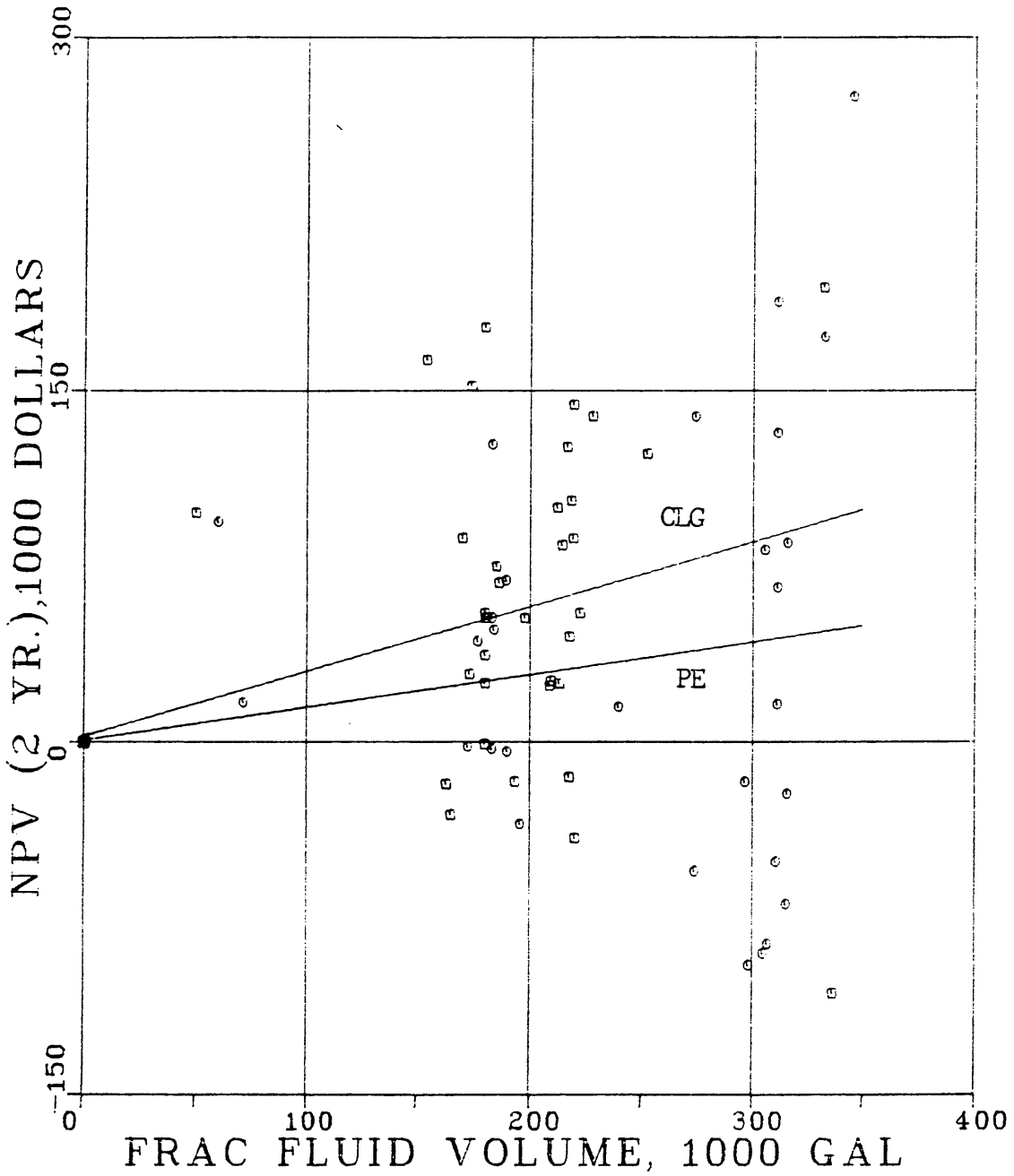


Figure 23. Comparison of NPV versus fluid volume for polymer emulsions and cross-linked gels. First order best-fit curves.

If the effects of different treatment fluids are neglected, Figure 22 suggests that higher sand concentrations result in higher initial producing rates.

### Comparison of Pillar and Conventional Packed Fractures

Tinsley and Williams (10) proposed a new proppant scheduling technique designed to place proppant in pillars within the fracture. The authors reason that the unpropped fracture between the proppant pillars will have a much higher conductivity than the propped portions. There are several assumptions used to develop this concept:

- 1) there is no mixing of proppant-laden slurry and spacer fluid;
- 2) the proppant does not crush or become embedded;
- 3) the fracture will close and trap proppant after injection ceases;
- 4) Poisson's ratio, Young's modulus, and fracture height are known with certainty;
- 5) the productivity ratio from McGuire and Sikora models well behavior.

There are several problems with these assumptions as they apply to the Muddy "J" sand:

- 1) turbulence, eddy currents and mixing most likely occur as fluids are pumped through perforations.
- 2) Nolte (25) reports that fracture closure times may be as long as 24 hours after pumping stops;
- 3) if fracture height is greater than estimated, the equations predict that some unpropped areas will close, resulting in essentially zero fracture conductivity;

- 4) the McGuire and Sikora productivity chart applies only for pseudo-steady state; it is not valid for a tight gas reservoir; and
- 5) the method is designed to benefit wells with permeabilities of 0.1 md, or more; the Muddy "J" generally has a maximum permeability of 0.05 md.

If significant fluid mixing does occur while pumping, the result is a much lower average proppant concentration and lower conductivity for equivalent fracture length. These points suggest that the "pillar fracture" technique would not be appropriate in the Muddy "J" sand.

Mean values of average sand concentration and job cost ratios are as follows:

	<u>Packed</u>	<u>Pillar</u>
Avg. Sand Concentration (lb/gal)	4.14	2.19
Job cost/sand wt. (\$/lb)	0.21	0.38
Job cost/fluid vol. (\$/lb)	0.86	0.84

Note that these values are very similar to those for cross-linked gels and polymer emulsions. Most pillar fracture treatments in T2N/R65W have used polymer emulsions, although some have been done with cross-linked gels. The comparisons of packed and pillar fractures are similar to the comparisons of the two fluid types, but the magnitudes of the variations in slopes are different.

Figures 24 and 25 indicate that there is virtually no difference in performance between packed and pillar fractures, for equivalent sand weights. The test for parallelism verifies this observation.

Packed fractures result in higher initial rates for equivalent fluid volumes, but not necessarily higher NPV, as shown in Figures 26 and 27. The test for parallelism indicates that packed fractures are superior at a 90% confidence interval (Figure 26). The slopes of Figure 26 are virtually equivalent at a 95% confidence interval. There is clearly no significant difference of slopes in Figure 27. As noted for Figure 22, Figure 26 suggests that higher average sand concentrations lead to higher initial producing rates. However, the incremental production is apparently partially offset by the increased sand costs, and there is no significant difference in economic performance of packed and pillar fractures. The difference in fracture fluid types clouds the issue somewhat, but "pillar fracs" do not appear to offer an economic advantage in T2N/R65W.

#### Low versus High Fluid Loss Treatments

Fracture fluid efficiency is strongly dependent on the fluid loss coefficient, as shown in Figure 28. A higher fluid efficiency means longer fracture lengths for equiva-

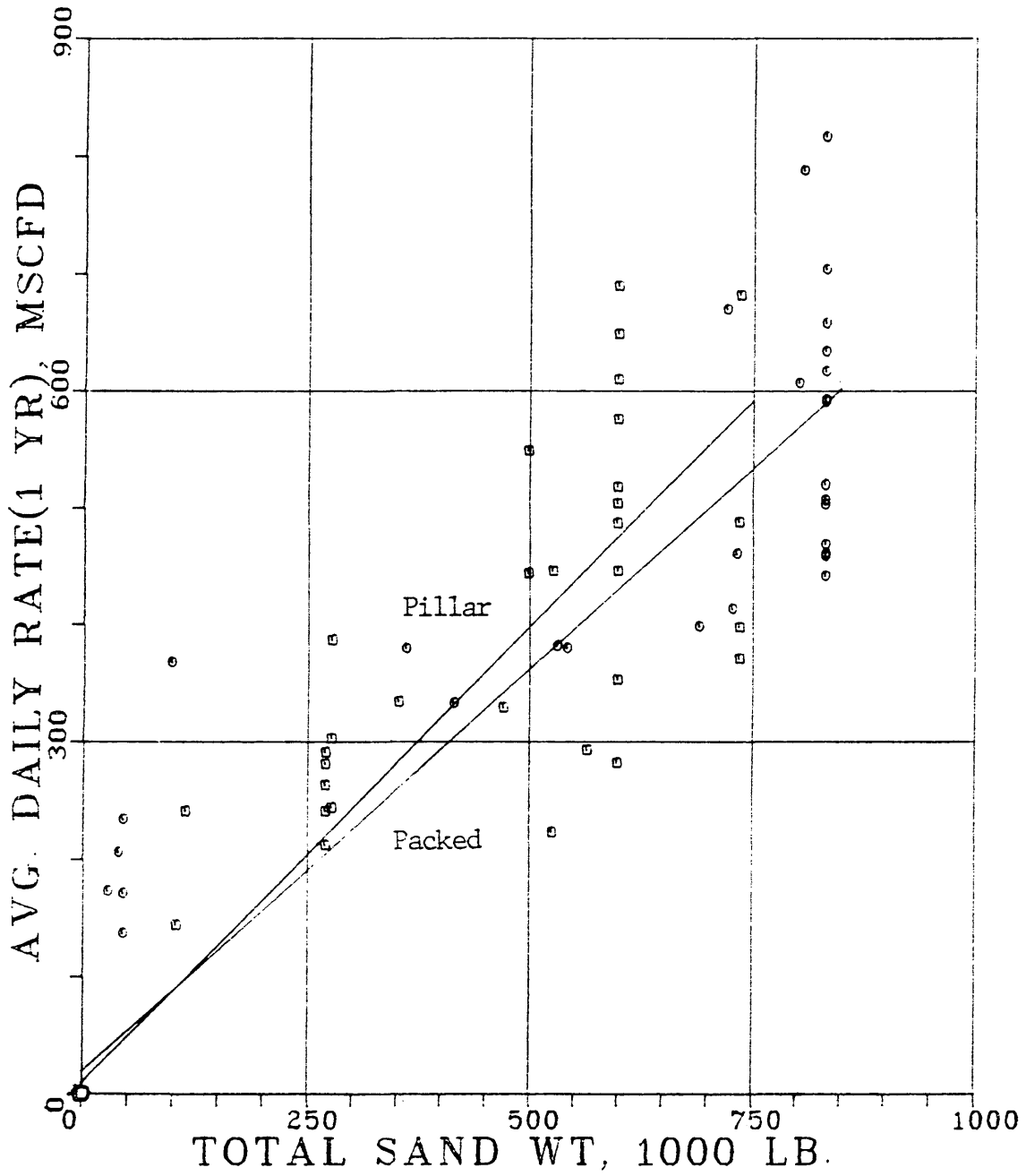


Figure 24. Comparison of initial producing rates versus propant weight for packed and pillar fracs. First order best-fit curves.

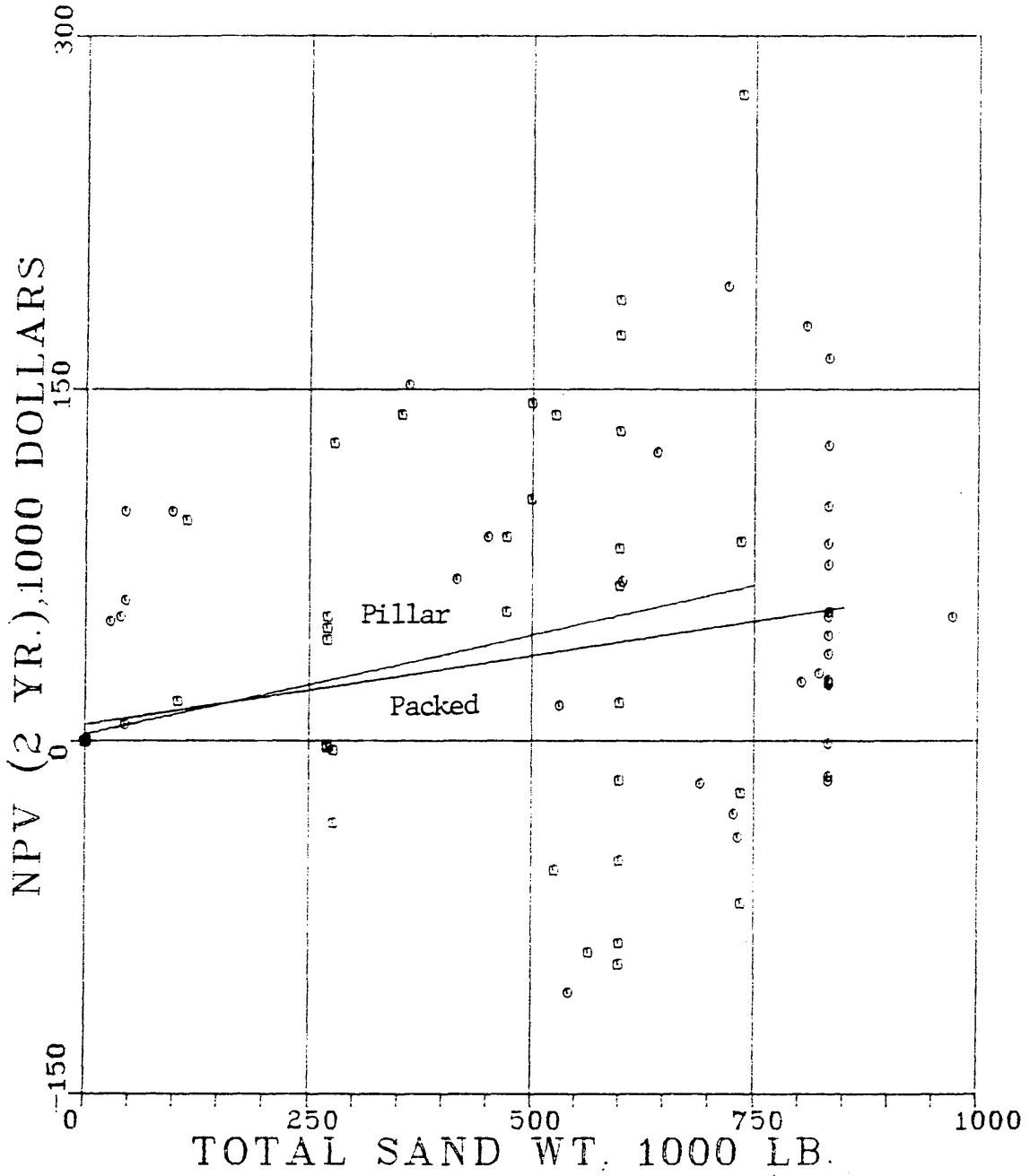


Figure 25. Comparison of NPV versus proppant weight for packed and pillar fracs. First order best-fit curves.

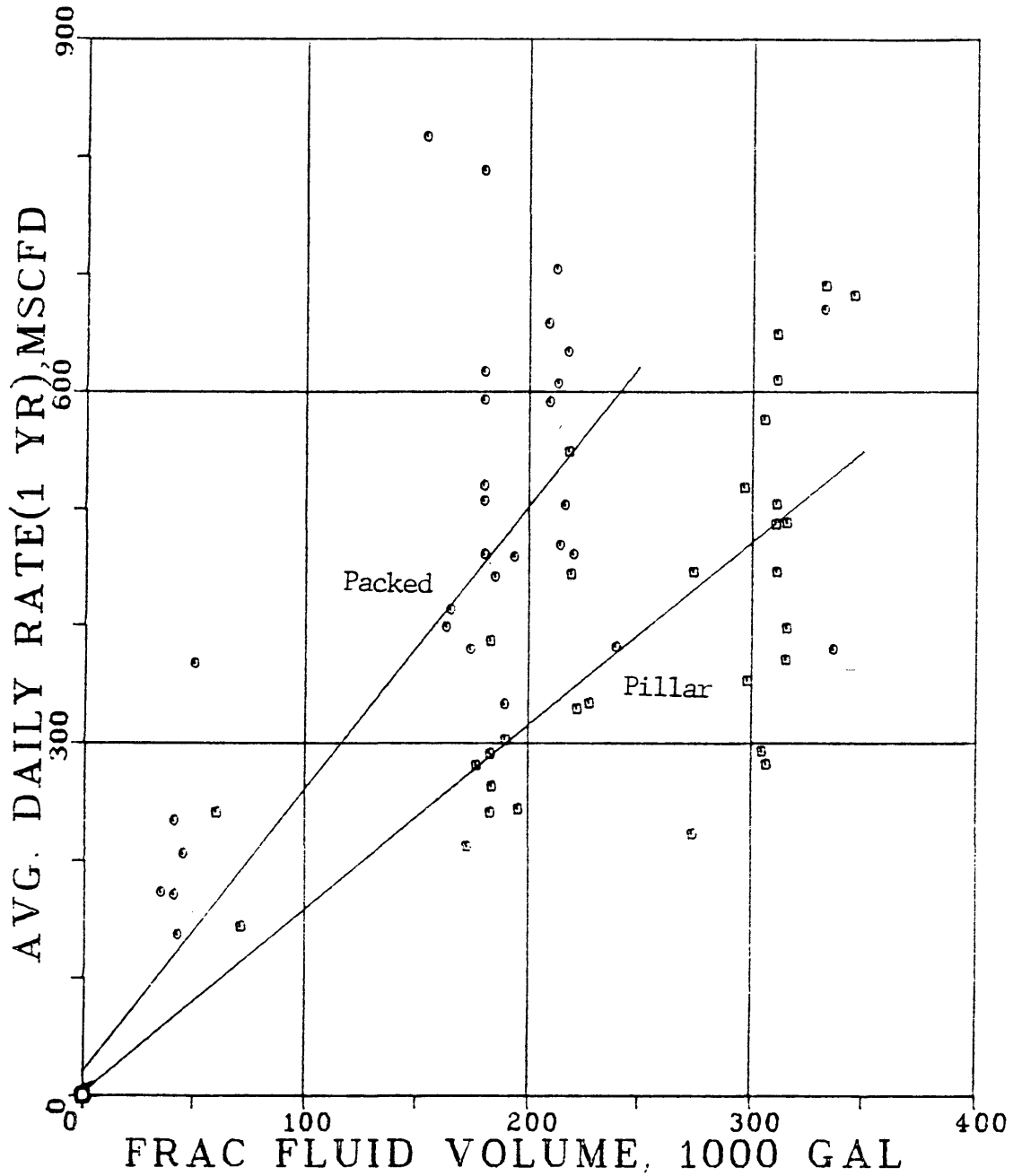


Figure 26. Comparison of initial producing rates versus fluid volume for packed and pillar fracs. First order best-fit curves.

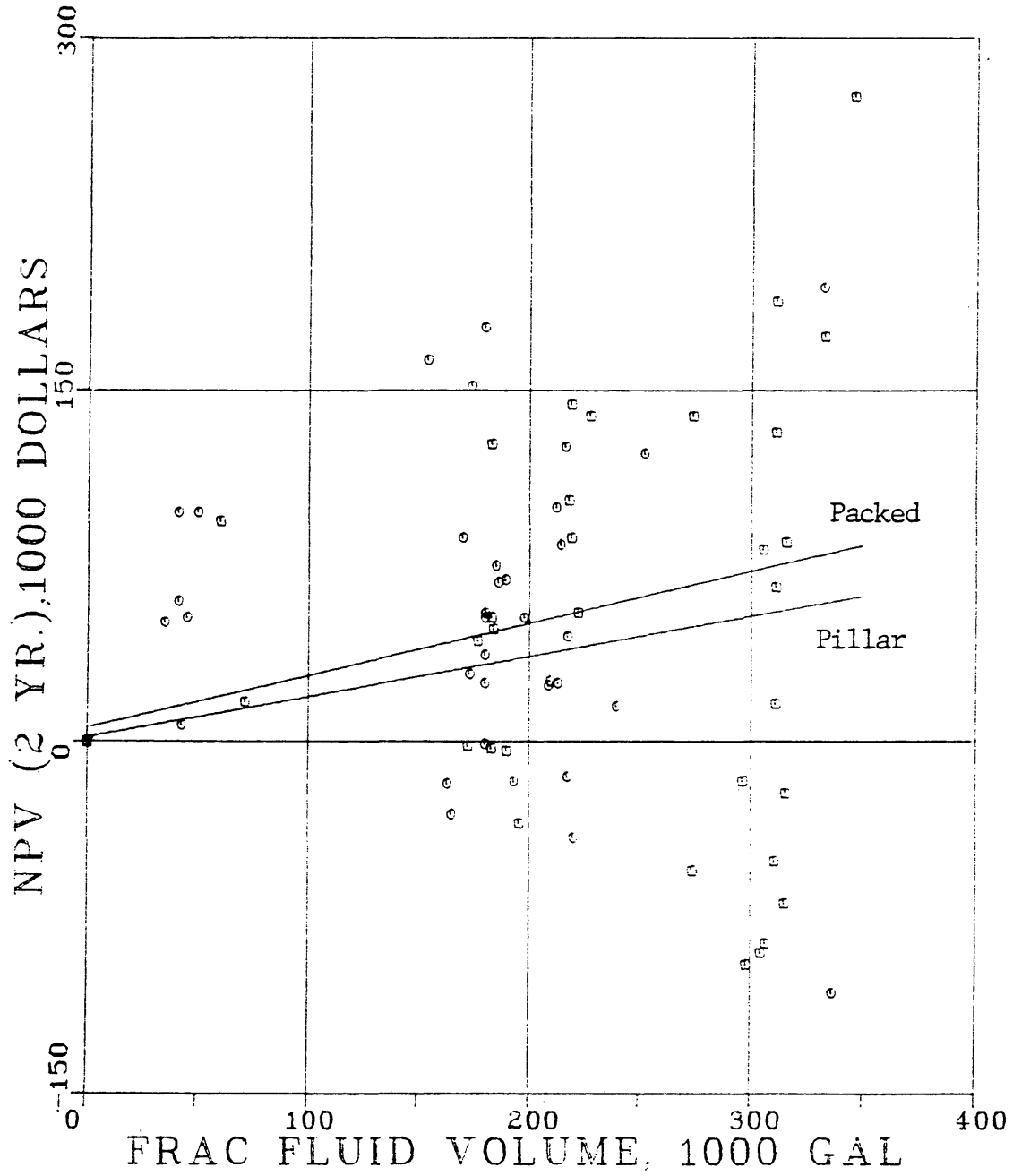


Figure 27. Comparison of NPV versus fluid volume for packed and pillar fracs. First order best-fit curves.

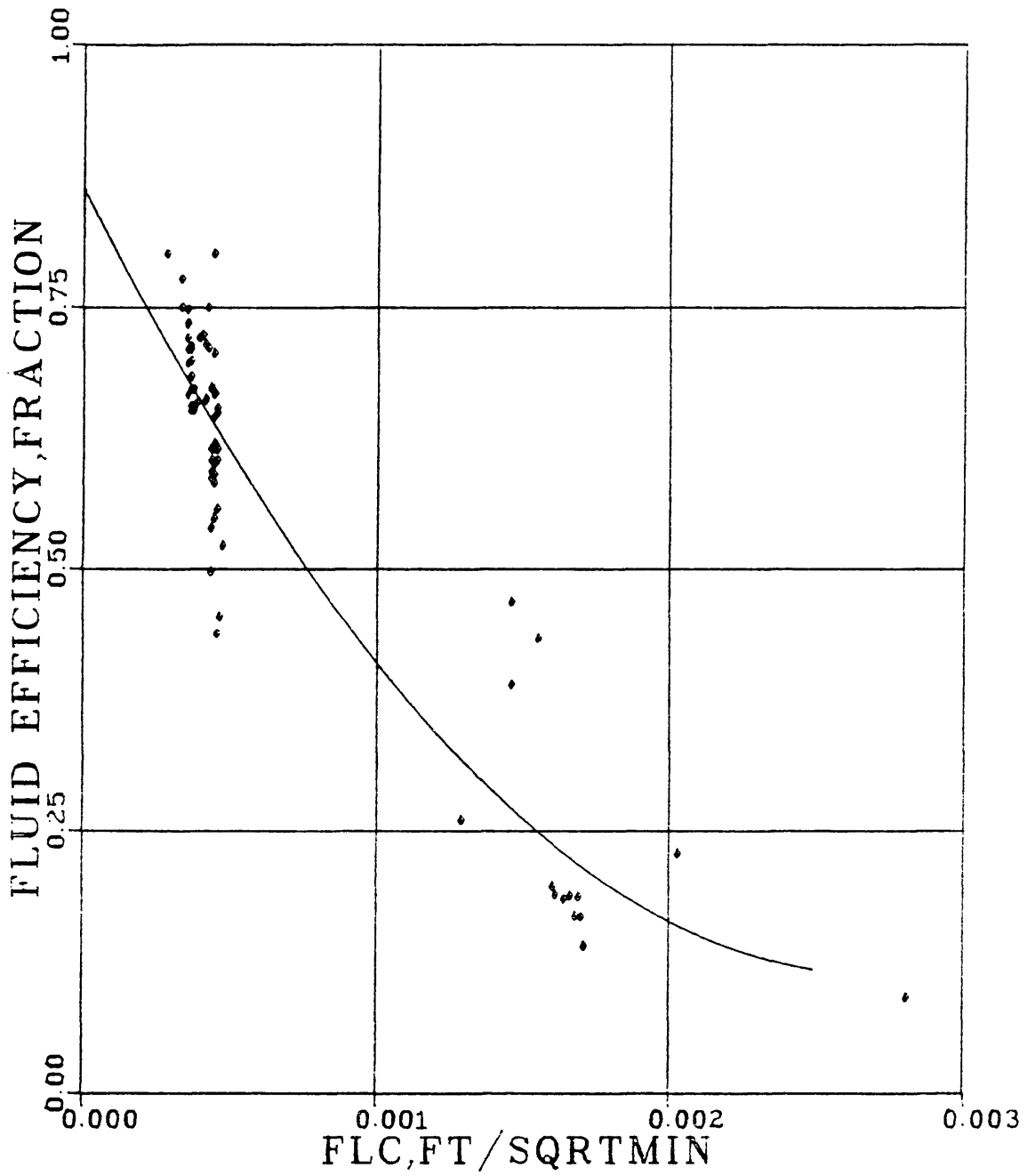


Figure 28. Fluid efficiency versus fluid loss coefficient for the treatments included in this report. Second order best-fit curve.

lent fluid volumes. Figure 29 presents created length versus fluid volume for treatments with low FLC (less than  $0.001 \text{ ft}/(\text{min})^{\frac{1}{2}}$ ) and high FLC (greater than  $0.001 \text{ ft}/(\text{min})^{\frac{1}{2}}$ ). Note that for 200,000 gallon treatments, the low-FLC fluids produce a fracture almost twice as long as for the high-FLC treatments. Considering the emphasis put on fracture length by so many authors, it is surprising that some operators do not use hydrocarbon in their cross-linked gels to reduce fluid loss. Moreover, higher leak-off rates generally mean that proppant concentrations must be reduced to avoid sand-outs, and the fracture is narrower. Table 7 presents the results of calculation of fracture dimensions for three treatments with different fluid loss coefficients. The sand concentration of the high-FLC fluids must be reduced to avoid a sand-out, based on the propped/created length ratio. However, it is conceivable that the higher fluid loss results in better proppant distribution. For a given pump rate, higher fluid loss results in smaller areas and higher velocities. Higher velocities may carry smaller proppant sizes to the fracture tip.

The mean values of average sand concentration and job cost ratios are as follows:

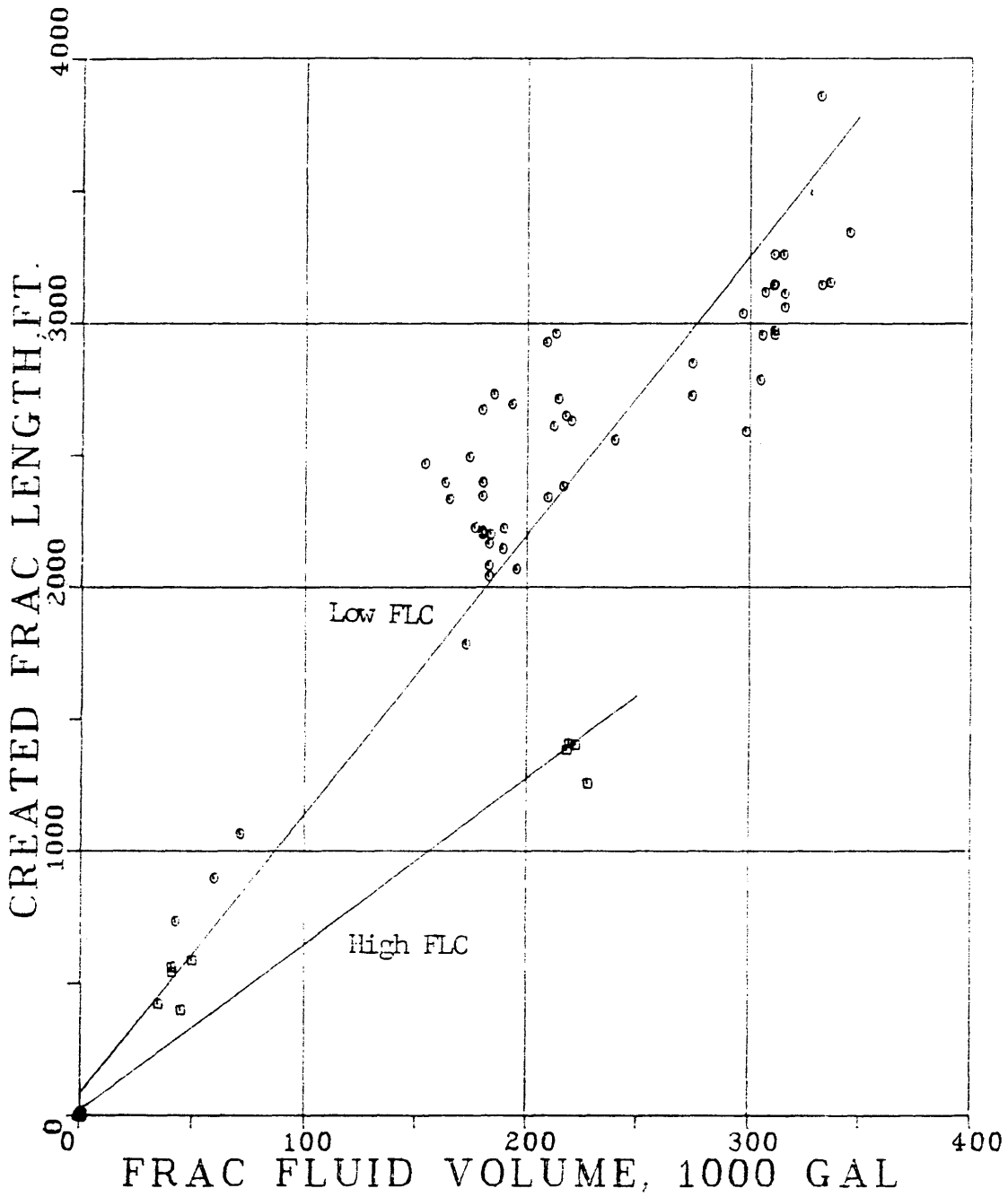


Figure 29. Created fracture length versus fluid volume for high fluid loss and low fluid loss jobs. First order best-fit curve.

Table 7

Fluid	Fluid Vol. (M gal)	Pad Vol. (M gal)	Sand Wt. (M lb)	FLC (ft/(min) <sup>1/2</sup> )	Max. Width (in)	Frac Length Created	Frac Length Propped
1	170	30	600	0.0005	0.5408	2794	2620
2	170	30	500	0.0010	0.4755	2178	2165
3	170	30	170	0.0020	0.3561	1467	1428

Table 7. Variation of fracture dimensions with fluid loss coefficient, using modified McLeod method.

ER-2989

	<u>Low FLC</u>	<u>High FLC</u>
Avg. sand concentration (lb/gal)	3.12	2.53
Job cost/sand wt. (\$/lb)	0.27	0.31
Job cost/fluid vol. (\$/gal)	0.86	0.79

The number of high fluid loss treatments is small (11), so the validity of drawing conclusions from Figures 30 to 33 is questionable. Figures 30, 31, and 33 indicate that the high fluid loss treatments may be superior. However, tests for parallelism indicate there are no differences in slope for Figures 30 through 33.

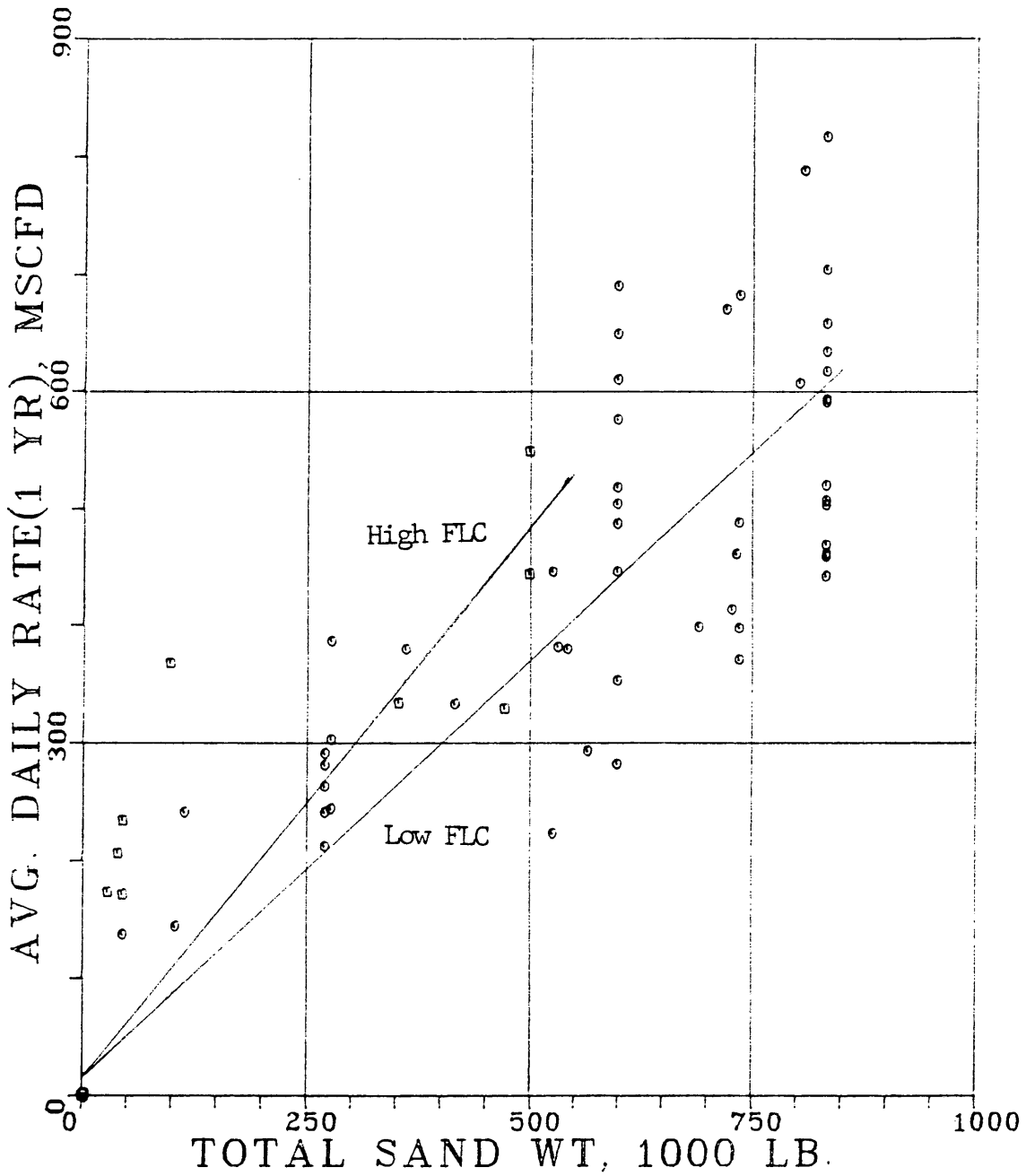


Figure 30. Comparison of initial producing rate versus proppant weight for high and low fluid loss. First order best-fit curves.

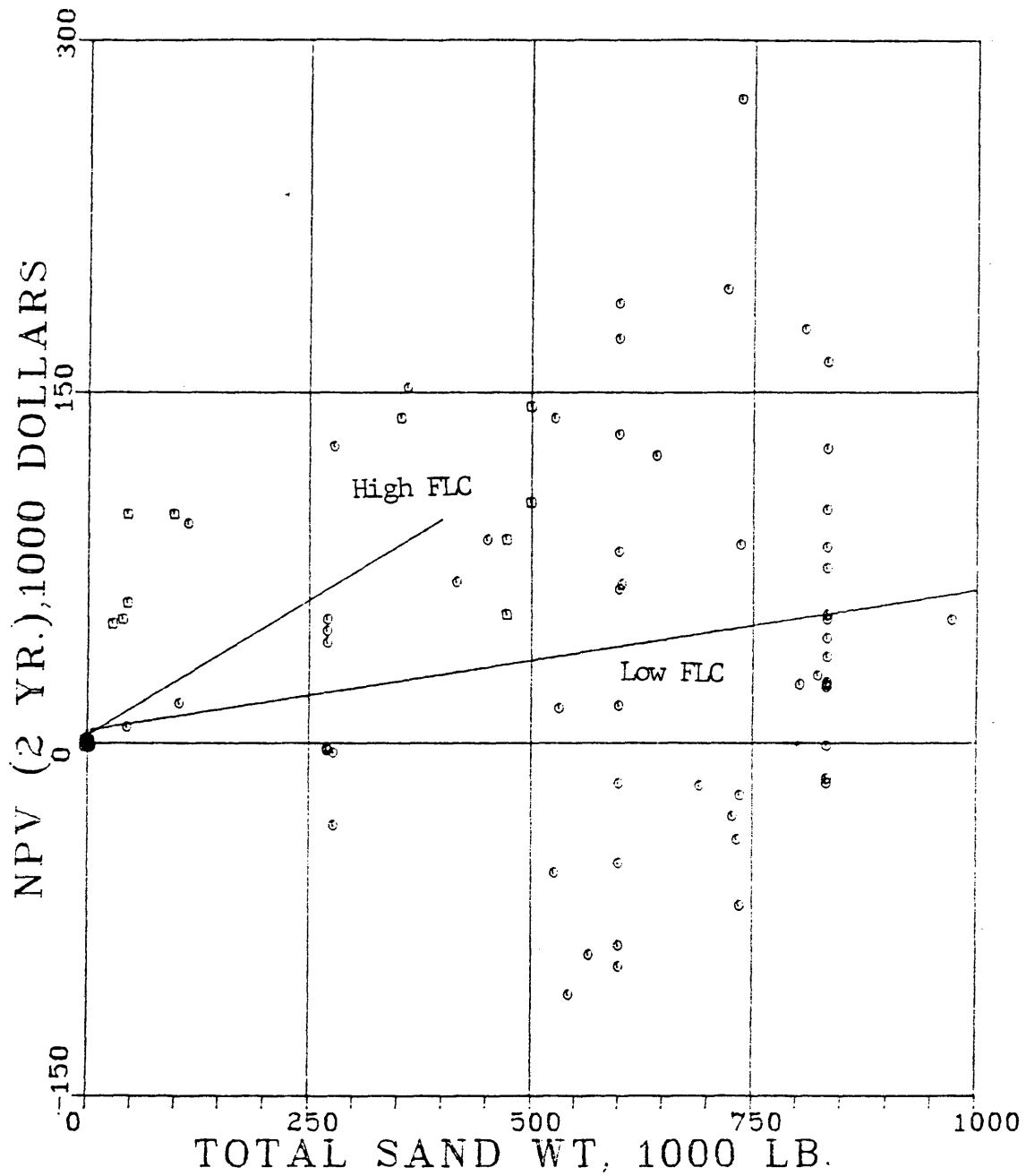


Figure 31. Comparison of NPV versus proppant weight for high and low fluid loss. First order best-fit curve.

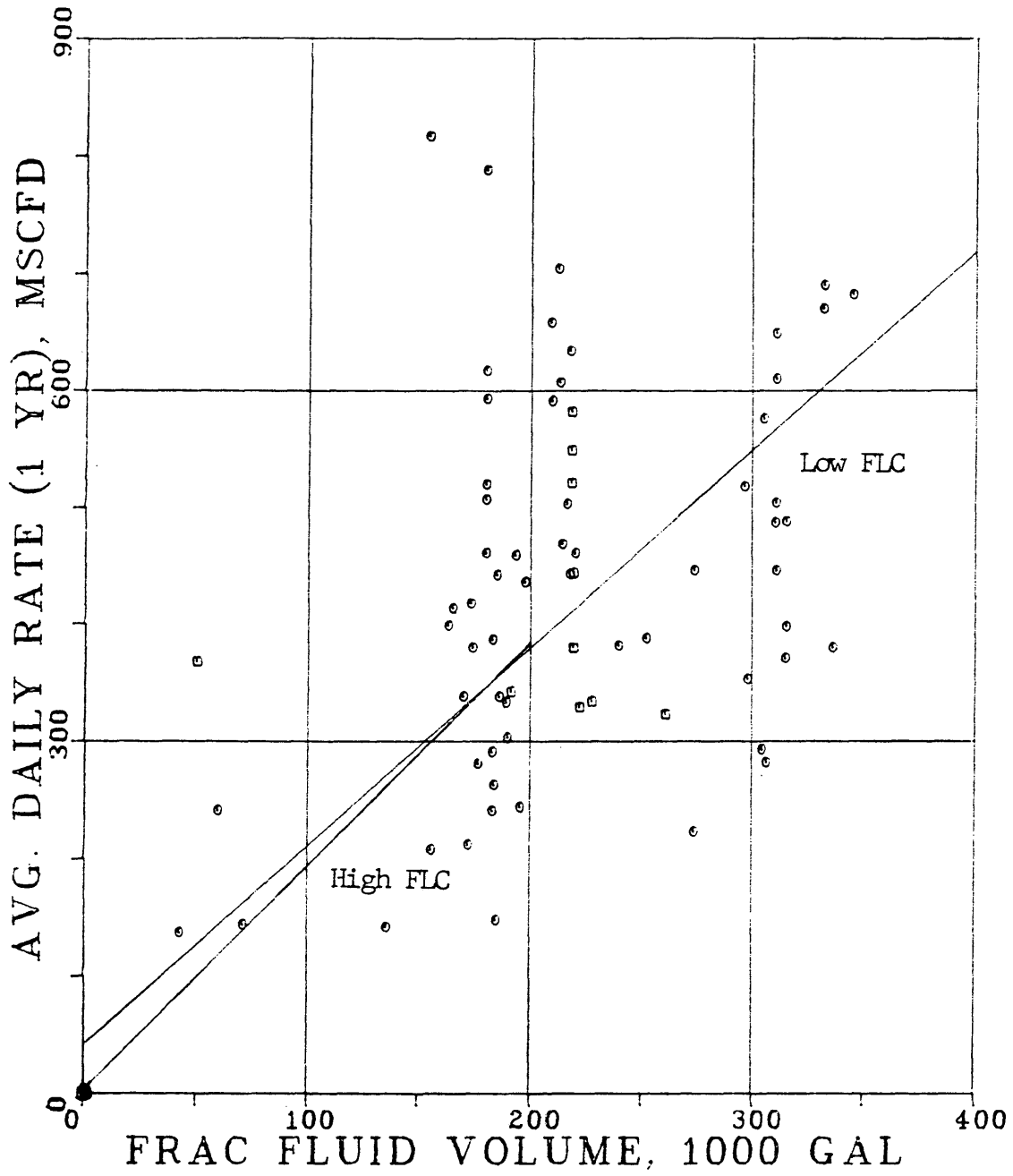


Figure 32. Comparison of initial producing rates versus fluid volume for high and low fluid loss. First order best-fit curves.

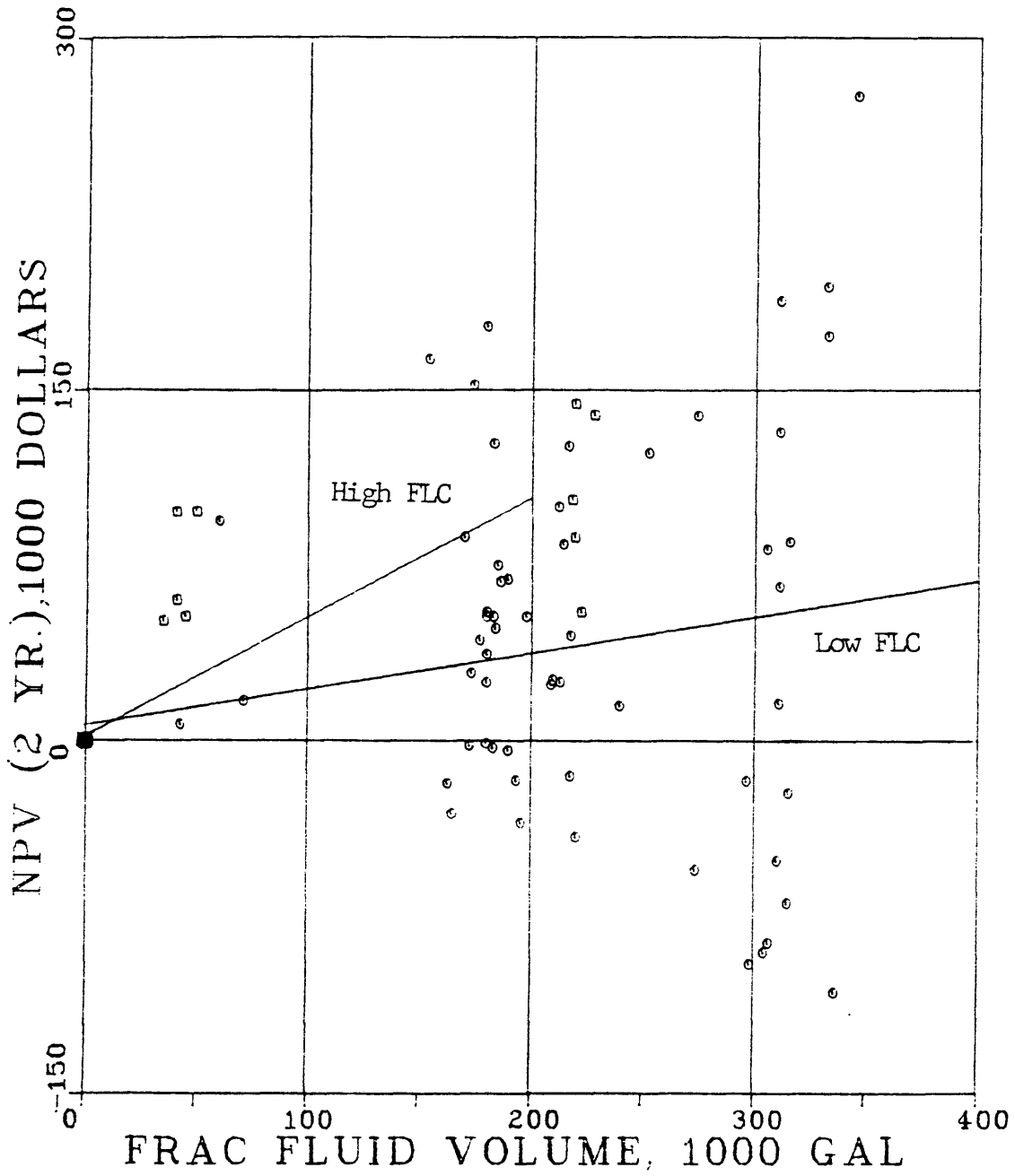


Figure 33. Comparison of NPV versus fluid volume for high and low fluid loss. First order best-fit curves.

### DISCUSSION OF THE VARIATIONS IN WELL PERFORMANCE

The results presented in the previous section clearly demonstrate the lack of correlation between fracture dimensions and well performance. Moreover, some of the comparisons of fluid types and proppant schedules have results which are much different than expected. Assuming permeability is relatively constant throughout T2N/R65W, there must be other reasons to explain the wide variations in well performance. Some possible explanations are discussed below.

#### Formation Damage due to Fluid Invasion

It is a well known fact that fluid invasion of sandstones containing clays can cause permanent damage. Jones and Owens (34) report that a 60,000 mg/L NaCl solution will typically reduce permeability 85% below the Klinkenberg permeability of a dry core. They also note that damage due to water or brine is more pronounced in lower permeability rocks, and recommend that fluid invasion be kept to a minimum during drilling and fracturing. Simon and Coon (35) suggest that fluid pH affects the degree of formation damage. They report that a pH of 4.0 to 6.0 causes less damage than a pH of 3.0 to 10.0. The addition of 5% methanol to a cross-linked gel can reduce the pH to a desired level (4). If this is true, it could explain the wide variation of performance for the wells treated with cross-linked gel.

Perhaps more important than the pH, is the length of time the formation is exposed to invasion fluids. Crafton and Wilderson (32) note that leaving even a stable emulsion in contact with the reservoir matrix for extended periods of time causes formation damage. They explain that the Muddy "J" sandstone has no continuous liquid phase, and that adsorption of surfactants may lead to increased relative permeability to water and imbibition of water. Naturally, the longer the formation is exposed to this condition, the greater the imbibition and damage. It would appear that the length of time required to recover fracture fluids might provide insight into the potential of a particular well. Unfortunately, this data is not commonly available, and could not be obtained for this report. However, consider that as treatment sizes increase, more fracture area is exposed to fluid invasion. If a formation is very heterogeneous, as the Muddy "J" is, some areas of the fracture may not produce back invasion fluid as rapidly as other areas. The imbibition process is likely to lead to the equivalent of permanent damage over a period of time. Under this scenario, part or all of the benefit of longer fracture lengths is lost.

#### The Concept of Effective Fracture Length

The reduction of fracture area due to imbibition, dis-

ER-2989

cussed above, can be thought of as a reduction of fracture length, if height is constant. Thus an "effective" fracture length can be defined as that portion of the propped fracture length which contributes to production. More specifically, it is that fracture length determined with a transient test model. As discussed earlier, the effective fracture length may be different for various models and assumptions of fracture conductivity. More important, the effective fracture length will generally not be equal to the propped length, nor will the ratio of effective/propped length be constant.

The physical significance of effective fracture length is demonstrated by the work of Branagan et al (36). They used cyclic injection of dry gas into shut-in Wattenberg gas wells in an attempt to restore production. Extensive pressure buildup tests were used before and after gas injection to check permeability. The authors noted a 19-fold increase in permeability due to gas cycling. However, if the permeability were assumed to remain constant, the effective fracture length would show an increase from 160 feet to 879 feet. The authors concluded that the gas cycling most likely removed high fluid saturations adjacent to the fracture face and restored gas permeability.

McMechan and Conway (37), in reviewing hydraulic fracturing in the Anadarko Basin, note that the combination of

high capillary pressure, low fracture conductivity and high gas mobility relative to water, allows early breakthrough of gas near the wellbore following treatment. This can lead to high water saturations in the fracture and effectively isolate most of the fracture from production. The same idea is expressed by Tannich (19). He makes the point that when selecting a design fracture length, one must consider whether fracture fluid can be removed from the wellbore. If not, the effective length will be shorter than the propped length.

Obviously, effective/design fracture lengths less than 1.0 may be caused by factors other than reduced gas permeability, as noted by Holditch et al (16):

- 1) the fracture is wider than the design indicates;
- 2) sand transport is inefficient and proppant settling may have occurred;
- 3) the actual fluid loss is larger than predicted;  
and
- 4) fracture height is greater than estimated.

The above discussion leads to the conclusion that effective fracture length is much more important than propped length in determining well performance. The literature generally fails to make the distinction between the two lengths with respect to fracture design. The results of this study strongly suggest that something more than a design propped fracture length is required in order to obtain realistic production forecasts for hydraulically fractured

tight-gas sands. Specifically, a technique that defines the effective/propped fracture length ratio is needed.

#### Other Factors Which Affect Performance

As previously stated, variations in formation permeability have not been considered in this study. A pressure build-up test is available for only one of the wells included in this report. The depositional environment of the Muddy "J" sand and inspection of logs suggests that reservoir quality may vary significantly between location.

Another factor which has not been addressed in this report is proppant size and concentration. Many treatments used large quantities of 100 mesh sand, which is currently used only for fluid loss control. Proppant schedules have changed and evolved over the years, and could be responsible for some of the variations in well performance.

The fracture dimension equations used in this study incorporate several simplifying assumptions. It is possible that errors in calculating propped fracture length are greater for some wells than for others. Some treatments may follow the model closely while others may deviate significantly. This is another argument for investigating propped/effective length relationships.

DISCUSSION OF FRACTURE DESIGN  
OPTIMIZATION PROCEDURES

General guidelines for fracture design optimization, based on the concept of effective fracture length, are proposed here. Application of the specific procedures is beyond the scope of this work, but they are generally well documented in the literature. The intent here is to discuss how various ideas might be combined to form a practical fracture design optimization procedure. The general steps of the procedure are as follows:

- 1) Determine the effective/propped fracture length ratio for the area of interest.
- 2) Select several treatment sizes, fluid types, etc.
- 3) Compute fracture dimensions using the modified McLeod method.
- 4) Compute an expected effective fracture length using the appropriate effective/propped length ratio.
- 5) Use an analytical model or type curves to forecast production.
- 6) Compute NPV for various treatments, and compare to find a desired treatment size.

Step 1 is the most difficult and time-consuming part of this procedure. It would require transient test analysis such as that proposed by Crafton et al (7), Agarwal et al (15), Bostic et al (38), or Holditch et al (39).

Ideally, Step 1 would have to be done only once, and the results could be applied to all subsequent treatments in a particular area. Alternately, an operator could simply

assume a constant effective/propped length ratio, such as 0.70, based on published results in the literature. Note that the particular model used in Step 1) should also be used to forecast production rates. If the analytical model of Crafton et al (7) is used in Steps 1) and 5), the whole procedure could be programed on a micro-computer.

This optimization procedure is ideally suited to re-fracturing candidates which have production history readily available. If a unique history match can be obtained, formation permeability can be determined, resulting in a more reliable production forecast.

The element of risk, with respect to performance, should be considered. This might be done by assigning a probability of economic success to ranges of fracture lengths. For example, propped lengths longer than 2000 feet in the Wattenberg field would have a reduced probability of success, as demonstrated by this study.

The use of a fracture design procedure based on the Modified McLeod method is well suited for use with typical field data. It is intended to fill the gap between sophisticated and expensive finite difference simulators, and the common practice of using a standard treatment for all wells in an area.

ER-2989

NOMENCLATURE

$a$	- length of semi-major axis of an ellipse
$b$	- length of semi-minor axis of an ellipse
$c_v$	- volume concentration of proppant
$c_w$	- weight concentration of proppant
$\bar{c}_w$	- avg. weight concentration of proppant
$c_w$	- final sand concentration pumped
$E$	- Young's modulus of elasticity
$E_f$	- overall fracture fluid efficiency
$E_s$	- slurry fluid efficiency
$F_{cd}$	- dimensionless fracture conductivity
$G$	- shear modulus
$h$	- fracture height
$k_f$	- fracture permeability
$k_r$	- reservoir permeability
$L$	- fracture half-length, wellbore to tip
$L_p$	- propped fracture half-length
$P_o$	- pressure within a crack
$q$	- total injection rate
$t_{de}$	- dimensionless time at external boundary
$V_{cs}$	- volume of fracture created by slurry
$V_{ct}$	- volume of fracture created by slurry and pad
$V_{fp}$	- fracture volume at the instant pumping stops

ER-2989

- $V_{fc}$  - volume of created fracture  
 $V_{fpc}$  - propped fracture volume after closure  
 $V_p$  - total proppant volume  
 $V_{si}$  - volume of slurry injected  
 $V_{fc}$  - volume of created fracture  
 $V_{fpc}$  - volume of propped fracture  
 $V_{li}$  - volume of liquid in slurry injected  
 $V_{pi}$  - volume of proppant injected  
 $w_{cw}$  - created fracture width at the wellbore  
 $w_{pw}$  - propped fracture width at the wellbore  
 $\bar{w}$  - overall avg. fracture width  
 $\bar{w}_p$  - avg. propped fracture width  
 $w(o,t)$  - created width at wellbore, at time  $t$   
 $w(x,t)$  - created width at location  $x$ , at time  $t$   
 $W_p$  - total weight of proppant  
 $x$  - incremental fracture half-length  
 $\nu$  - Poisson's ratio  
 $\mu$  - fracture fluid viscosity  
 $\phi_f$  - in-situ porosity of proppant in fracture  
 $\rho_p$  - density of proppant

ER-2989

$w_{av}$  - vertical avg. fracture width

$w_{al}$  - avg. fracture width over the length

REFERENCES

1. Matuszczak, R.A., "Wattenberg Field, Denver Basin, Colorado," The Mountain Geologist, Vol. 10, No. 3, p. 99-105, (July 1973).
2. Fast, C.R., Holman, G.B., and Covlin, R.J., "The Application of Massive Hydraulic Fracturing to the Tight Muddy "J" Formation, Wattenberg Field, Colorado", Journal of Petroleum Technology, Vol. 29, p. 10-16, (January 1977).
3. Parrot, D.I., and Long, M.G., "A Case History of Massive Hydraulic Refracturing in the Tight Muddy "J" Formation," SPE Paper 7936, presented at the 1979 SPE Symposium on Low-Permeability Gas Reservoirs, (May 1979).
4. Harp, L.J., "Another Significant Step in the Evolution of Stimulation Treatments in the Muddy "J" Sand - Wattenberg Field," SPE Paper 9037, presented at SPE Rocky Mountain Regional Meeting, (May 1980).
5. Roberts, C.N., "Fracture Optimization in a Tight Gas Play: Muddy "J" Formation, Wattenberg Field, Colorado," SPE/DOE Paper 9851, presented at the 1981 SPE/DOE Symposium on Low Permeability Gas Reservoirs, (May 1981).
6. Holditch, S.A., Jennings, J.W., and Neuse, S.H., "The Optimization of Well Spacing and Fracture Length in Low Permeability Gas Reservoirs," SPE Paper 7496, pre-

ER-2989

sented at the 53rd Annual Fall Technical Conference of SPE, (October 1978).

7. Crafton, J.W., et al, "A Practical Model for Evaluating a Well Producing from a Tight Gas Formation," SPE/DOE Paper 10841, presented at the 1982 SPE/DOE Unconventional Gas Recovery Symposium, Pittsburg, PA.
8. Crowell, R.F. and Jennings, A.R.: "A Diagnostic Technique for Restimulation Candidate Selection," SPE Paper 7556, presented at SPE 53rd Annual Technical Conference, (Oct. 1978).
9. McLeod, H.O., Jr.: "A Simplified Approach to Design of Fracturing Treatments Using High Viscosity Cross-Linked Fluids," SPE Paper 11614 presented at 1983 SPE/DOE Low Permeability Gas Reservoir Symposium, Denver, March 13-16.
10. Tinsley, J.M., and Williams, J. R. Jr.: "A New Method for Providing Increased Fracture Conductivity and Improving Stimulation Results," Journal of Petroleum Technology, Vol. 27, (Nov. 1975), p. 1319-1325.
11. McGuire, W.J. and Sikora, V.J.: "The Effect of Vertical Fractures on Well Productivity," Trans., AIME (1960) Vol. 219, 401-03.
12. Veatch, R.W., Jr. and Crowell, R.F.: "Joint Research Operations Programs Accelerate Massive Hydraulic Frac-

ER-2989

- turing Technology," J. Pet. Tech. (Dec. 1982) 2763-75.
13. Geertsma, J. and DeKlerk, F.: "A Rapid Method of Predicting Width & Extent of Hydraulically Induced Fractures," J. Pet. Tech. (Dec. 1969) 1571-81.
  14. Gringarten, A.C., et al, "Unsteady-State Pressure Distributions Created by a Well with a Single Infinite-Conductivity Vertical Fracture," SPE Journal (Aug. 1974) p. 347-360, Trans., AIME, V. 253.
  15. Agarwal, R.G., Carter, R.D. and Pollock, C.B.: "Evaluation and Performance Prediction of Low-Permeability Gas Wells Stimulated by Massive Hydraulic Fracturing," J. Pet. Tech. (March 1979) 362-72.
  16. Holditch, S.A. and Lee, W.J., "Fracture Evaluation with Pressure Transient Tests in Low-Permeability Gas Reservoirs Part II: Field Examples," SPE Paper 7930, presented at the 1979 SPE Symposium on Low Permeability Gas Reservoirs, (May 1979).
  17. Spencer, C.W., "Geologic Aspects of Tight Gas Reservoirs in the Rocky Mountains Region," SPE/DOE Paper 11647, presented at the SPE/DOE Symposium on Low Permeability Gas Reservoirs, (1983).
  18. Rosepiler, M.J., "Calculation and Significance of

- Water Saturations in Low Porosity Shaly Gas Sands," SPE Paper 10910, presented at the 1982 SPE Cotton Valley Symposium of SPE, (May 1982).
19. Tannich, J.D.: "Liquid Removal from Hydraulically Fractured Gas Wells," Jour. of Pet. Tech., Vol. 27 (Nov. 1975), p. 1309-1317.
  20. Perkins, T.K. and Kern, L.R.: "Widths of Hydraulic Fractures," J. Pet. Tech. (Sept. 1961) 937-49.
  21. Nordgren, R.D.: "Propagation of a Vertical Hydraulic Fracture," Soc. Pet. Engr. J. (Aug 1972) 306-14.
  22. Khristianovitch, S.A. and Zheltov, Yu.P., "Formation of Vertical Fractures by Means of Highly Viscous Fluids," Proceedings of 4th World Petroleum Congress, Vol. II, 1955, p. 579.
  23. Erdle, J.C. et al: "Results of Hydraulic Fracturing Treatment BHP Analysis in Peru," SPE Paper 10310 presented at the 1981 SPE Annual Technical Conference, San Antonio, Texas, Oct. 5-7.
  24. Barree, R.D., "Development of a Numerical Simulator for Three-Dimensional Hydraulic Fracture Propagation in Heterogeneous Media, in partial fulfillment of requirements for Doctor of Philosophy, Colorado School of Mines, 1984.
  25. Nolte, K.G.: "Fracture Design Considerations Based on Pressure Decline," SPE Paper 10911 presented at the

ER-2989

- 1982 SPE Cotton Valley Symposium, Tyler, Texas, May 20.
26. Dobkins, T.A.: "Procedures, Results, and Benefits of Detailed Fracture Treatment Analysis," SPE Paper 10130, presented at SPE 56th Annual Technical Conference, (Oct. 1981).
  27. Nolte, K.G.: "Determination of Fracture Parameters from Fracturing Pressure Decline," SPE Paper 8341 presented at the 1979 SPE Annual Technical Conference, Las Vegas, Sept. 23-26.
  28. Schlottman, B.W., Miller, W.K, II and Lueders, R.K.: "Massive Hydraulic Fracture Design for the East Texas Cotton Valley Sands," SPE Paper 10133 presented at the 1981 SPE Annual Technical Conference, San Antonio, Texas, Oct. 5-7.
  29. Gulbis, J., "Dynamic Fluid Loss or Fracturing Fluids," SPE Paper 12154, presented at the SPE 58th Annual Technical Conference, (Oct. 1983).
  30. Laboratory Report No. F11-B010-78, Halliburton Services, Duncan, Oklahoma, (March 1978).
  31. Penny, G.S., Conway, M.W. and Lee, W.S.: "Control and Modeling of Fluid Leak-Off During Hydraulic Fracturing," SPE Paper 12486, presented at the Sixth SPE Symposium on Formation Damage Control, (Feb. 1984).

ER-2989

32. Crafton, J.W. and Wilderson, C.R., "Individual Well Treatment, Operation and Performance in Wattenberg Field, Colorado," Unpublished, Liberal, Kansas (1974).
33. Kleinbaum, D.G., and Kupper, L.L., Applied Regression Analysis and Other Multivariable Methods, Duxbury Press, Massachusetts (1978), pp. 23-29, 97-102.
34. Jones, F.O., and Owens, W.W., "A Laboratory Study of Low Permeability Gas Sands," Journal of Petroleum Technology, Vol. 32, p. 1631-1640, (September 1989)
35. Simon, D.E. and Coon, R.M.: "Evaluation of Fluid pH Effects on Low Permeability Sandstones," SPE Paper 6010 presented at SPE 51st Annual Technical Conference (Oct. 1976).
36. Branagan, P.T., Cotner, G. and Gettman, G.: "Evidence of Permeability Enhancement Through Cyclic Dry Gas Injection," SPE/DOE Paper 9854, presented at the 1981 Symposium on Low Permeability Gas Reservoirs, (1981)
37. McMechan, D.E. and Conway, M.W.: "Hydraulic Stimulation Treatments in the Fletcher Field in the Deep Anadarko Basin," SPE/DOE Paper 11604, presented at the 1981 Symposium on Low Permeability Gas Reservoirs (Mar 1983)
38. Bostic, J.N., Agarwal, R.G. and Carter, R.D., "Combined Analysis of Postfracturing Performance and Pressure

ER-2989

- Buildup Data for Evaluating an MHF Gas Well," Journal of Petroleum Technology, Vol. 32, (October 1980), p. 1711-1719.
39. Holditch, S.A., Lee, W.J. and Gist, R., "An Improved Technique for Estimating Permeability, Fracture Length, and Fracture Conductivity from Pressure Buildup Tests in Low Permeability Gas Wells," SPE Paper 9885, presented at the SPE/DOE Symposium on Low Permeability Gas Reservoirs, (May 1981).
  40. Carter, R.D., "Derivation of the General Equation for Estimating the Extent of the Fractured Area," Drilling and Production Practice, API, Dallas, Texas (1957).
  41. Geertsma, J., and Haafkens, R., "A Comparison of the Theories for Predicting Width and Extent of Vertical Hydraulically Induced Fractures," Transactions of the ASME, Vol. 101, (March 1979).
  42. Crafton, J.W., class notes from "Advanced Well Design", CSM, (Fall 1984).
  43. Sneddon, I.N., and Elliot, H.A., "The Opening of a Griffith Crack Under Internal Pressure," Quarterly of Applied Math., Vol. 4, (1946), p. 262.
  44. Cooke, C.E. Jr., "Conductivity of Fracture Proppants in Multiple Layers," Journal of Pet. Tech, Vol. 25, (1973), pp. 1101-1107.

APPENDIX A: Derivation of the Propped Fracture Length Equation Proposed by McLeod (9).

The following discussion presents a derivation of equations [10] and [11] of McLeod (9). This derivation has not been presented nor confirmed by McLeod, but does result in the same equations proposed by him. It is shown here as a prelude to the modifications presented in Appendix B.

McLeod (9) uses the fracture area equation of Carter (40), and the width equations shown by Geertsma and deKlerk (13) for Perkins and Kern (20) to solve iteratively for created width and length. Geertsma and Haafkens (41) present an excellent comparison of these equations with expected results, and the reader may consult this work for further reference.

Two assumptions are used to derive the formula for propped width, equation [10] of McLeod. The assumptions are stated as equations [3] and [4], and repeated here,

$$V_{si} = V_{fc} \quad [3]$$

where  $V_{si}$  = volume of slurry injected.

$$V_{fc} = \text{volume of created fracture.}$$

and,

$$V_{pi} = V_{fp}(1-\phi_f) \quad [4]$$

ER-2989

where  $V_{pi}$  = volume of proppant injected.  
 $V_{fp}$  = volume of propped fracture.  
 $\phi_f$  = in-situ porosity of proppant in the fracture.

Note that Eq. 3 assumes there is no fluid leak-off for the final fluid segment. The volume concentration of proppant can be found from the weight concentration as follows:

$$c_v = c_w \text{ (lb/gal) } * 1/\rho_p \text{ (cc/gr) } * (454\text{gr/lb) } * \\ (\text{ft}/30.48 \text{ cm})^3 * (7.48 \text{ gal/ft}^3) \\ c_v = c_w (.120/\rho_p) \quad [A1]$$

where  $c_v$  = volume concentration of proppant, gal - prop/gal - fluid.  
 $c_w$  = weight concentration of proppant, lb - prop/gal - fluid.  
 $\rho_p$  = density of proppant, gm/cc.

In a similar manner, the total proppant volume is:

$$V_p = W_p (.120/\rho_p) \quad [A2]$$

where  $V_p$  = volume of proppant, gal.  
 $W_p$  = total proppant weight, lb.

If proppant density is taken to be 2.65 gm/cc, the equations become:

$$c_v = .0452 c_w \\ V_p = .0452 W_p$$

Returning to Eq. 3, the slurry volume of the final segment can be written:

$$V_{si} = V_{li} (1 + .045 c_w)$$

where  $V_{li}$  = volume of proppant ladden liquid pumped, gal

$c_w$  = final average sand concentration pumped, lb/gal - fluid

Eq. 3 can be written as:

$$V_{li} (1 + .045 c_w) = 2w_{cw}hx \quad [A3]$$

where  $w_{cw}$  = created fracture width at the well-bore

$h$  = fracture height

$x$  = fracture half-length created by  $V_{si}$

Solving for  $V_{li}$

$$V_{li} = (2w_{cw}hx)/(1 + .045c_w)$$

Eq. 4 can be written as:

$$V_{li} (.045c_w) = 2w_{pw}hx (1-\phi_f) \quad [A4]$$

where  $w_{pw}$  = propped fracture width at the well-bore

Substituting Eq. A3 into A4 leads to:

$$w_{pw} = w_{cw} \left[ \frac{(.045c_w)}{(1 + .045c_w)} \right] \frac{1}{(1-\phi_f)}$$

If  $\phi_f$  is taken as 0.40, the result is:

$$w_{pw} = .0753 w_{cw} \left[ \frac{c_w}{(1 + .045c_w)} \right] \quad [A5]$$

ER-2989

If the packed fracture width is assumed to be constant for the entire fracture, the average width is equal to the width at the wellbore. The propped length can be determined using a volumetric relationship,

$$V_{fpc} = 2\bar{w}_p hL_p (1-\phi_f) \quad [A6]$$

where  $V_{fpc}$  = propped fracture volume after closure

$\bar{w}_p$  = avg. propped fracture width, in

$h$  = fracture height, ft

$L_p$  = propped fracture half-length, ft

Assuming  $\bar{w}_p = w_{pw}$  and  $\phi_f = 0.40$ , and converting to field units,

$$L_p = .0604 \left[ \frac{W_p}{\bar{w}_p h} \right] \approx .60^{1/2} \left[ \frac{W_p}{h} \right] \quad [A7]$$

*Total propped length*  
*Eqn A5*

Eq. A5 and A7 are virtually identical to equations 10 and 11 of McLeod.

The following discussion is presented to demonstrate that the McGuire and Sikora charts are not generally suitable for tight-gas reservoirs. The transition to pseudo-steady state occurs when

$$t_{de} \approx 0.25$$

where

$$t_{de} = (.0002645 kt) / (\phi \mu c r_e^2)$$

$k$  = reservoir permeability, md

$t$  = time, hr  
 $\phi$  = porosity, fraction of 1.00  
 $\mu$  = reservoir fluid viscosity, cp  
 $c$  = total compressibility, 1/psi  
 $r_e$  = drainage radius, ft

Setting  $t_{de} = 0.25$  and solving for the time required to reach pseudo-steady state,

$$t_{pss} = \frac{\phi \mu c r_e^2}{.0002645k} t_{de}$$

For a typical Muddy "J" Wattenberg well, the solution is:

$$\begin{aligned}
 t_{pss} &= \frac{(.12)(.02)(.0002)(1489)^2}{.0002645(.01)} \quad (0.25) \\
 &= 100,587 \text{ Hrs} \\
 &= \underline{11.5 \text{ Years}}
 \end{aligned}$$

In other words, a Muddy "J" well would have to produce continuously for 11.5 years to reach pseudo-steady state. The McGuire and Sikora charts are of little practical use for such a well.

APPENDIX B: Modification of the McLeod Method

The following discussion is based on personal communication with Dr. James Crafton (42). The derivation is a condensed version of his work.

Sneddon & Elliot (43) present an equation for the displacement of the fracture face of a two-dimensional crack,

$$w(y) = \left[ \frac{2(1-\nu^2)P_0}{E} \right] (a^2 - y^2)^{\frac{1}{2}} \quad [B1]$$

where  $w(y)$  = crack width at the  $y$  location of the major axis of an ellipse  
 $\nu$  = Poisson's ratio  
 $E$  = Young's modulus of elasticity  
 $P_0$  = pressure within the crack in excess of stress  
 $a$  = maximum length of the crack

Eq. B1 has the form of an ellipse,

$$\frac{y^2}{a^2} + \frac{w^2}{b^2} = 1 \quad (2)?$$

where

$$b = \frac{w(1-\nu^2)P_0 a}{E}$$

= maximum width of the ellipsoidal crack

The average crack width is then

$$w_{av} = \frac{\int_0^a w(y) dy}{\int_0^a dy}$$

$$\begin{aligned}
&= \frac{1}{a} \int_0^a w(y) dy \\
&= \frac{2(1-\nu^2)P_0}{aE} \int_0^a (a^2 - y^2)^{\frac{1}{2}} dy \\
&= \frac{b}{a^2} \left[ y(a^2 - y^2)^{\frac{1}{2}} + a^2 \sin^{-1}(y/a) \right]_0^a \\
&= \frac{\pi}{4} b
\end{aligned}$$

$$w_{av} = .785b \quad [B2]$$

Perkins and Kern (20) use Eq. B1 and the flow equation of a slot to derive their width equation for a fracture,

$$w(o,t) = 3.0045 \left[ \frac{q\mu L(1-\nu)}{G} \right]^{\frac{1}{4}} \quad [B3]$$

where

- q = flowrate into one fracture wing
- L = fracture length
- G = shear modulus

The width at any location x, can be found from:

$$w(x,t) = 3.0045 \left[ \frac{q\mu(L-x)(1-\nu)}{G} \right]^{\frac{1}{4}}$$

and

$$\begin{aligned}
\frac{w(x,t)}{w(o,t)} &= \frac{(L-x)^{\frac{1}{4}}}{L^{\frac{1}{4}}} \\
&= (1-f_1)^{\frac{1}{4}}
\end{aligned}$$

where

$$f_1 = x/L$$

The average fracture width along the length is then:

$$\begin{aligned} w_{al} &= w(o,t) \int_0^1 (1-f_1)^{\frac{1}{4}} df_1 \\ &= w(o,t) \left[ -(4/5)(1-f_1)^{5/4} \right]_0^1 \\ w_{al} &= 4/5 w(o,t) \end{aligned} \quad [B4]$$

From Eq. B2, the average width in the vertical direction is:

$$w_{av} = .785 w(o,t) \quad [B5]$$

Combining Eq. B4 and B5, the average width overall is:

$$\begin{aligned} \bar{w} &= (.7854)(.80)w(o,t) \\ &= .62832 w(o,t) \end{aligned} \quad [B6]$$

Eq. B6 is used in the iterative solution for created fracture length, created fracture width, and apparent fluid viscosity. The fracture length is from Carter's (40) area equation,

$$L = \frac{\bar{w}qf(x)}{8\pi c^2 h} \quad [B7]$$

where  $f(x) = e^{x^2} \operatorname{erfc}(x) + 2x/\pi^{\frac{1}{2}} - 1$

$$x = \frac{2c}{\bar{w}} (\pi t)^{\frac{1}{2}}$$

$c$  = fluid loss coefficient

The equations for propped fracture dimensions are derived using Eq. 6, as discussed in the body of this report. Specifically,

ER-2989

$$E_s = V_{cs}/V_{si} \quad [6]$$

where

$E_s$  = frac fluid (slurry) efficiency

$V_{cs}$  = volume of fracture created by slurry

$V_{si}$  = volume of slurry injected

The volume of the fracture when pumping stops is:

$$V_{fp} = V_{li} * E_s + .045 W_p \quad [B8]$$

Also, when pumping stops,

$$V_{fp} \cong 2hL_p \bar{w}_p \quad [B9]$$

where

$L_p$  = final propped fracture length

Eq. B9 assumes that the fracture tip closes, but the average fracture width does not change significantly when pumping stops.

Rewriting Eq. 4 for total proppant volume,

$$V_{fpc} = 2hL_p \bar{w}_p (1-\phi_f) \quad [B10]$$

where

$V_{fpc}$  = propped fracture volume after closure

Solving for  $\bar{w}_p$

$$\bar{w}_p = \frac{.045 W_p}{2hL_p (1-\phi_f)} \quad [B11]$$

ER-2989

Substituting Eq. B8 and B9

$$\begin{aligned}
 \bar{w}_p &= \frac{.045 W_p}{2h(1-\phi_f)} * \frac{2h\bar{w}}{V_{li}E_s + .045 W_p} \\
 &= \frac{.045 \bar{c}_w V_{li}}{(1-\phi_f)} * \frac{\bar{w}}{V_{li}E_s + .045 \bar{c}_w V_{li}} \\
 &= \frac{\bar{w}}{(1-\phi_f)} * \frac{.045 \bar{c}_w}{(E_s + .045 \bar{c}_w)}
 \end{aligned}$$

where

$$\bar{c}_w = \text{overall avg. proppant concentration,} \\
 \text{lb/gal-fluid}$$

Substituting Eq. B6 and taking  $\phi_f = .30$ , from ref. 44,

$$\begin{aligned}
 \bar{w}_p &= \frac{.62832 w(o,t)}{.70} * \frac{.045 \bar{c}_w}{E_s + .045 \bar{c}_w} \\
 &= .0404 w(o,t) \left[ \frac{\bar{c}_w}{(E_s + .045 \bar{c}_w)} \right] \quad [B12]
 \end{aligned}$$

Solving Eq. B11 for  $L_p$ , and  $\phi_f = .30$ , and converting to consistent units,

$$L_p = .0518 \left[ \frac{W_p}{h \bar{w}_p} \right] \quad [B13]$$

Eq. B12 and B13 are used to calculate propped fracture lengths for this report. Note that Eq. B12 is similar to Eq. A5,

ER-2989

which represents McLeod's equation 10. The main difference is the inclusion of the fluid efficiency term,  $E_s$ , in Eq. B12, which leads to the conclusion that McLeod assumes a fluid efficiency of 1 (i.e., no fluid loss). The difference in the coefficients, 0.0753 and 0.0404, is due to the different in-situ porosities assumed, and converting to an average created width with the 0.62832 multiplier. Equations B13 and A7 are identical except for the in-situ porosities.

ER-2989

APPENDIX C: Fracture Treatment Data and Fracture Dimensions.

Tables C1 - C4 contain treatment data and results of fracture calculations for the wells studied in this report.

"Frac no." signifies original completions (1) or re-fracture treatments (2).

TABLE C1 - FLUID VOLUMES AND SAND WEIGHTS

Well No.	Frac No.	Fluid Type	Fluid Vol (M Gal)	Pad Vol (M Gal)	Sand Wt (M Lb)	Max SCC 1 (PPG)
101	1	EMUL	155	21	270	4.0
102	1	EMUL	281	29	599	6.0
103	1	GEL H2O	182	26	832	7.0
104	1	GEL H2O	191	26	832	7.0
105	1	GEL H2O	30	5	28	1.5
105	2	GEL H2O	131	25	360	5.0
106	1	GEL H2O	144	30	360	4.0
107	1	GEL H2O	131	55	602	6.0
108	1	GEL H2O	140	45	600	6.0
109	1	EMUL	162	21	270	4.0
110	1	EMUL	168	21	277	6.0
111	1	GEL H2O	139	26	727	7.0
112	1	GEL H2O	154	26	832	7.0
113	1	EMUL	268	29	599	6.0
114	1	GEL H2O	154	26	832	7.0
115	1	GEL H2O	194	26	732	5.0
118	1	OIL GEL	37	5	45	1.5
119	1	EMUL	277	29	599	6.0
122	1	GEL H2O	135	19	832	8.0
123	1	GEL H2O	183	26	832	7.0
124	1	GEL H2O	190	26	832	7.0
125	1	EMUL	65	6	104	4.0
125	2	GEL H2O	111	25	366	5.0
126	1	EMUL	302	29	599	6.0
127	1	GEL H2O	153	26	807	8.0
128	1	GEL H2O	140	30	450	6.0
129	1	EMUL	168	21	415	4.0
130	1	EMUL	286	29	735	6.0

<u>Well No.</u>	<u>Frac No.</u>	<u>Fluid Type</u>	<u>Fluid Vol (M Gal)</u>	<u>Pad Vol (M Gal)</u>	<u>Sand Wt (M Lb)</u>	<u>Max SCC 1 (PPG)</u>
132	1	GEL H20	167	26	832	9.0
133	1	GEL H20	36	5	45	1.5
134	1	GEL H20	158	26	832	7.0
135	1	GEL H20	191	26	832	7.0
136	1	GEL H20	171	26	971	8.0
137	1	EMUL	151	21	270	4.0
138	1	EMUL	267	29	599	6.0
139	1	GEL H20	154	26	832	7.0
140	1	GEL H20	186	26	832	7.0
141	1	EMUL	281	29	599	6.0
143	1	GEL H20	219	30	842	5.0
144	1	GEL H20	311	25	542	5.0
145	1	EMUL	162	21	277	6.0
146	1	EMUL	315	29	735	6.0
147	1	GEL H20	154	26	832	7.0
149	1	EMUL	52	8	114	4.0
149	2	GEL H20	161	30	300	4.0
150	1	EMUL	244	29	525	6.0
151	1	GEL H20	169	50	471	6.0
152	1	GEL H20	39	6	39	1.0
154	1	EMUL	174	21	277	6.0
159	1	GEL H20	40	10	97	4.0
161	2	GEL H20	168	50	499	6.0
162	1	EMUL	281	29	599	6.0
163	1	GEL H20	172	50	471	6.0
165	2	GEL H20	236	25	515	5.0
166	1	GEL H20	168	50	499	6.0
167	1	GEL H20	169	50	499	6.0
168	1	EMUL	162	21	270	4.0
169	1	EMUL	281	29	599	6.0

<u>Well No.</u>	<u>Frac No.</u>	<u>Fluid Type</u>	<u>Fluid Vol (M Gal)</u>	<u>Pad Vol (M Gal)</u>	<u>Sand Wt (M Lb)</u>	<u>Max SCC 1 (PPG)</u>
170	1	GEL H20	188	26	832	7.0
171	1	GEL H20	154	26	832	7.0
173	1	GEL H20	177	50	352	4.0
174	1	EMUL	162	21	270	4.0
175	1	EMUL	275	29	599	6.0
176	1	GEL H20	186	26	802	7.0
177	1	GEL H20	35	6	45	1.5
178	1	EMUL	281	29	599	6.0
182	1	GEL H20	271	60	720	5.0
183	1	GEL H20	169	83	641	6.0
184	1	GEL H20	168	50	499	6.0
188	1	EMUL	244	29	525	6.0
190	1	EMUL	210	29	531	4.0
193	1	EMUL	285	29	735	6.0
195	1	GEL H20	147	26	822	7.0
196	1	EMUL	275	29	565	6.0
197	1	EMUL	286	29	735	6.0
198	1	GEL H20	148	15	690	7.0

Notation: 1 - Maximum sand concentration pumped

TABLE C2 - FRAC FLUID PROPERTIES

Well No.	Frac No.	Ge1 CC 1 (Lb/M Gal)	n'	k'	FLC (Ft/Min* $\frac{1}{2}$ )	ATP <sup>2</sup> (PSIG)	ATR <sup>3</sup> (BPM)	HC <sup>4</sup> Used	SF/SL Ratio
101	1	60	.440	.05700	.00050	3900	28	Y	.73
102	1	60	.480	.03500	.00050	4950	26	Y	.75
103	1	60	.680	.01300	.00040	2800	30	Y	.00
104	1	60	.680	.01300	.00040	2400	35	Y	.00
105	1	40	.630	.00300	.00240	3100	30	N	.00
105	2	50	.850	.00190	.00040	2800	35	Y	.00
106	1	60	.573	.01290	.00050	3000	25	Y	.00
107	1	60	.720	.00650	.00040	2600	35	Y	.00
108	1	60	.720	.00650	.00040	2700	35	Y	.00
109	1	60	.440	.05700	.00050	4100	28	Y	1.40
110	1	60	.440	.05700	.00050	4200	26	Y	1.40
111	1	50	.633	.01870	.00050	2600	35	Y	.00
112	1	50	.633	.01870	.00050	2800	35	Y	.00
113	1	60	.480	.03500	.00050	6450	12	Y	.75
114	1	50	.633	.01870	.00050	2800	35	Y	.00
115	1	60	.680	.01300	.00040	3000	30	Y	.00
118	1	0	.205	.19500	.00050	3500	41	Y	.00
119	1	60	.440	.05700	.00050	4450	28	Y	.38
122	1	60	.680	.01300	.00040	2200	30	Y	.00
123	1	50	.633	.01870	.00050	2300	35	Y	.00
124	1	30	.656	.02700	.00040	2550	35	Y	.00
125	1	60	.440	.05700	.00050	4500	25	Y	1.13
125	2	50	.539	.02210	.00050	2600	35	Y	.00
126	1	60	.440	.05700	.00050	4200	27	Y	.75
127	1	60	.680	.01300	.00040	2500	28	Y	.00
128	1	60	.720	.00650	.00040	1700	30	Y	.00
129	1	60	.440	.05700	.00050	4500	22	Y	.00
130	1	60	.440	.05700	.00050	4350	25	Y	.75

Well No	Frac No.	Gel CC 1 (Lb/M Gal)	n'	k'	FLC (Ft/Min* $\frac{1}{2}$ )	ATP <sup>2</sup> (PSIG)	ATR <sup>3</sup> (BPM)	HC <sup>4</sup> Used	SF/SL Ratio
132	1	60	.680	.01300	.00040	3500	35	Y	.00
133	1	60	.470	.02100	.00200	3700	42	N	.00
134	1	60	.680	.01300	.00040	2350	29	Y	.00
135	1	60	.680	.01300	.00040	2600	35	Y	.00
136	1	50	.633	.01870	.00050	2650	35	Y	.00
137	1	60	.440	.05700	.00050	3000	25	Y	1.40
138	1	60	.440	.05700	.00050	4200	26	Y	.75
139	1	50	.633	.01870	.00050	2700	35	Y	.00
140	1	60	.680	.01300	.00040	2500	35	Y	.00
141	1	60	.480	.03500	.00050	3000	30	Y	.75
143	1	35	.608	.04100	.00040	2450	35	Y	.00
144	1	35	.608	.04100	.00040	2180	35	Y	.00
145	1	60	.440	.05700	.00050	4300	25	Y	1.50
146	1	0	.470	.08000	.00040	4450	25	N	.75
147	1	30	.656	.02700	.00040	2500	35	Y	.00
149	1	50	.520	.03900	.00050	4000	26	Y	.75
149	2	50	.720	.00260	.00200	2300	30	N	.67
150	1	60	.440	.05700	.00050	4400	24	Y	.68
151	1	50	.720	.00260	.00200	3100	35	N	.30
152	1	20	.860	.00007	.00300	3800	30	N	.00
154	1	60	.440	.05700	.00050	6200	11	Y	1.40
159	1	50	.608	.02300	.00220	2450	30	N	.00
161	2	50	.720	.00260	.00200	2300	30	N	.30
162	1	60	.440	.05700	.00050	3800	22	Y	.75
163	1	50	.720	.00260	.00200	2900	30	N	.30
165	2	50	.720	.00260	.00200	5300	21	N	.50
166	1	50	.720	.00260	.00200	3300	30	N	.30
167	1	50	.720	.00260	.00200	3000	30	N	.30
168	1	60	.440	.05700	.00050	4400	26	Y	1.40
169	1	60	.440	.05700	.00050	4200	28	Y	.75

Well No.	Frac No.	Ge1 CC 1 (Lib/M Gal)	n'	k'	FLC (Ft/Min* $\frac{1}{2}$ )	ATP <sup>2</sup> (PSIG)	ATR <sup>3</sup> (BPM)	HC <sup>4</sup> Used	SF/SL Ratio	5
170	1	30	.656	.02700	.00040	2500	35	Y	.00	
171	1	50	.633	.01870	.00050	2200	35	Y	.00	
173	1	60	.573	.01290	.00210	2200	20	N	.70	
174	1	60	.440	.05700	.00050	3850	30	Y	1.40	
175	1	60	.480	.03500	.00050	6400	15	Y	.75	
176	1	60	.680	.01300	.00040	2000	30	Y	.00	
177	1	60	.470	.02100	.00200	3400	45	N	.00	
178	1	60	.440	.05700	.00050	4200	28	Y	.75	
182	1	60	.680	.01300	.00040	3000	35	Y	.00	
183	1	60	.680	.01300	.00040	2800	34	N	.00	
184	1	50	.720	.00260	.00200	2650	30	N	.30	
188	1	60	.440	.05700	.00050	4350	22	Y	.68	
190	1	60	.440	.05700	.00050	2600	17	Y	.00	
193	1	50	.570	.02400	.00050	4250	30	Y	.66	
195	1	35	.608	.04100	.00040	0	35	Y	.00	
196	1	60	.480	.03500	.00050	4450	27	Y	.75	
197	1	60	.440	.05700	.00050	4400	21	Y	.75	
198	1	60	.680	.01300	.00040	2300	35	Y	.00	

## Notation:

- 1 - Gelling agent concentration
- 2 - Avg. treatment pressure
- 3 - Avg. treatment rate
- 4 - Was hydrocarbon used in treatment fluid (yes/no)
- 5 - Ratio of spacer fluid/slurry volume for pillar-fracs

TABLE C3 - CREATED FRACTURE DIMENSIONS

Well No.	Frac No.	$\mu$ l (CP)	$E_f$ 2 (Vol/Vol)	$W_{cw3}$ (In)	Lc4 (Ft)
101	1	222.9	0.6138	0.4931	2224.
102	1	245.7	0.5566	0.5457	3260.
103	1	195.6	0.6534	0.5200	2927.
104	1	504.4	0.7346	0.6682	2652.
105	2	85.9	0.6588	0.4243	2531.
105	1	22.1	0.2279	0.1856	421.
106	1	76.3	0.5222	0.3772	2492.
107	1	141.7	0.6724	0.4914	2760.
108	1	270.2	0.7097	0.5646	2522.
109	1	564.3	0.6723	0.6087	2040.
110	1	330.1	0.6199	0.5339	2222.
111	1	217.1	0.6538	0.5242	2334.
112	1	596.7	0.7112	0.6652	2201.
113	1	919.9	0.4973	0.5907	2589.
114	1	303.3	0.6674	0.5736	2395.
115	1	518.6	0.7099	0.6461	2631.
118	1	354.8	0.8012	0.4618	734.
119	1	365.8	0.5998	0.6072	3117.
122	1	189.3	0.6724	0.4942	2466.
123	1	782.0	0.7238	0.7226	2339.
124	1	1059.4	0.7772	0.7832	2383.
125	1	457.9	0.7063	0.4772	1064.
125	2	148.0	0.6494	0.4604	2036.
126	1	540.4	0.6154	0.6649	3146.
127	1	194.7	0.6518	0.4991	2671.
128	1	273.9	0.6975	0.5353	2346.
129	1	504.3	0.6149	0.5642	2145.
130	1	550.9	0.6042	0.6510	3061.
132	1	257.3	0.6987	0.5669	2693.
133	1	159.1	0.4684	0.3523	541.

<u>Well No.</u>	<u>Frac No.</u>	<u><math>\mu</math> l (CP)</u>	<u><math>E_f</math> 2 (Vol/Vol)</u>	<u><math>W_{cw3}</math> (In)</u>	<u><math>Lc_4</math> (Ft)</u>
134	1	194.2	0.6563	0.5059	2731.
135	1	504.3	0.7337	0.6680	2649.
136	1	374.2	0.6742	0.6120	2516.
137	1	1314.7	0.7209	0.7068	1782.
138	1	372.7	0.5903	0.5950	3036.
139	1	303.3	0.6678	0.5737	2396.
140	1	502.9	0.7354	0.6651	2611.
141	1	699.0	0.6634	0.7169	2958.
143	1	526.3	0.7291	0.6894	2879.
144	1	919.5	0.7497	0.8109	3155.
145	1	331.8	0.6153	0.5258	2164.
146	1	731.4	0.6672	0.7143	3343.
147	1	531.7	0.7475	0.6565	2344.
149	1	706.2	0.7504	0.5148	898.
149	2	32.1	0.1844	0.2666	1232.
150	1	375.0	0.5816	0.5748	2848.
151	1	32.2	0.1873	0.2898	1469.
152	1	2.1	0.0908	0.1012	397.
154	1	311.3	0.4376	0.4167	2067.
159	1	180.6	0.3890	0.3411	587.
161	2	44.9	0.1888	0.3009	1428.
162	1	572.3	0.5875	0.6318	2972.
163	1	32.8	0.1688	0.2769	1403.
165	2	46.4	0.1358	0.2666	1218.
166	1	32.7	0.1678	0.2758	1384.
167	1	44.8	0.1846	0.2996	1408.
168	1	467.1	0.6455	0.5728	2081.
169	1	367.2	0.5998	0.6093	3147.
170	1	396.4	0.7211	0.6327	2713.
171	1	597.2	0.7152	0.6660	2211.
173	1	275.0	0.2568	0.4183	1307.
174	1	311.1	0.6456	0.5439	2201.

<u>Well No.</u>	<u>Frac No.</u>	<u><math>\mu</math>l (CP)</u>	<u>E<sub>f</sub> 2 (Vol/Vol)</u>	<u>W<sub>cw3</sub> (In)</u>	<u>Lc4 (Ft)</u>
175	1	287.9	0.4539	0.4828	2955.
176	1	196.0	0.6558	0.5218	2961.
177	1	90.4	0.4325	0.3140	561.
178	1	367.1	0.5999	0.6091	3145.
182	1	200.2	0.6518	0.5824	3857.
183	1	265.6	0.6838	0.5874	3095.
184	1	54.3	0.1973	0.3153	1424.
188	1	553.3	0.5931	0.6130	2724.
190	1	411.1	0.5391	0.5253	2558.
193	1	332.3	0.6036	0.6100	3260.
195	1	694.4	0.8006	0.6974	2285.
196	1	942.7	0.6608	0.7412	2784.
197	1	408.8	0.5484	0.5809	3113.
198	1	251.6	0.7132	0.5474	2395.

## Notation:

- 1 - Apparent viscosity
- 2 - Fluid efficiency
- 3 - Created width at the wellbore
- 4 - Created length

TABLE C4 - PROPPED FRACTURE DIMENSIONS

Well No.	Frac No.	W <sub>fpc</sub> (in)	L <sub>p</sub> (ft)	C <sub>a1</sub> (lb/ft <sup>2</sup> )	F <sub>cd</sub>
101	1	0.0502	2064.	0.484	23.20
102	1	0.0723	3179.	0.698	41.38
103	1	0.1120	2849.	1.082	51.88
104	1	0.1268	2518.	1.224	64.13
105	2	0.0605	2283.	0.584	39.15
105	1	0.0261	412.	0.252	568.24
106	1	0.0603	2290.	0.582	76.84
107	1	0.1043	2215.	1.006	63.47
108	1	0.1088	2115.	1.051	68.49
109	1	0.0551	1880.	0.532	26.67
110	1	0.0513	2073.	0.495	41.38
111	1	0.1252	2228.	1.209	71.82
112	1	0.1529	2088.	1.476	88.91
113	1	0.0895	2568.	0.864	56.45
114	1	0.1382	2310.	1.334	74.48
115	1	0.1125	2496.	1.086	59.39
118	1	0.0265	651.	0.256	720.67
119	1	0.0765	3006.	0.738	44.85
122	1	0.1302	2452.	1.257	67.15
123	1	0.1435	2224.	1.386	79.60
124	1	0.1429	2234.	1.380	78.99
125	1	0.0397	1006.	0.383	39.94
125	2	0.0773	1818.	0.746	60.22
126	1	0.0758	3032.	0.732	49.04
127	1	0.1198	2585.	1.156	59.96
128	1	0.0830	2082.	0.801	55.77
129	1	0.0778	2046.	0.751	74.12
130	1	0.0944	2989.	0.911	48.52
132	1	0.1241	2573.	1.198	61.78
133	1	0.0341	507.	0.329	550.39

Well No.	Frac. No.	$W_{fpc}$ (in)	$L_p$ (ft)	$C_{a1}$ (lb/ft <sup>2</sup> )	$F_{cd}$
134	1	0.1206	2647.	1.164	58.82
135	1	0.1269	2516.	1.225	64.21
136	1	0.1514	2460.	1.462	74.93
137	1	0.0638	1623.	0.616	45.34
138	1	0.0784	2932.	0.757	46.50
139	1	0.1381	2311.	1.333	74.43
140	1	0.1290	2476.	1.245	66.05
141	1	0.0816	2816.	0.788	49.30
143	1	0.1190	2716.	1.148	56.80
144	1	0.0693	3002.	0.669	33.34
145	1	0.0527	2016.	0.509	41.08
146	1	0.0875	3224.	0.844	43.14
147	1	0.1454	2196.	1.403	81.37
149	1	0.0540	811.	0.521	65.23
149	2	0.0751	1533.	0.725	111.49
150	1	0.0739	2725.	0.713	48.75
151	1	0.1049	1723.	1.012	77.58
152	1	0.0303	494.	0.292	297.14
154	1	0.0528	2015.	0.509	43.22
159	1	0.0674	552.	0.651	178.09
161	2	0.1125	1702.	1.086	82.77
162	1	0.0799	2876.	0.771	47.82
163	1	0.1054	1714.	1.018	78.27
165	2	0.1010	1957.	0.975	96.41
166	1	0.1104	1735.	1.065	80.07
167	1	0.1132	1692.	1.092	83.57
168	1	0.0538	1926.	0.519	25.72
169	1	0.0757	3036.	0.731	44.21
170	1	0.1235	2584.	1.192	61.33
171	1	0.1525	2094.	1.472	88.47
173	1	0.0973	1388.	0.939	120.92
174	1	0.0508	2038.	0.491	16.54

<u>Well No.</u>	<u>Frac. No.</u>	<u>W<sub>fpc</sub> (in)</u>	<u>L<sub>p</sub> (ft)</u>	<u>C<sub>a1</sub> (lb/ft<sup>2</sup>)</u>	<u>F<sub>cd</sub></u>
175	1	0.0772	2978.	0.745	45.46
176	1	0.1071	2872.	1.034	49.88
177	1	0.0334	517.	0.323	487.12
178	1	0.0758	3034.	0.731	44.26
182	1	0.0823	3400.	0.784	33.56
183	1	0.1059	2324.	1.022	58.77
184	1	0.1149	1667.	1.109	85.73
188	1	0.0775	2599.	0.748	52.04
190	1	0.0826	2467.	0.797	47.32
193	1	0.0886	3184.	0.855	43.98
195	1	0.1503	2098.	1.451	87.34
196	1	0.0821	2642.	0.792	53.23
197	1	0.0913	3090.	0.881	46.05
198	1	0.1122	2360.	1.083	62.71

Notation:

1 - Areal Sand Concentration after closure

APPENDIX D: Procedure for Economic Calculations.

Net Present Value and undiscounted Profit/Investment ratio are calculated using constant operating costs and gas prices, as shown in Table 5. The procedure used is as follows:

- 1) Data is organized for each well using the system 1022 Program, ECONF.DMC. The data includes well number, fracture treatment information, and cumulative production at yearly intervals.
- 2) Treatment costs are computed by adding fluid, proppant, hydraulic horsepower and fixed costs, as follows:

$$\text{FLDCST} = \text{GELVOL} * \text{GELCST} + \text{HCVOL} * \text{HLCST} + \text{MEVOL} * \text{MECST}$$

where           FLDCST = total fluid cost  
                   GELVOL = gel volume, gal  
                   HCVOL  = hydrocarbon volume, gal  
                   MEVOL  = methanol volume, gal

The total treatment cost is,

$$\text{JOB CST} = \text{FLDCST} + \text{SANDWT} * \text{SND CST} + \text{HHP} * \text{HHPCST} + \text{SETCST}$$

- 3) The program enters a loop to compute revenues, net present value (NPV) and profit/investment (PI) for n years as follows:

$$\text{Gross revenue} = (\text{CUMPRO}(n) - \text{CUMPRO}(n-1)) * \text{Gas Price}$$

$$\text{Net Revenue} = (\text{Gross revenue}) * \text{NRI} * (1 - \text{SEVTAX}) + (1 - \text{ADVAL})$$

where CUMPRO = cumulative production at n  
years

NRI = net revenue interest, fraction

SEVTAX = severance tax, fraction

ADVAL = advalorem tax, fraction

NOI(n) = net revenue - yearly operating cost

where NOI(n) = net operating income for year n

$NPV(n) = NPV(n-1) + (NOI(n)/(1 + i)^{n-\frac{1}{2}})$   
If  $n = 1$ , then  $NPV(n) = NPV(n) - JOBCST$

CUMNOI = CUMNOI + NOI(n)

PI(n) = (CUMNOI/JOBCST) - 1

- 4) The program computes NPV and PI for each year until it encounters a cumulative production of zero or until the desired number of years are executed. The program then returns to step 2 for a new well.

ER-2989

APPENDIX E: Structure of the 1022 Data Base used for this Study.

The system 1022 data base management system on the Colorado School of Mines DEC10 #2 (MUNCH) computer is used to store and organize the data used in this report. Nine data sets make up the data base, as follows:

<u>Primary Data Sets</u>	<u>Description</u>	<u>Source</u>
BASDAT	Basic Well Data	PI Scout Cards Colorado O&GC
PRODAT	Monthly Production Data	Panhandle Eastern Pipeline Co.
FRCDAT	Fracture Treatment Data	Fracture treatment reports from Amoco, Coors, Macey & Mershon, MGF, and Vessels
VOLDAT	Volumetric Data	Well Logs from Various Sources
GASDAT	Gas Analysis	Laboratory Reports
<u>Secondary Data Sets</u>	<u>Description</u>	<u>Source</u>
FRCDIM	Fracture Dimensions	MCLEOD.FOR Program
CUMPRO	Yearly Cumulative Production & Recoveries	CUMPRO.DMC Program
DAYRA	Avg. Daily Production Rates	CUMPRO.DMC Program
ECONF	Job Cost, NPV and P/I Ratio	ECONF.FOR Program

ER-2989

Complete descriptions of the contents of each data set may be found in corresponding description files, with the .DMD extension. The primary data sets are those which contain raw data collected from respective sources. Secondary data sets contain data generated by the programs listed.

The system 1022 permits the construction of simple programs such as the one used to generate the CUMPRO and DAYRA data sets above. These programs have a .DMC file extension, and are used to generate reports to check data entries and data files to use in plotting. The command programs currently available are:

<u>.DMC Program</u>	<u>Output File</u>	
	<u>Name</u>	<u>Contents</u>
PRODAT	PRODAT.CHK	Monthly Production Data
FRCDAT	FRCDAT.CHK	Fracture Treatment Data
VOLDAT	VOLDAT.CHK	Volumetric Data
CUMPRO	CUMPRO.DMI DAYRA.DMI	Cumulative Prod. Data Avg. Daily Rates
MCLEOD	MCLEOD.DAT	Data required to run MCLEOD.FOR
ECONF	ECONF.DAT	Data required to run ECONF.FOR
YR1 YR2 YR8	YR1.DAT YR2.DAT YR8.DAT	Data for all Wells with one, two, or eight Years of Production. Used for Plots.
TFLUID	EMUL.DAT	Data for Emulsion Treat- ments

<u>.DMC</u> <u>Program</u>	<u>Output File</u>	
	<u>Name</u>	<u>Contents</u>
	XLGEL.DAT	Data for Cross-linked Gel Treatments
PFRAC	PILFRC	Data for Pillar Frac Treatments
	PACFRC	Data for Packed Frac Treatments
FLC	HIFLC	Data for High FLC Treat- ments
	LOFLC	Data for Low FLC Treat- ments

Files and programs can be transferred from the DEC10 #2 to the DEC10 #1 with the use of the KERMIT program. All plots were run on the DEC10 #1.

APPENDIX F: Procedure to Test for Parallelism of Slopes

The procedure to test for parallelism is taken from Ref. 33. An example of the calculations for Figure 21 and results from all calculations are presented. The equations used are:

$$S_{\hat{\beta}_{1A}}^2 = \frac{S_{y|xA}^2}{(n-1)S_{xA}^2} \quad [F1]$$

where  $S_{\hat{\beta}_{1A}}^2$  = variance of the estimated slope  $\hat{\beta}_{1A}$  for data group A.

$S_{y|xA}^2$  = residual mean square error for data group A.

$n$  = number of sample data points for group A.

$S_{xA}^2$  = sample variance of x's for data group A.

The test statistic is:

$$Z = \frac{\hat{\beta}_{1A} - \hat{\beta}_{1B}}{\left[ S_{\hat{\beta}_{1A}}^2 + S_{\hat{\beta}_{1B}}^2 \right]^{1/2}} \quad [F2]$$

where

$\hat{\beta}_{1A}$  = estimated slope for group A

$\hat{\beta}_{1B}$  = estimated slope for group B

The value of Z is compared to the Student's t value for a 95% confidence interval. The Student's t value represents the upper 95% point of the standard normal distribution of the test statistic. For the cases investigated, the Student's t is equal to 1.990. The results for figure 21 are as follows:

	<u>CLG</u>	<u>PE</u>
$S_{y x}$	99.1212	63.3697
$S_x^2$	10714.48	3725.03
n	84	79
$\hat{\beta}_1$	0.16507	0.2915
$S_{\hat{\beta}}^2$	0.11048	0.13821

$$Z = 0.82 < 1.99$$

Since Z is less than the Student's t value, the hypothesis that the slopes are equal is not rejected. The alternative hypothesis that the slopes are equal is accepted with a 95% confidence interval.

The results for all comparisons of slopes are as follows:

<u>Figure</u>	<u>Z</u>	<u>Conclusion (C.I. = 95%)</u>
20	1.79	Slopes are equal
21	0.82	Slopes are equal
22	2.43	Slopes are not equal
23	1.67	Slopes are equal
24	1.59	Slopes are equal
25	0.74	Slopes are equal
26	1.96	Slopes are not equal for a confidence interval of 94%
27	1.06	Slopes are equal
30	0.43	Slopes are equal
31	0.85	Slopes are equal
32	0.23	Slopes are equal
33	1.22	Slopes are equal